# Factors influencing cellular radiosensitivity and survival curve analysis.

By RHEA DESAI, B.Sc.

A Thesis Submitted to the Department of Biology
and the School of Graduate Studies of McMaster University
in Partial Fulfilment of the Requirements
for the Degree of Doctor of Philosophy

| | |
|---|---|
| TITLE: | Factors influencing cellular radiosensitivity and survival curve analysis. |
| AUTHOR: | Rhea Desai<br>B.Sc. Biology – McMaster University |
| SUPERVISOR: | Dr. Carmel Mothersill |
| COMMITTEE: | Dr. Colin Seymour<br>Dr. Jonathon Stone<br>Dr. Juliet Daniel |
| NUMBER OF PAGES: | xvi, 149 |

# Abstract

Investigating variance in radiosensitivity amongst cell populations contributes to the overall improvement in our understanding of the effects of low dose ionizing radiation. The aim of this thesis was to investigate factors influencing radiosensitivity through analysis of survival curves. The radiation-induced bystander effect and low dose hyperradiosensitivty were observed to help elucidate relationships between these phenomena.

First heterogeneity of a cell population was investigated and seven clonal lines of an HCT 116 p53 wild type cell line were derived. Survival curves with a wide range of dose points (0.5 to 15 Gy) were developed and curves were fitted with the linear-quadratic and multi-target models. The McMaster Taylor Radiobiology Cesium-137 source was used for all irradiations in this thesis. Here it was evident that the multi-target model provided a better fit and further analysis revealed a relationship between the curve shoulder and toxicity of bystander effect signals. Clonal lines with a large shoulder size did not show evidence of the radiation induced bystander effect. Since the lowest dose point in curves was 0.5 Gy, a more focused look was taken in the low dose range.

Survival curves were again produced for all clonal lines adding data to now include six dose points in the low dose region (below 0.5 Gy). Survival curves were re-analyzed with this extensive data set including doses from 0.01 to 15 Gy and now instances of hyperradiosensitivty were evident in all cell lines. The linear-quadratic model did not provide a meaningful fit to the data and so the induced-repair model was used and found to be appropriate in low doses. It was concluded that whether the radiation-induced bystander effect was produced or not, low dose effects such as hyperradiosensitivity may contribute to the overall radiosensitivity of a cell line.

Finally, sex of the cell line was investigated using four cell lines. Of the four cell lines, two were included as controls for radiosensitivity. These two cell lines were null for the protein Artemis which assists in the repair of double strand DNA breaks. Thus, when this protein is not functioning as normal, radiosensitivity is induced in the cell line. Through medium transfer bystander effect assays a greater reduction in cell survival was observed in the normal female cell line compared to the normal male cell line.

In conclusion, this thesis contributes to the understanding of low dose effects and non-targeted effects of ionizing radiation. Understanding these mechanisms both separately and in combination may contribute to the betterment of radiation therapies and radiation protection.

# Acknowledgements

As I sit down to (finally) write these acknowledgements, I am filled with so much joy and gratitude. I feel so grateful to have taken on this academic journey which not only expanded my perspectives but filled my life with people and opportunities I could not find elsewhere.

First, thank you to Dr. Carmel Mothersill. Carmel, thank you for taking a chance on my younger self and guiding me through the challenges of academia and life. It has been such a rewarding experience to have been your student over these past years. You have pushed me to think critically to solve problems in and out of the lab and have been an amazing mentor. The compassion you show for your students has made difficult times that much easier and definitely does not go unnoticed. Your interest in my leadership goals and activities has helped me find my true values in the work I pursue and has made me optimistic for all that is to come.

A sincere thank you to Dr. Colin Seymour for showing me what it is to be a researcher, to challenge stereotypes and to approach problems with an open mind. The conversations we have had over the years have broadened my perspectives and have taught me things you can't read in books! Thank you to Dr. Jonathon Stone and Dr. Juliet Daniel for pushing me at my committee meetings while being supportive of my work. From undergraduate classes to sitting on academic and social committees, it has been a pleasure to work with you and learn from you along the way.

Thank you to all the lab friends - you have made my time in the lab fun even when experiments don't seem to work out. Special thank you to Nathan, Andrej and Megan for all of your support. Nathan, you made my early days in the lab a great experience and really set me up for success! Andrej and Megan, thank you for being there to talk through problems whether they be about lab work or not, and for

stepping in to help out when getting to the lab was tough. I really appreciate you all for your positive energy and support.

To my friends Erica and Lindy, you two have been around for the highs and lows and never wavered in your support even when you had your own stuff going on. I truly appreciate all the times you have listened to my excessive rants and all the times you forced me to relax and enjoy the ride. A big thank you to the friends I met in my earliest days at Mac. Claire, Emily, Sarah and Zahra, you guys have given me so much joy since we've met and have supported me to lean into who I really am. Your support to take on new jobs, roles and degrees means the world. Even in times when I was barely scraping by, you all have reminded me to never set limits to my dreams. I'm grateful to have met such inspiring women and can't wait for all that we accomplish in this life!

Of course, I can't forget my homie for life, James. I feel so grateful to have met you back in undergrad and for all the support and love you have provided since. I think it is sooo rare to find someone with the same values, goals and ambitions and I cannot wait to continue reaching all of our goals together. We constantly push each other to learn more about the world around us so that we can contribute in meaningful ways and for this I am forever grateful.

Lastly, thank you to my family who have demonstrated firsthand, that no goal is too hard to achieve, and no problem is too hard to overcome. Growing up living with and learning from my grandparents created a bond I can never forget. Bhai, thank you for making fun of me since we were kids and putting me in compromising positions that I *think* have helped make me become the resilient person I am today. Thank you Shui, you have taught me the importance and value of independence. Finally, thank you to my parents. You have sacrificed so much so that I could have the life of my choosing and I am eternally grateful. Without you all, I would not be able to achieve any of the goals I set out for myself. Thank you.

# Declaration of Academic Achievement

I declare that all work submitted in this thesis is my own work and does not involve plagiarism or academic dishonesty.

I certify that I have read this thesis and that, in my opinion, it is fully adequate in scope and in quality, as a dissertation for the degree of Doctor of Philosophy.

# Contents

# List of Figures

# List of Tables

# List of Acronyms & Symbols

| | |
|---|---|
| **CHART** | Continuous, Hyperfractionated, Accelerated Radiotherapy |
| **CHO** | Chinese Hamster Ovary Cells |
| **CJ176** | Primary Fibroblast (male, Artemis-null) Cells |
| **CNSC** | Canadian Nuclear Safety Commission |
| **CT-Scan** | Computed Tomography Scan |
| **DMEM** | Dulbecco's Modified Eagle Medium |
| **DNA** | Deoxyribonucleic Acid |
| **DSB** | Double Strand Break |
| **EDTA** | Ethylenediaminetetraacetic Acid |
| **FBS** | Fetal Bovine Serum |
| **F02/385** | Primary Fibroblast (female, Artemis-null) Cells |
| **Gy** | Gray |
| **HaCaT** | Immortalized Human Epithelial Cells |
| **HCT 116** | Human Colon Carcinoma Cells |
| **HeLa** | Immortalized Cell Line |
| **HPV-G** | Human Papilloma Virus Transfected Keratinocyte Line G Cells |
| **HRS** | Hyperradiosensitivity |
| **ICCM** | Irradiated Cell Culture Medium |
| **IR** | Ionizing Radiation |
| **IR** | Induced-Repair |
| **IRR** | Increased Radioresistance |
| **LNT** | Linear No-Threshold |
| **LQ** | Linear-Quadratic |

| | |
|---|---|
| **MRT** | Microbeam Radiation Therapy |
| **NHEJ** | Non-homologous End Joining |
| **NTE** | Non-Targeted Effect |
| **PC3** | Human Prostate Cancer Cell Line |
| **PE** | Plating Efficiency |
| **RIBE** | Radiation Induced Bystander Effect |
| **RPMI 1640** | Roswell Park Memorial Institute Growth Medium |
| **RS-SCID** | Radiosensitive-Severe Combined Immunodeficiency |
| **SEM** | Standard Error of the Mean |
| **SW48** | Colon Carcinoma Cells |
| **T98G** | Human Glioma Cell Line |
| **UV** | Ultraviolet |
| **1BR.3** | Primary Fibroblast (male) Cells |
| **48BR** | Primary Fibroblast (female) Cells |

| | |
|---|---|
| $\alpha$ | Coefficient for cell killing proportional to dose (linear-quadratic model) |
| $\alpha s$ | Slope at very low dose (induced-repair model) |
| $\alpha r$ | Coefficient for cell killing proportional to dose at high doses (induced-repair model) |
| $\beta$ | Coefficient for cell killing proportional to square of dose (linear-quadratic & induced-repair model) |
| ***D or d*** | Dose |
| $d_c$ | Dose constant |
| $D_q$ | Quasi-Threshold Number |
| $D_0$ | Reciprocal of final slope |
| $D_{10}$ | Decade Killing Dose |
| $n$ | Extrapolation number |
| $S$ | Survival Fraction |

# Chapter 1 - Introduction

## 1.1 Research Motivation

The goal of this project is to determine fundamental heterogeneity in clonal progeny of cell populations exposed to ionising radiation using cell survival models commonly used to estimate cell death following radiation exposure. A main aim is to reduce the uncertainty associated with low dose ionizing radiation exposures. This is necessary to gain trust from the public during a period of time that finds governments and industry keen on the increased use of nuclear energy. Along with this particular interest in the nuclear industry, findings in this field provide information to better develop radiation protection guidelines and standards.

A large portion of this project involves comparing parameters of commonly used models such as the multi-target, linear-quadratic and induced-repair used to model survival curves obtained through experimentation on cell populations. Here we work with an HCT 116 p53 positive cell line, clones derived from this HCT 116 cell

line and finally cell lines with variation in sex (1BR.3, CJ176, 48BR and F02/385). This investigation into the heterogeneity of clonal cell lines as well as variations arising from less investigated factors such as the sex of the person from whom the cell line was derived, assists in furthering the radiobiological understanding of cellular response to targeted and non-targeted ionizing radiation. This work is relevant to radiation therapy, diagnostic imaging (ex. CT scans, mammography) and radiation protection.

While diagnostic imaging is used regularly in clinical settings, there remains hesitancy accepting these tests due to perceived cancer risk. Data gathered on the differences of clonal radiosensitivity will also pay particular attention to low doses of radiation below 0.5 Gy to elucidate any phenomena that occur at very low doses. Further research accounting for sex-effects will also focus on low doses. This research will investigate anomalies of cell death and survival at low doses commonly overlooked in many radiobiological studies focusing on the effects of high dose radiation. This research will help further our understanding of factors involved in determining individual radiation responses. There is great uncertainty concerning low dose effects due to a number of genetic, environmental and lifestyle factors and thus we aim to assess the factors involved in the variation of response to radiation. This specific type of science is necessary to understand the complexity of adding

ionizing radiation exposure to an environment while maintaining the surrounding ecosystem.

## 1.2 Project Aim & Thesis Outline

The aim of this thesis is to better understand lose dose effects in the context of the radiation induced bystander effect (RIBE) and hyperradiosensitivity (HRS) while considering other factors that add complexity to low dose effects such as sex. Specifically, we look at clonal heterogeneity and variance in sex on overall radiosensitivity. The following outlines each chapter of this thesis.

**Chapter 2** introduces relevant radiation biology principles, current survival curve models and the historical context of the non-targeted effects of ionizing radiation. This chapter also highlights current problems in low dose research as well as areas where research is lacking with respect to factors such as sex of the donor.

**Chapter 3** (Paper I) investigates the clonal heterogeneity of a common cell line, used to investigate non-targeted effects such as the radiation induced bystander effect (RIBE) and low dose hyperradiosensitivity (HRS). Seven clonal cell lines are derived from the parent populations and are investigated for differences in radiosensitivity. Survival curve models are used to better understand the cell lines' response to ionizing radiation.

**Chapter 4** (Paper II) takes a more focused look at the effects of low dose ionizing radiation. Using clonal cell lines previously derived in Chapter 3. Low dose irradiations are conducted in order to investigate HRS and the transition of cells to a more radioresistant response.

**Chapter 5** (Paper III) continues work in the low dose range to investigate often overlooked factors influencing individual response to ionizing radiation. Here we take particular interest in sex as literature has suggested a difference in response to direct irradiation between males and females, however, less is known on the influence of sex on the outcome of non-targeted effects of ionizing radiation.

**Chapter 6** summarizes the findings presented in this thesis and discusses the significance of the findings in the context of improved treatment and radiation protection.

# Chapter 2 - Background

## 2.1 Contextualizing Radiobiology

Radiobiology studies the impact of radiation on biological systems. The electromagnetic spectrum comprises various types of radiation ranging from radio waves all the way to radiation in the ionizing part of the spectrum[1]. This includes gamma rays and X-rays. Ionizing radiation is comprised of radiation with short wavelengths, high frequency and high energy. The complexity in radiobiology studies lies where ionizing radiation produces effects that are damaging to living systems or may alter their normal behaviours [1,2]. When radiation of high energy penetrates a cell, tissue or organism, ionization occurs either in biomolecules (direct ionization) or in the water surrounding them. The ionised molecules and free radicals formed can then react with biomolecules (indirect effect of radiation) . The way in which ionizing radiation events can lead to cellular damage or cell death is the premise upon which the study of radiobiology lies.

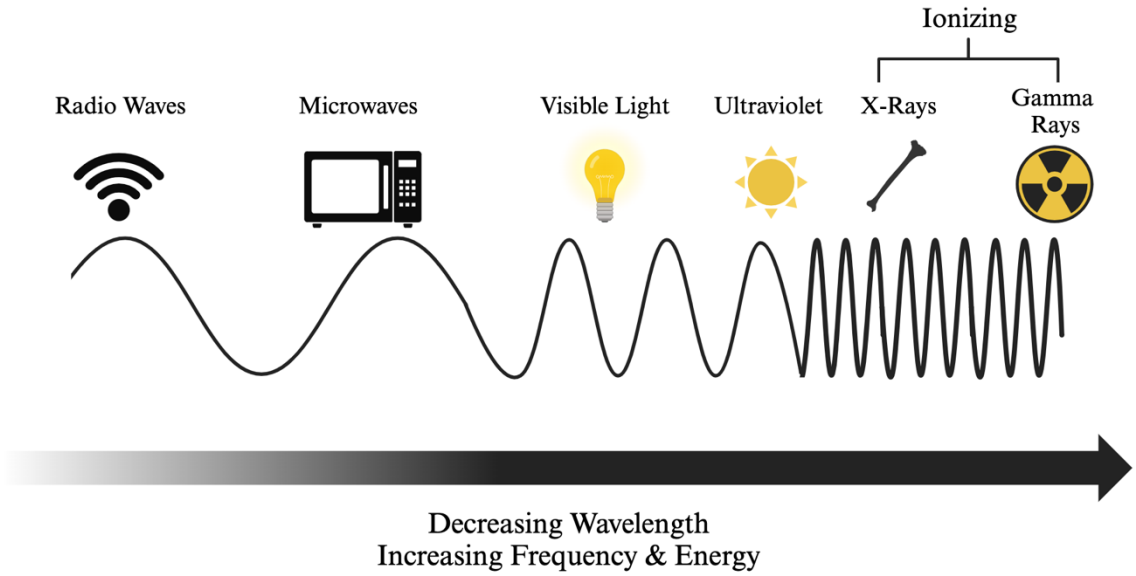


**Figure 2.1:** The electromagnetic spectrum. Radio waves, microwaves and visible light are found lower on the spectrum. Ultraviolet light is not considered ionizing but can cause photochemical reactions that can be damaging to tissues. This thesis utilizes gamma radiation via a Cesium-137 source.

## 2.2 Low Dose Effects

While there is an overall agreement that direct ionizing radiation in high doses defined as above 0.5 Gy have the potential to produce damaging effects, non-targeted effects are an area of research that explores effects in neighbouring populations. Non-targeted effects (NTEs) refer to ionizing radiation-like effects in biological systems where there is not a direct deposition of energy[3–7]. While DNA is accepted as a primary and critical target for the targeted effects of ionizing radiation, there is less

certainty about critical targets following non-targeted radiation exposure. Work by Murphy and Norton, in 1915, noted effects in organs that were distant from the site of direct exposure in X-ray irradiated mice [8]. These effects were initially described as *indirect effects* but are now referred to as non-targeted effects and were not given much attention until further research on NTEs in the 1980s. Today, indirect effects of radiation refers to the ionization of water that then proceeds to react with a molecule of interest due to the formation of reactive species. Non-targeted effects now have more distinct categories: abscopal effects, clastogenic effects, genomic instability, and radiation-induced bystander effects (RIBE). With consideration to low dose effects, low dose hyperradiosensitivity (HRS) is also of interest showing how cells may die at a greater than expected level at such low doses. Under such conditions, the challenge lies in estimating risk to a patient, community, or ecosystem as many NTEs add to the degree of damage experienced by a living cell, tissue, or organism. It is worth noting the first instance of an adaptive response to ionizing radiation was observed using lymphocyte culture. A group of cells were cultured in the presence of radioactive thymidine and then were subject to a high dose of radiation. These cells were found to develop fewer chromosomal aberrations compared to the control group which only received an acute high dose of radiation[9,10]. Radiation hormesis is thought to be due to low doses of radiation which contribute to the initiation of protective cellular processes [11,12]. This thesis will pay particular attention to RIBE and hyperradiosensitivity (HRS) described in greater detail later in this chapter.

### 2.2.1 Hyperradiosensitivity (HRS) and Increased Radioresistance (IRR)

Many phenomena can come into play impacting our understanding of dose-response relationships. One of these, hyperradiosensitivity (HRS) refers to a greater than expected sensitivity to low doses (below 0.5 Gy) radiation exposure often followed by a transition to increased radioresistance (IRR). Many expectations to response following low dose exposure come from models such as linear no threshold and linear-quadratic models. In 1985 using mice skin to study low dose radiation, Joiner *et al.* found that their results fit the linear-quadratic model for X-ray exposure down to 0.75 Gy fractional doses but at even lower doses there was more radiosensitivity than initially expected [13]. Later in 1993 Marples and Joiner confirmed a transition from HRS to IRR in Chinese hamster V79-379A cells showing lower survival for X-ray doses below 0.6 Gy than predicted by the linear-quadratic model [14]. Further work using human cell lines also reported instances of HRS/IRR. Wouters and Skarsgard showed human tumor cells which received a single X-Ray dose of 0.05 to 4 Gy, the linear-quadratic model fit data below 1 Gy but below this dose displayed an enhanced level of sensitivity [15]. A dose rate of 0.51 Gy/min was used for doses up to 1.6 Gy and a dose rate of 2.21 Gy/min was used for doses from 2 to 4 Gy. They suggested that the cell population to be hypersensitive and as damage

is sustained by the cell takes a more resistant response[15]. Following this in 1996, Wouters *et al.* examined very low dose responses of five human tumour cell lines known to display variation in radiosensitivity[16]. They found that the four most resistant cell lines displayed HRS in low doses followed by IRR in the range of 0.3 to 0.7 Gy[16]. Lambin *et al*. also reported supporting evidence that doses below 1 Gy showed an increased effectiveness of X-rays[17]. Research using the human radioresistant T98G cell line investigated HRS with respect to phases of the cell cycle and confirmed low dose HRS in the whole cell population rather than radiosensitive subpopulations[18]. These previously mentioned studies concluded more pronounced HRS/IRR transition in human cells compared to the original Chinese hamster V79 cells. Since much of this initial work emphasized HRS in low doses, other models such as the induced-repair model were introduced to better describe low dose effects. Both the induced-repair and linear-quadratic model are described in further detail in section 2.5.

Research into low dose HRS/IRR has demonstrated evidence *in vivo* and shows potential for the betterment of fractionated radiotherapy. In general, reports by Joiner *et al.* on mouse skin[13] and kidneys[19] and Parkins and Fowler on lungs[20] show that the total dose needed to produce damage is decreased when the dose per fraction is below 1 Gy [21]. Continuous, hyperfractionated, accelerated radiotherapy (CHART), originally conducted at Mount Vernon Hospital in the United Kingdom, was able to produce high levels of tumour control in progressed head, neck and bronchial

carcinomas[22]. This fractionated approach to treat progressed tumours was encouraging and further trials were conducted. A report published in 1997 showed that locally advanced non-small-cell lung cancer treated using CHART led to a significant improvement in survival of patients[23]. Further understanding of low dose radiation and associated effects could help significantly improve such therapy types. To gain a therapeutic advantage while exploiting HRS/IRR would mean that more sensitivity must occur in the cancer or tumour tissue than in normal tissues. Thus low dose curve fitting parameters outlined in section 2.5 are of interest to investigate sensitivity in low doses as well as the rate of transition for HRS to IRR. Skov *et al.* investigated the low dose response of three hamster cell lines which deficiencies in DNA repair[24]. A cell line defective in the subunit of DNA-PK complex that repairs double strand break was found to have an exponential survival response (no IRR) and a cell line defective in nucleotide excision repair responded in the same manner. In the third cell line with base-excision repair deficiency showed HRS/IRR and thus it was suggested that this phenomenon is linked to the repair mechanisms of double strand break (DSB) repair and nucleotide excision repair[24]. In 2002, work by Mothersill *et al.* again emphasizes the presence of HRS in low doses and how this effect results in a larger amount of cell killing than the classical understanding of DNA DSB break repair[25]. Here they tested 13 cell lines and saw variation in expression of RIBE and HRS and suggested that cell lines displaying large RIBE responses don't show HRS and those that show HRS do not show RIBE[25]. However, this conclusion was modified later (see below).

Previous work by our group has reported a relationship between cells showing the HRS/IRR response and adaptive responses. The adaptive response refers to a biological process by which radioresistance to a challenging dose is formed after receiving a small priming dose[26–28]. In 2009, Ryan *et al.* show that an adaptive response is detected in documented HRS cell lines, meaning an increase in cell survival was observed[27]. Work by Fernandez-Palomo *et al.* took a further look at the T98G (shows HRS) cell line and HaCaT (does not show HRS) cell lines and aimed to show a link between RIBE and HRS[29]. When using a mix-match protocol of donor and reporter cell lines, it was found that RIBE occurred when T98G donor cells were used on both T98G and HaCaT cell lines but that there was some relationship to dose where RIBE was only achieved below 1 Gy. When HaCaT donor cells were used, an increased survival fraction was found in reporter T98G cell but decreased in HaCaT cells[29]. A large amount of the research mentioned in this section emphasizes that studies at high doses cannot accurately be extrapolated to low doses and thus continued interest in low dose effects such as HRS/IRR is necessary.

## 2.3 Non-Targeted Effects

The low dose range of ionizing radiation is defined as below 0.5 Gy and is relevant in a variety of real-world settings. From occupational exposures and environmental protection to the use of low dose radiation for radiation therapies and diagnostic imaging, low dose ionizing radiation is of particular interest due to the possible effects it may have on a population. These effects vary from our high dose understanding of radiation effects. While it is understood that high dose exposures lead to an overall linear dose-response relationship[1,2], phenomena occurring in low doses results in a more non-linear relationship [3,4,21]. In low doses, it has been noted that effects are not directly proportional to the dose received since there are several factors (ex. age, sex, comorbidities) that also contribute to sensitivity in this region. These low dose effects have created a sense of uncertainty in the low dose range, creating difficulties when advising the general public regarding the various effects of radiation.

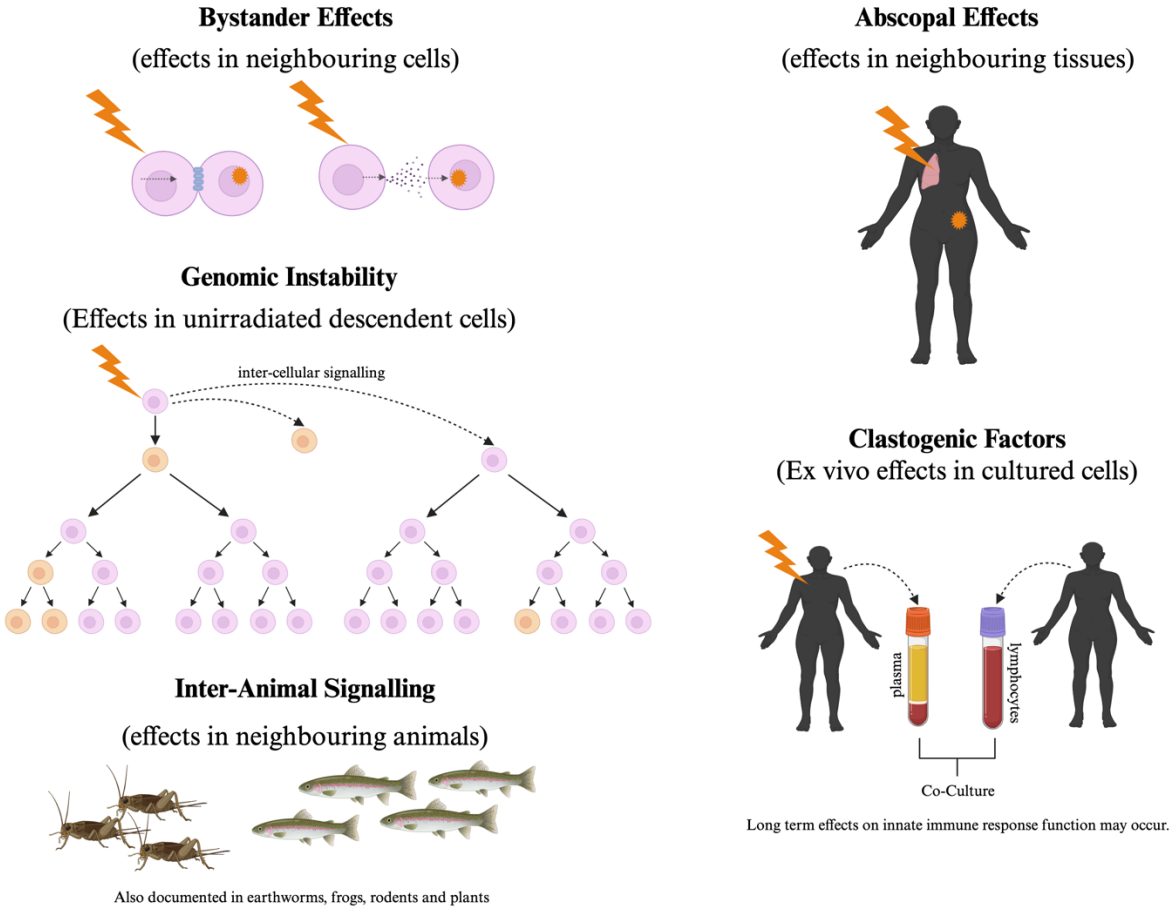


**Figure 2.2:** Examples of documented non-targeted effects of ionizing radiation. In all cases, ionizing radiation is not directly applied to the cell or organism however effects are observed in the non-irradiate counterpart (Figure courtesy of Dr. Carmel Mothersill).

### 2.3.1 Radiation-Induced Bystander Effect (RIBE)

Radiation-induced bystander effects refers to a response in a cell, tissue or organism which did not receive a direct deposition of ionizing radiation but responded to signals from an irradiated counterpart[6,7,30]. RIBE has been demonstrated as a communication through gap junctions[31,32] as well as soluble factors[33–36]. More recently, RIBE has also been described through physical factors such as biophotons[37,38] and at the population level in organisms such as fish[39] and crickets[40]. Research has shown RIBE both *in vitro* and *in vivo* however the work presented in this thesis make use of the RIBE medium transfer assay documented further in chapters 3 to 5.

Literature dated to 1953 [6,7] has shown cells producing NTEs with Parsons *et al.* who reported changes in sternum bone marrow in children who received spleen irradiation for chronic granulocytic leukemia[41]. This study clearly emphasized findings that a radiation-induced effect may be observed in distant and unirradiated tissues. About 10 years later, in 1962, Souto *et al.* gave evidence that rats injected with plasma or ultrafiltrates of blood from irradiated rats or sheep developed many mammary tumours compared to the non-irradiated animals[42]. The tumours developed at a significantly higher rate in the irradiated groups compared to the unirradiated. This effect is known as a NTE via clastogenic factors. Later in 1967, work by Hollowell and Littlefield built on the report of clastogenic factors and found that

plasma from X-ray irradiated patients was able to induce chromosomal aberrations in lymphocyte culture[43]. Further research by Hollowell *et al.* found plasma collected from radiotherapy patients has a similar effect regarding chromosomal damage[44,45]. The chromosomal changes were found to be the formation of dicentrics, chromatid breaks, and chromatid exchanges and translocations and was a significant finding which shed light on the fact that even NTEs could result in the change of genetic information similar to the well understood mechanisms of direct radiation[43–45]. Similarly, Goh and Sumner found in 1968, that some sort of transferable substance is produced following total-body irradiation which also produced chromosomal damage in unirradiated lymphocytes[46]. To build on these findings Littlefield *et al.* looked at effects of donor and recipient populations and saw an apparent variation in response[45].

While irradiations to pregnant females is understood to be dangerous due to the developing fetus, studies by Goyanes-Vallaescusa in 1971 also found NTEs in lymphocytes from human children and from young rabbits' [47]. Their mothers had been irradiated but received only nonpelvic irradiations and that before time of gestation. This group suggested a transplacental migration of the chromosome-breaking factor in plasma to be the reason for this damage transfer to offspring[47]. Continued work on clastogenic factors by Faguet *et al.* showed an increase in clastogens after whole-body irradiation using rats[48]. They concluded that "This activity is not due to radiation-induced depletion of protective factors nor to

chemical-physical changes of normal plasma components but results from circulating factors released by irradiated cells" [48]. Following this result, research on atomic bomb survivors by Pant and Kamada concluded the presence of the factor in plasma even 31 years post-exposure[49]. Pant and Kamada used blood plasma to conduct experiments and observed this effect in leukocytes. In comparison they also looked at the blood plasma of patients who underwent x-rays and a control population. An interesting and significant conclusion was that these clastogenic factors could have effects decades after an initial high dose radiation exposure[49]. Many of these findings confirmed the presence of cytotoxic effects of radiation on unirradiated cells and tissues.

The more modern studies of RIBE began with Nagasawa and Little in 1992 who at that moment in time challenged basic concepts in radiobiology. The classical understanding that living cells exposed to ionizing radiation would experience some type of cellular recovery, mutation or total cell inactivation was now being extensively challenged with large volumes of research indicating the possibility for NTEs to come into play. The 1992 study by Nagasawsa and Little investigated low fluence alpha particles applied to cell cultures[50]. The main idea put forward here was that if these alpha particles were applied in a way that only some cells would receive a direct deposition of ionizing energy, sister chromatid exchanges would be measured in more cells than were hit directly. Other laboratories also challenged key radiobiology principles including Seymour *et al.* in 1986 who found that when mammalian cells are

irradiated cells in survivor colonies have the potential to carry lethal mutations[51]. Sometimes these lethal mutations may only be detectable after numerous divisions. Plating efficiencies were investigated, and it was found that plating efficiencies decreased to levels less than those of unirradiated cell populations. Alper *et al.* in 1988 built on Seymour *et al.'s* 1986 finding and concluded that "lethal mutations induced in mammalian cells are for the most part associated with the shoulder regions of survival curves"[52]. The rationale of this perspective explained that this region of the curve is representative of an initial and fast acting repair mechanism which was no longer prominent with an increase in dose[52]. In 1988 Born and Trott tested clonogenic ability of the progeny of irradiated cells *in vitro* through consecutive replating of irradiated cultures[53]. Their experiments allowed for about 5 to 25 divisions to occur after cell plating. Born and Trott's finding that there was no difference in plating efficiency or clonogenic survival results between an irradiated group and non-irradiated group did not support Seymour *et al.* and Alper *et al.*'s findings[53]. Later research by Pampfer and Streffer investigated chromosome damage in mouse fetuses following zygote irradiation[54]. It was found that cells derived from skin biopsies of mouses fetuses that were irradiated with X-rays at the zygote stage had increased chromosome aberration levels and was the first instance of reporting chromosome instability in fetal fibroblasts following zygote irradiation[54]. Various findings by Chang and Little investigated delayed reproductive death in Chinese hamster ovary cells tying in the previously mention work on delayed lethal effects in the form of clonogenic surviving ability[55–57].

First, they found that with a reduction in clonogenic ability, the progeny of surviving CHO cells showed other abnormalities such as decreased ability to attach to culture dishes and slower cell cycle progression[55]. It was suggested here that damage carried by surviving progeny of irradiated cells can still propagate over many mitotic cycles[55]. They termed this effect as *delayed reproductive death* after the realization that a reduction in clonogenic ability persisted in cloned progeny of CHO cells following X-ray irradiation[55,56]. Results of follow up studies suggested DNA double-strand breaks and their associated endogenous repair processes are involved in the induction of delayed reproductive death in CHO cells[56,57]. Similarly, a study by Kadhim *et al.* reported "exposure to alpha particles (but not X-rays) produced a high frequency of non-clonal aberrations in the clonal descendants, compatible with alpha-emitters inducing lesions in stem cells that result in the transmission of chromosomal instability to their progeny"[58]. Later work by Brown and Trott with HeLa cells found that when clones of HeLa cells were irradiated with high dose X-rays, reduced plating efficiency and clonal heterogeneity of progeny of irradiated surviving cells were observed[59]. Plating efficiency was decreased and continued for more than 20 population doublings[59]. Today it is expected that there will be some effect to surviving progeny of irradiated biological material however all of the research mentioned here significantly helped shift the mindset of experts in the field believing that effects of radiation occur only in the DNA of target cells[6].

In 1997 Mothersill and Seymour reported the significant finding of an observed decrease "in cloning efficiency in unirradiated normal and malignant epithelial cell lines receiving medium from irradiated cultures"[60]. Medium irradiated without cells and that of a fibroblast line had no effect on unirradiated fibroblasts. However, medium from irradiated epithelial cells had a significantly toxic effect on unirradiated cultures of these cells. This effect demonstrated using epithelial cells was dependent on the number of cells present at the time of irradiation and could be observed in culture medium taken from cells even after only 30 minutes had elapsed after irradiation before medium harvest. They noted these findings to suggest a factor involved with RIBE to be cell-derived[60]. Following this finding Azzam *et al.* reported the significance of intercellular communication in RIBE[32]. Levels of expression of TP53, CDKN1A, CDC2, CCNB1 and RAD51 were investigated, and it was found that "TP53 and CDKN1A is significantly reduced in the presence of the gap junction inhibitor lindane and in irradiated low-density cell populations"[32]. CDKN1A plays a critical role in G1 cell cycle arrest. Therefore, it was an interesting finding to see that at doses where only 2% of nuclei would be hit with an alpha particle track of radiation, CDKN1A induction was reported in a significantly larger population of cells than predicted[32]. Further research by Azzam *et al.* was significant in confirming the role of gap junctions in RIBE. They found that lindane (connexin-43 function inhibitor) was effective in halting transduction of RIBE to non-irradiated neighbouring cells[31,32].

Research by various groups such as the 1998 and 2003 studies by Khan *et al.* showed that even shielded regions of an organism could experience NTEs. For example Khan *et al.* used rats with shielded lung areas and found that these shielded regions resulted in increased micronuclei formation when the not shielded lung parts are irradiated[61,62]. Another finding in 2003 highlighted a possible benefit of NTEs. Here mice were implanted with tumors into the midline dorsum and then underwent high dose fractionated radiations of the leg[63]. When compared to the control group they found that the tumors in the midline dorsum grew significantly slower[63]. However later reports in 2008 by Mancuso *et al.* revealed an increase in occurrence of medulloblastoma when heads of animals were shielded compared to whole-body irradiations[64]. Previous work by our group showed RIBE in both non-irradiated brain areas and bladders of normal and tumour bearing rats[65,66].

Further work on RIBE has proven that exposure of cell cultures or tissue explants to low doses of gamma radiation can produce increased levels of abnormal behaviour in cells never directly irradiated. In 2001, Seymour and Mothersill found human keratinocytes to show RIBE following radiation exposures of 0.01 to 0.5 Gy [67]. They found the magnitude of RIBE to be generally constant across these doses but to saturate in the range of 0.03 to 0.05 Gy [67]. Lyng *et al.* studied, medium collected form irradiated cells and its ability to induce mobilization of intracellular calcium, loss of mitochondrial membrane potential and increase in reactive oxygen species on cells not directly exposed to ionizing radiation[68]. Some of these events

are involved in early initiation of the apoptotic cascade. Using this RIBE medium transfer assay where medium collected from irradiated human keratinocytes is transferred to unirradiated keratinocytes, rapid calcium flux, loss of mitochondrial membrane potential, increase in apoptotic cells and reactive oxygen species and a significant reduction in clonogenic survival were observed again giving evidence to the relevance of NTEs, in particular RIBE [68]. Also in 2001, Mothersill *et al.* reported the significance of RIBE for cancer risk assessment and treatment plans. Here they signified the relevance of such low dose effects *in vivo* [69]. In this study fragments of human tissues were irradiated *ex vivo* and medium was subsequently collected an added to unirradiated explants or cell lines. It was found that a signal or factor in the collected medium could induce cell death and protein expression in the unirradiated counterparts and these effects were transmissible to progeny[69]. Another aspect of RIBE worth mentioning is the role of photons. First, Le *et al.* showed that irradiation using tritium ($^{3}H$, low energy beta emitter) has the ability to produce photon emission in human keratinocytes[70]. Later studies emphasized the biological relevance of photon emission from beta-irradiated cells and found that UV photons emitted from directly from irradiated cells influence RIBE in neighbouring cell populations. This gave evidence of a physical mechanism for RIBE [37,38,70].

Other notable findings on RIBE by our group have investigated entire organisms *in vivo*. In 2006 it was reported that fish irradiated with a whole-body dose of 0.5 Gy (dose rate of 0.1 Gy/min) release soluble factors into water which induce

RIBE in unexposed fish [39]. Tissue culture explants were derived from the fish and used to examine RIBE. It was found that RIBE response varied depending on the tissue type and that gill and fin explant cultures showed the most notable RIBE response[39]. More recently in 2023, Li *et al.* demonstrated RIBE in crickets. It was found that "cohabitated males and females matured significantly faster with no significant difference in maturation weight than non-cohabitated populations"[40]. This finding is a novel demonstration of RIBE where introduction of irradiated organisms influences development of non-irradiated populations. Effects were found to be sex dependent [40].

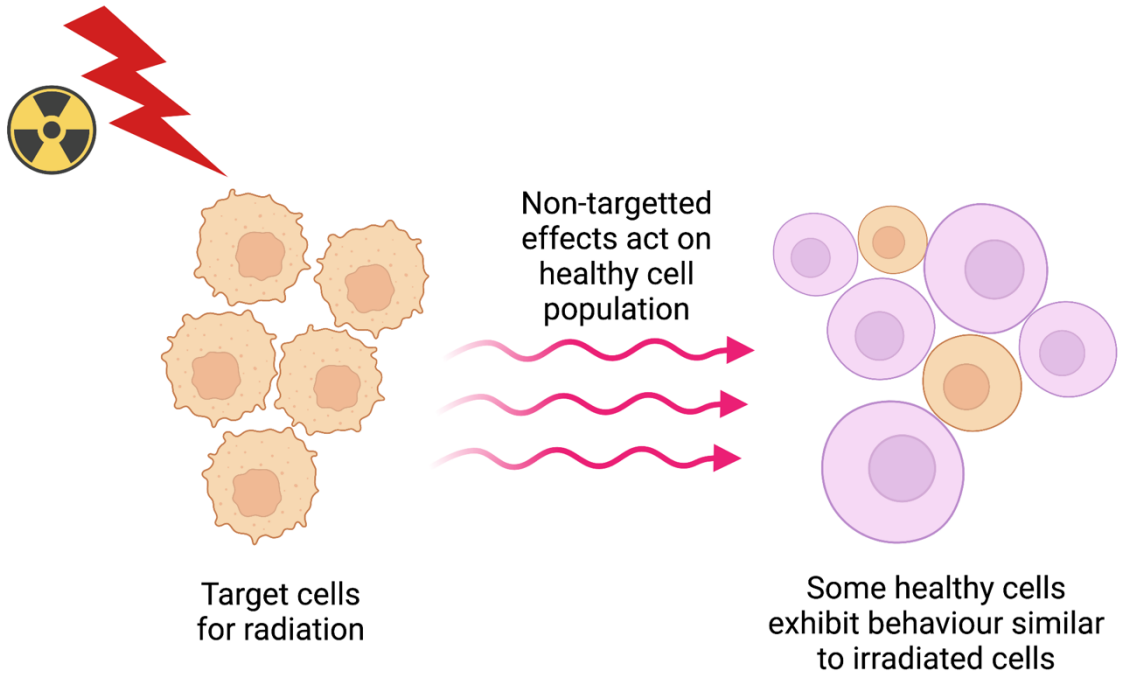


**Figure 2.3**: A representation of the non-targeted effects of ionizing radiation. Cells in orange destined to receive a dose of radiation (left) are hit with ionizing radiation and subsequently release a signal that triggers the purple non-targeted or healthy cell populations (right) to exhibit changes in behaviour or cellular characteristics.

### 2.3.2 Low doses and the influence of sex on radiosensitivity

As previously described, low dose effects add to the uncertainty of radiation advisory in terms of occupational, environment and clinical exposures. To add to the complexity of low dose radiation, factors such as sex have been found to have influence on exposure outcomes. In general, more is understood about the targeted effects of ionizing radiation and the same can be said with respect to sex.

Current regulatory bodies have indicated a greater risk associated with females exposed to ionizing radiation. Much of this risk is associated with the female reproductive system and dose guidelines aim to protect these most sensitive tissues and organs. However, attention must be drawn to the scarcity of research considering sex in low dose exposures and NTEs.

Previous work by the Kovalchuk research group has suggested bystander effects in males and females may be distinct due to differences found through direct radiation exposures [71–73]. In a 2001 study by Mothersill *et al.* it was concluded that females had an overall greater sensitivity to RIBE signals compared to their male counterparts. While the main focus of this study was not on sex-differences in NTEs, they did note one of the first instances where a significant difference in cell survival was observed between sexes following the RIBE medium transfer assays[69]. Furthermore, to build on findings of targeted ionizing radiation exposure and sex, Koturbash *et al.* found a selective response through bystander effect experiments[74]. A greater change was observed in spleens of male mice, but sex differences were significantly less prominent when gonads were surgically removed. In 2022, a student in our group analyzed published bystander data available in literature to find any commonalities in factors influencing RIBE. Of these factors, sex of the cell line was analyzed, and it was concluded that female cell lines produced a larger reduction in cell survival compared to male cell lines in RIBE experiments [75]. Further investigations on NTEs in the context of sex-linked effects is needed.

## 2.4 Modelling

Modelling radiobiology has proven to be difficult as researchers aim to find balance between a physical understanding true to their knowledge of ionizing radiation risk and exposure, and a mathematical equation that accurately describes a full spectrum of radiation damage from low to high doses. Survival curves are used to describe the relationship between radiation dose and the proportion of cells that survive and thus curve fitting models are developed to estimate dose-response. Many models also have a range of applicability as will be discussed in this section. Something less discussed is the applicability of these models. Whether it be for assessing cancer risk to high dose exposures, the effects of acute or chronic low dose radiation or for advisory of new nuclear projects, it is necessary to be critical of modeling in order to truly understand and communicate the range and applicability of each model. The following highlights models commonly used in the field of radiobiology with implications for radiation therapy and the radiation protection of parts of an ecosystem.

### 2.4.1 Linear No Threshold Model

The linear no threshold (LNT) model assumes cancer risk increases with increasing dose. The LNT model is used internationally by many health agencies and nuclear regulators including the Canadian Nuclear Safety Commission (CNSC) to help determine dose limits for workers and community members however it does not account for the possibility of low dose effects [76]. The LNT model has been challenged by various scientists who suggest that it does not accurately represent biological effects especially at low doses [77,78]. Both RIBE and HRS oppose this model with various findings reported at low doses.

### 2.4.2 Multi-Target Model

The multi-target model was an early model used to predict the cell killing. The multi-target model describes dose response relationships with the following mathematical equation and constant parameters.

$$S(D) = 1 - \left(1 - e^{-\frac{D}{D_0}}\right)^n \tag{2.1}$$

| | | |
|---|---|---|
| Where: | S | Survival Fraction |
| | D | Dose |
| | $D_0$ | Reciprocal of the final slope |
| | $D_1$ | Reciprocal of the initial slope |
| | $D_q$ | Quasi-threshold dose |
| | $n$ | Extrapolation number |

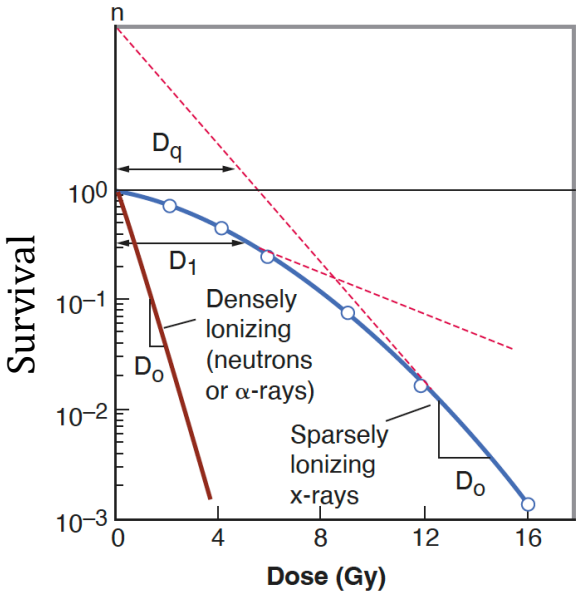


**Figure 2.4:** An example of the multi-target model on a log-linear plot with reference to curve fitting parameters. Graph from Radiobiology for the Radiobiologist [1].

The reciprocal of the final slope, $D_0$, also represents the dose required to reduce survival fraction to 37% for the linear portion. The parameter $D_0$ can be proven as the reciprocal of the final slope by differentiating the survival fraction in log-linear space and taking the limit as the dose becomes infinite.

The following converts Equation 2.1 into log-linear space:

$$\ln(S) = \ln\left(1 - \left(1 - e^{-\frac{D}{D_0}}\right)^n\right)$$

Then differentiating both sides of the equation to get the slope of the line with respect to the dose.

$$\frac{\partial}{\partial D}\ln(S) = \frac{1}{1 - \left(1 - e^{-\frac{D}{D_0}}\right)^n} * \frac{-n}{D_0}\left(\frac{\left(1 - e^{-\frac{D}{D_0}}\right)^n}{\left(e^{\frac{D}{D_0}} - 1\right)}\right)$$

Finally, taking the limit where the dose becomes large, we find the final slope the model reaches.

$$\lim_{D\to\infty}\frac{\partial}{\partial D}\ln(S) = -\frac{n}{D_0}\frac{1}{\left(1 - \left(1 - e^{-\frac{D}{D_0}}\right)^n\right)\left(e^{\frac{D}{D_0}}\right)} = -\frac{1}{D_0}$$

Therefore, the final slope, $-1/D_0$, is evident and it is seen that the parameter $D_0$ is the reciprocal of the final slope.

The extrapolation number, $n$, gives the width of the shoulder of the curve which determines the radioresistance at lower doses. Meaning a higher $n$ value will have less cell killing at low doses. There is another parameter related to the extrapolation number called the quasi-threshold dose, $D_q$, which is where the extrapolated backward linear portion intersects with the x-axis at the survival fraction of 1. This threshold is the dose that backward extrapolation would produce no effect on cell killing although this is not actually true. The three parameters are related by the following equation:

$$\ln(n) = \frac{D_q}{D_0}$$

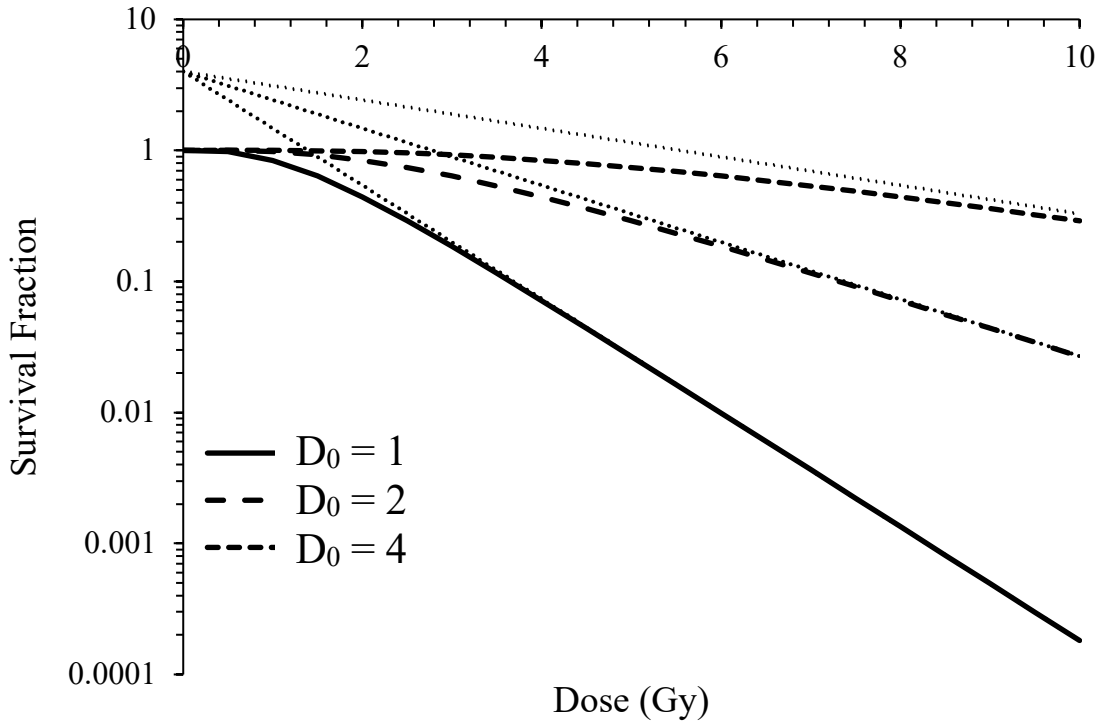


**Figure 2.5:** The effect of changing $D_0$ in the multi-target model with a constant $n$ value of 4. This shows how the final slope, $D_0$, changes but all lines backwards extrapolate to the same $n$ value on the y-axis. The small, dotted lines represent the backwards extrapolation of each line in the legend from infinity.

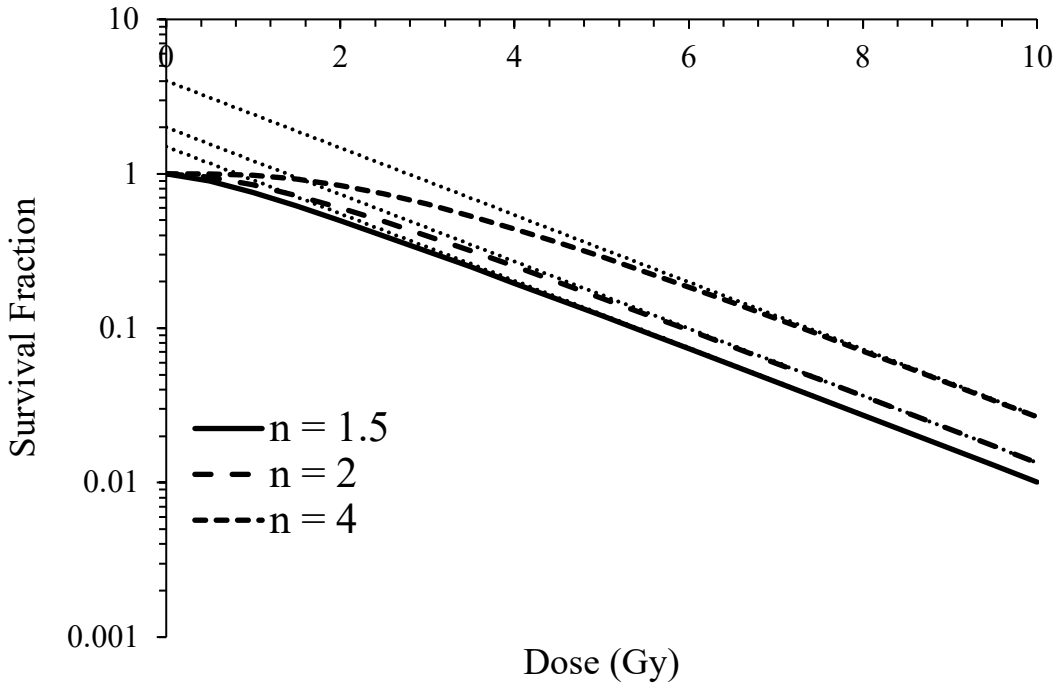


**Figure 2.6:** The effect of changing *n* in the multi-target model with a constant $D_0$ value of 2. This shows that all curves reach the final slope but extrapolate to a different *n* value (small, dotted lines). Lines with larger *n* values evidently have a wider shoulder.

The above graphs, Figure 2.5 and 2.6, show the effect of each parameter. The multi-target model is sufficient at modelling high doses and attempts to address changes in low doses but not all low dose effects are captured. As shown in the math in this section, there are no terms to describe low dose effects such as HRS and IRR.

### 2.4.3 Linear-Quadratic Model

The linear-quadratic model is currently used for various clinical and radiation protection purposes and therefore was revisited in this thesis. It attempts to address early radiobiological findings that a majority of chromosome aberrations are a result of two separate ionizing breaks in DNA. The linear-quadratic model describes dose response relationships with the following mathematical equation and constant parameters.

$$S(D) = e^{-\alpha D - \beta D^2} \tag{2.2}$$

| | | |
|---|---|---|
| Where: | S | Survival Fraction |
| | D | Dose |
| | $\alpha$ | Coefficient for cell killing proportional to dose |
| | $\beta$ | Coefficient for cell killing proportional to square of dose |

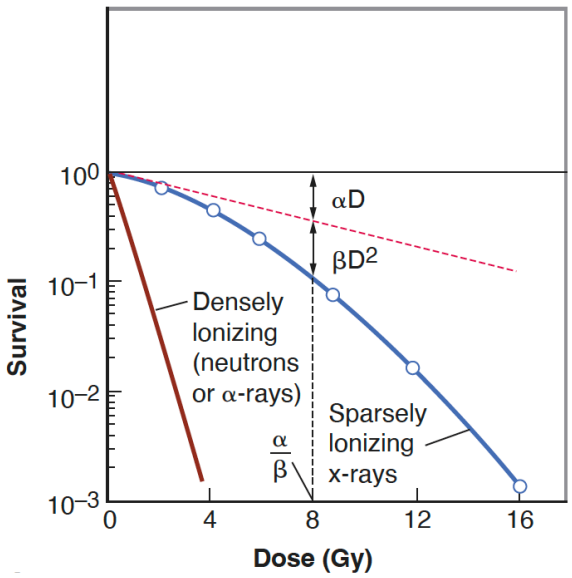


**Figure 2.7:** An example of the linear-quadratic model on a log-linear plot with reference to curve fitting parameters. Graph from Radiobiology for the Radiobiologist [1].

The cell killing from the proportional $\alpha$ term and squared proportional $\beta$ term are equivalent when:

$$\alpha D = \beta D^2$$

Which rearranges to a dose of:

$$D = \frac{\alpha}{\beta}$$

This represents the dose when the majority of cell killing transitions from $\alpha$ to $\beta$ killing. The cell killing in high doses continuously bends with no final straight portion on a log-linear plot, unlike what is observed experimentally in some

experimental data. After seven or more decades of cell killing the model is not applicable.

A decade is defined as the dose required to kill 90% of the cell population. Which can be calculated from the linear portion of the survival fraction.

$$S(D) = e^{-\alpha D}$$

The $\alpha$ term is the slope in the log-linear space but if the reciprocal to the dose is used it defines the dose in which 63% of the cell population is killed. This is also one standard deviation of cell killing.

$$\alpha = \frac{1}{D_0}$$

The decade killing dose can be found by setting the survival fraction to 0.1 or 10% and solving for the resulting dose. The decade killing dose is proportional to the standard deviation of killing dose or the reciprocal of the slope of the line.

$$S(D) = 0.1 = e^{-\frac{D}{D_0}}$$

$$\ln(0.1) = -\frac{D}{D_0}$$

$$D = D_{10} = D_0 * 2.3$$

Again, it is worth noting that while this model is widely used in the field, it does not contain curve fitting parameters which help accurately describe low dose effects such as HRS to IRR. The Linear-Quadratic model is an adequate representation in doses in the first few decades of cell killing and its advantage is the simplicity of having only two parameters.

### 2.4.4 Induced-Repair Model

The induced repair model is an adaptation on the linear-quadratic model to improve its capability in the low dose region. The induced-repair model makes $\alpha$ a function of the dose to account for the hyperradiosensitivity in low doses followed by an induced-repair response. The general formula is given by:

$$S(D) = e^{-\alpha(D)*D-\beta D^2} \tag{2.3}$$

One of the proposed $\alpha$ functions by Lambin *et al.* is shown below [79].

$$\alpha(D) = \alpha r * \left(1 + \left(\frac{\alpha s}{\alpha r} - 1\right) e^{-\frac{D}{D_c}}\right) \tag{2.4}$$

| | | |
|---|---|---|
| Where: | S | Survival Fraction |
| | $D$ | Dose |
| | $\alpha r$ | Coefficient for cell killing proportional to dose at high doses |
| | $\alpha s$ | Slope at very low doses |
| | $\beta$ | Coefficient for cell killing proportional to square of dose |
| | $D_c$ | Dose Constant |

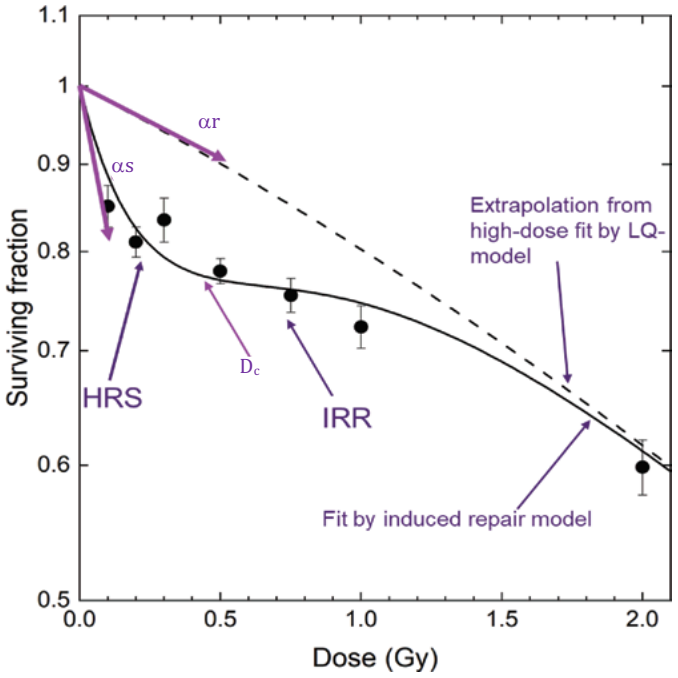


**Figure 2.8**: An example of the induced-repair model on a log-linear plot. The linear-quadratic model (LQ - dotted line) is also shown on this plot as a comparison to the improved induced-repair model (solid line). Graph from Radiobiology Textbook [2].

In this model, $\alpha r$ is cell killing proportional to the dose at high doses. It is like the $\alpha$ in the linear-quadratic model at higher doses. This can be seen when $D \gg D_c$,

the term for the $\alpha$ function simplifies to $\alpha r$. The other $\alpha$ constant, $\alpha s$, is the slope of the survival curve at 0 dose. This is seen by taking the derivative of the survival fraction in log-linear space and setting the dose to zero as seen below:

First, the full induced repair model is made by taking the general induced-repair model equation (2.3), with equation (2.4) substituted for the $\alpha$ component as described by Lambin *et al* [79].

$$\mathrm{S(D)} = e^{-\alpha_r * \left(1+\left(\frac{\alpha s}{\alpha r}-1\right)e^{-\frac{D}{D_c}}\right) * D - \beta D^2} \tag{2.5}$$

Setting equation 2.5 in log-linear space:

$$\ln\big(S(D)\big) = -\alpha r * \left(1 + \left(\frac{\alpha s}{\alpha r} - 1\right) e^{-\frac{D}{D_c}}\right) * D - \beta D^2$$

Take the derivative to find the slope of the curve in log-linear space:

$$\frac{\partial}{\partial D}\ln\big(S(D)\big) = -\alpha r * \left(1 + \left(\frac{\alpha s}{\alpha r} - 1\right) e^{-\frac{D}{D_c}}\right) + \left(\frac{-\alpha r}{D_c} e^{-\frac{D}{D_c}} + \frac{\alpha s}{D_c} e^{-\frac{D}{D_c}}\right) * D - 2\beta D$$

Finally, set dose=0 to find the initial slope $\alpha s$:

$$\frac{\partial}{\partial D}\ln\big(S(0)\big) = -\alpha r * \left(1 + \left(\frac{\alpha s}{\alpha r} - 1\right)\right) = -\alpha s$$

The dose constant, $D_c$, shows a characteristic dose used to describe the transition from HRS to IRR. The following math shows that $D_c$ is a local minimum value representing the dose at which HRS is at a maximum and a transition to IRR begins.

To find the local minimum, one can take the derivative of the induced repair model equation described directly above and set it to zero. A slope of zero is when the local minimum is reached. The local minimum is expected in the low dose region so the reader will notice the $\beta$ term is neglected in the following proof. It is evident that a chain rule must be used and the equation S'(D) can only equate to zero when $f'(D)$ equals zero.

$$\mathrm{S(D)} = e^{f(D)}$$

Using chain rule: $$\mathrm{S'(D)} = f'(D)e^{f(D)}$$

$$\mathrm{S'(D)} = 0 \quad when \quad f'(D) = 0$$

$$f'(D) = e^{-\frac{D}{D_c}}\left(\left(-\alpha r\left(1 - e^{\frac{D}{D_c}}\right) - \alpha s\right) + \left(\frac{-\alpha r}{D_c} + \frac{\alpha s}{D_c}\right) * D\right) = 0$$

There will only be a minimum point if $\alpha s \gg \alpha r$ so we can approximate when adding terms that $\alpha r = 0$,

$$(-\alpha s) + \left(\frac{\alpha s}{D_c}\right) * D = 0$$

$$D = D_c$$

Therefore, the dose constant also approximates the valley where HRS turns into IRR. However, effects from large beta values or when $\frac{\alpha s}{\alpha r}$ is small can influence the exact HRS/IRR transition point. Overall, the induced-repair model provides a meaningful dose-response relationship in the low dose range.

## 2.5 References


1 Hall EJ, Giaccia AJ. Radiobiology for the Radiologist. 7th ed. Lippincott Williams & Wilkins 2012.

2 Baatout S, Dostál M, Válek V. Radiobiology Textbook. 2023.

3 Kadhim M, Salomaa S, Wright E, et al. Non-targeted effects of ionising radiation—Implications for low dose risk. Mutation Research/Reviews in Mutation Research. 2013;752:84–98.

4 Mothersill C, Rusin A, Seymour C. Low doses and non-targeted effects in environmental radiation protection; where are we now and where should we go? Environmental Research. 2017;159:484–90.

5 Dickey JS, Zemp FJ, Martin OA, et al. The role of miRNA in the direct and indirect effects of ionizing radiation. Radiat Environ Biophys. 2011;50:491–9.

6 Mothersill C, Rusin A, Fernandez-Palomo C, et al. History of bystander effects research 1905-present; what is in a name? International Journal of Radiation Biology. 2018;94:696–707.

7 Mothersill C, Seymour C. Radiation-Induced Bystander Effects: Past History and Future Directions. Radiation Research. 2001;155:759–67.

8 Murphy JB, Norton JJ. The effect of x-ray on the resistance to cancer in mice. Science. 1915;42.

9 Olivieri G, Bodycote J, Wolff S. Adaptive Response of Human Lymphocytes to Low Concentrations of Radioactive Thymidine. Science. 1984;223:594–7.

10 Wolff S. The adaptive response in radiobiology: evolving insights and implications. Environmental Health Perspectives. 1998;106.

11 Calabrese EJ. The Maturing of Hormesis as a Credible Dose-Response Model. Nonlinearity in Biology, Toxicology, Medicine. 2003;1:154014203902499.

12 Calabrese EJ, Stanek EJ, Nascarella MA, et al. Hormesis Predicts Low-Dose Responses Better Than Threshold Models. Int J Toxicol. 2008;27:369–78.

13 Joiner MC, Denekamp J, Maughan RL. The Use of 'Top-up' Experiments to Investigate the Effect of Very Small Doses Per Fraction in Mouse Skin. International Journal of Radiation Biology and Related Studies in Physics, Chemistry and Medicine. 1985;49:565–80.

14 Marples B, Joiner MC. The Response of Chinese Hamster V79 Cells to Low Radiation Doses: Evidence of Enhanced Sensitivity of the Whole Cell Population. Radiation Research. 1993;133:41.

15 Wouters BG, Skarsgard LD. The Response of a Human Tumor Cell Line to Low Radiation Doses: Evidence of Enhanced Sensitivity. Radiation Research. 1994;138:S76.

16 Wouters BG, Sy AM, Skarsgard LD. Low-Dose Hypersensitivity and Increased Radioresistance in a Panel of Human Tumor Cell Lines with Different Radiosensitivity. Radiation Research. 1996;146:399.

17 Lambin P, Marples B, Fertil B, et al. Hypersensitivity of a Human Tumour Cell Line to Very Low Radiation Doses. International Journal of Radiation Biology. 1993;63:639–50.

18 Short, C. Mayes, M. Woodcock, H. Jo S. Low dose hypersensitivity in the T98G human glioblastoma cell line. International Journal of Radiation Biology. 1999;75:847–55.

19 Joiner MC, Johns H. Renal Damage in the Mouse: The Response to Very Small Doses per Fraction. Radiation Research. 1988;114:385.

20 Parkins CS, Fowler, J F. The linear quadratic fit for lung function after irradiation with X-rays at smaller doses per fraction than 2 Gy. Br J Cancer. 1986;53:320–3.

21 Joiner MC, Marples B, Lambin P, et al. Low-dose hypersensitivity: current status and possible mechanisms. International Journal of Radiation Oncology*Biology*Physics. 2001;49:379–89.

22 Dische S, Saunders MI. Continuous, hyperfractionated, accelerated radiotherapy (CHART): an interim report upon late morbidity. Radiotherapy and Oncology. 1989;16:65–72.

23 Saunders M, Dische S, Barrett A, et al. Continuous hyperfractionated accelerated radiotherapy (CHART) versus conventional radiotherapy in non-small-cell lung cancer: a randomised multicentre trial. The Lancet. 1997;350:161–5.

24 Skov K, Marples B, Matthews JB, et al. A Preliminary Investigation into the Extent of Increased Radioresistance or Hyper-Radiosensitivity in Cells of Hamster Cell Lines Known to Be Deficient in DNA Repair. Radiation Research. 1994;138:S126.

25 Mothersill C, Seymour CB, Joiner MC. Relationship between Radiation-Induced Low-Dose Hypersensitivity and the Bystander Effect. Radiation Research. 2002;157:526–32.

26 Ryan LA, Seymour CB, O'Neill-Mehlenbacher A, et al. Radiation-induced adaptive response in fish cell lines. Journal of Environmental Radioactivity. 2008;99:739–47.

27 Ryan LA, Seymour CB, Joiner MC, et al. Radiation-induced adaptive response is not seen in cell lines showing a bystander effect but is seen in lines showing HRS/IRR response. International Journal of Radiation Biology. 2009;85:87–95.

28 Cohen J, Vo NTK, Seymour CB, et al. Parallel comparison of pre-conditioning and post-conditioning effects in human cancers and keratinocytes upon acute gamma irradiation. International Journal of Radiation Biology. 2019;95:170–8.

29 Fernandez-Palomo C, Seymour C, Mothersill C. Inter-Relationship between Low-Dose Hyper-Radiosensitivity and Radiation-Induced Bystander Effects in the Human T98G Glioma and the Epithelial HaCaT Cell Line. Radiation Research. 2016;185:124–33.

30 Seymour CB, Mothersill C. Radiation-induced bystander effects — implications for cancer. Nat Rev Cancer. 2004;4:158–64.

31 Azzam EI, De Toledo SM, Little JB. Direct evidence for the participation of gap junction-mediated intercellular communication in the transmission of damage signals from α-particle irradiated to nonirradiated cells. Proc Natl Acad Sci USA. 2001;98:473–8.

32 Azzam EI, De Toledo SM, Gooding T, et al. Intercellular Communication Is Involved in the Bystander Regulation of Gene Expression in Human Cells Exposed to Very Low Fluences of Alpha Particles. Radiation Research. 1998;150:497.

33 Le M, Fernandez-Palomo C, McNeill FE, et al. Exosomes are released by bystander cells exposed to radiation-induced biophoton signals: Reconciling the mechanisms mediating the bystander effect. PLoS ONE. 2017;12:e0173685.

34 Ariyoshi K, Miura T, Kasai K, et al. Radiation-Induced Bystander Effect is Mediated by Mitochondrial DNA in Exosome-Like Vesicles. Sci Rep. 2019;9:9103.

35 Kumar Jella K, Rani S, O'Driscoll L, et al. Exosomes Are Involved in Mediating Radiation Induced Bystander Signaling in Human Keratinocyte Cells. Radiation Research. 2014;181:138–45.

36 Mothersill C, Seymour CB. Cell-Cell Contact during Gamma Irradiation Is Not Required to Induce a Bystander Effect in Normal Human Keratinocytes: Evidence for Release during Irradiation of a Signal Controlling Survival into the Medium. Radiation Research. 1998;149:256.

37 Le M, McNeill FE, Seymour CB, et al. Modulation of oxidative phosphorylation (OXPHOS) by radiation- induced biophotons. Environmental Research. 2018;163:80–7.

38 Le M, Mothersill CE, Seymour CB, et al. An Observed Effect of p53 Status on the Bystander Response to Radiation-Induced Cellular Photon Emission. Radiation Research. 2017;187:169.

39 Mothersill C, Smith R, Wang J, et al. Biological Entanglement–Like Effect After Communication of Fish Prior to X-Ray Exposure. Dose-Response. 2018;16:155932581775006.

40 Li X, Seymour CB, Mothersill C, et al. Investigation of presence and impact of radiation-induced bystander effect in Acheta domesticus. International Journal of Radiation Biology. 2023;1–12.

41 Parsons WB, Watkins CH, Pease GL, et al. Changes in sternal marrow following roentgen-ray therapy to the spleen in chronic granulocytic leukemia. Cancer. 1954;7:179–89.

42 Souto J. Tumour Development in the Rat induced by Blood of Irradiated Animals. Nature. 1962;195:1317–8.

43 Hollowell J, Littlefield L. Chromosome aberrations induced by plasma from irradiated patients. A brief report. J S C Med Assoc. 1967;63:437–42.

44 Hollowell JG, Littlefield LG. Chromosome Damage Induced by Plasma of X-Rayed Patients: An Indirect Effect of X-Ray. Experimental Biology and Medicine. 1968;129:240–4.

45 Littlefield LG, Hollowell JG, Pool WH. Chromosomal Aberrations Induced by Plasma from Irradiated Patients: An Indirect Effect of X Radiation: Further Observations and Studies of a Control Population. Radiology. 1969;93:879–86.

46 Goh K-O, Sumner H. Breaks in Normal Human Chromosomes: Are They Induced by a Transferable Substance in the Plasma of Persons Exposed to Total-Body Irradiation? Radiation Research. 1968;35:171.

47 Goyanes-Villaescusa V. Chromosomal abnormalities in lymphocytes of children and baby rabbits born from mothers treated by X-irradiation before pregnancy. A transplacentary plasmatic chromosome-Damaged factor? Blut. 1971;22:93–6.

48 Faguet GB, Reichard SM, Welter DA. Radiation-induced clastogenic plasma factors. Cancer Genetics and Cytogenetics. 1984;12:73–83.

49 Pant G, Kamada N. Chromosome aberrations in normal leukocytes induced by the plasma of exposed individuals. Hiroshima J Med Sci. 1977;26:149–54.

50 Nagasawa H, Little JB, Tsang NM, et al. Effect of Dose Rate on the Survival of Irradiated Human Skin Fibroblasts. Radiation Research. 1992;132:375.

51 Seymour CB, Mothersill C, Alper T. High Yields of Lethal Mutations in Somatic Mammalian Cells that Survive Ionizing Radiation. International Journal of Radiation Biology and Related Studies in Physics, Chemistry and Medicine. 1986;50:167–79.

52 Alper T, Mothersill C, Seymour CB. Lethal Mutations Attributable to Misrepair of Q-lesions. International Journal of Radiation Biology. 1988;54:525–30.

53 Born R, Trott KR. Clonogenicity of the Progeny of Surviving Cells after Irradiation. International Journal of Radiation Biology. 1988;53:319–30.

54 Pampfer S, Streffer C. Increased Chromosome Aberration Levels in Cells from Mouse Fetuses after Zygote X-irradiation. International Journal of Radiation Biology. 1989;55:85–92.

55 Chang WP, Little JB. Delayed Reproductive Death in X-irradiated Chinese Hamster Ovary Cells. International Journal of Radiation Biology. 1991;60:483–96.

56 Chang WP, Little JB. Evidence That DNA Double-Strand Breaks Initiate the Phenotype of Delayed Reproductive Death in Chinese Hamster Ovary Cells. Radiation Research. 1992;131:53.

57 Chang WP, Little JB. Persistently elevated frequency of spontaneous mutations in progeny of CHO clones surviving X-irradiation: association with delayed reproductive death phenotype. Mutation Research/Fundamental and Molecular Mechanisms of Mutagenesis. 1992;270:191–9.

58 Kadhim MA, Macdonald DA, Goodhead DT, et al. Transmission of chromosomal instability after plutonium a-particle irradiation. 1992;355.

59 Brown DC, Trott KR. Clonal Heterogeneity in the Progeny of HeLa Cells Which Survive X-irradiation. International Journal of Radiation Biology. 1994;66:151–5.

60 Seymour CMAC. Medium from irradiated human epithelial cells but not human fibroblasts reduces the clonogenic survival of unirradiated cells. International Journal of Radiation Biology. 1997;71:421–7.

61 Khan MA, Hill RP, Van Dyk J. Partial volume rat lung irradiation: An evaluation of early DNA damage. International Journal of Radiation Oncology*Biology*Physics. 1998;40:467–76.

62 Khan MA, Van Dyk J, Yeung IWT, et al. Partial volume rat lung irradiation; assessment of early DNA damage in different lung regions and effect of radical scavengers. Radiotherapy and Oncology. 2003;66:95–102.

63 Camphausen K, Moses M, Menard C, et al. Radiation Abscopal Antitumor Effect Is Mediated through p53. Cancer Research. 2003;63:1990–3.

64 Mancuso M, Pasquali E, Leonardi S, et al. Oncogenic bystander radiation effects in Patched heterozygous mouse cerebellum. Proc Natl Acad Sci USA. 2008;105:12445–50.

65 Fernandez-Palomo C, Schültke E, Bräuer-Krisch E, et al. Investigation of Abscopal and Bystander Effects in Immunocompromised Mice After Exposure to Pencilbeam and Microbeam Synchrotron Radiation. Health Physics. 2016;111:149–59.

66 Fernandez-Palomo C, Schültke E, Smith R, et al. Bystander effects in tumor-free and tumor-bearing rat brains following irradiation by synchrotron X-rays. International Journal of Radiation Biology. 2013;89:445–53.

67 Seymour CB, Mothersill C. Relative Contribution of Bystander and Targeted Cell Killing to the Low-Dose Region of the Radiation Dose–Response Curve. Radiation Research. 2000;153:508–11.

68 Lyng FM, Seymour CB, Mothersill C. Production of a signal by irradiated cells which leads to a response in unirradiated cells characteristic of initiation of apoptosis. Br J Cancer. 2000;83:1223–30.

69 Mothersill C. Individual variation in the production of a `bystander signal' following irradiation of primary cultures of normal human urothelium. Carcinogenesis. 2001;22:1465–71.

70 Le M, McNeill FE, Seymour C, et al. An Observed Effect of Ultraviolet Radiation Emitted from Beta-Irradiated HaCaT Cells upon Non-Beta-Irradiated Bystander Cells. Radiation Research. 2015;183:279.

71 Besplug J, Burke P, Ponton A, et al. Sex and tissue-specific differences in low-dose radiation-induced oncogenic signaling. International Journal of Radiation Biology. 2005;81:157–68.

72 Pogribny I, Raiche J, Slovack M, et al. Dose-dependence, sex- and tissue-specificity, and persistence of radiation-induced genomic DNA methylation changes. Biochemical and Biophysical Research Communications. 2004;320:1253–61.

73 Kovalchuk O, Burke P, Besplug J, et al. Methylation changes in muscle and liver tissues of male and female mice exposed to acute and chronic low-dose X-ray-irradiation. Mutation Research/Fundamental and Molecular Mechanisms of Mutagenesis. 2004;548:75–84.

74 Koturbash I, Kutanzi K, Hendrickson K, et al. Radiation-induced bystander effects in vivo are sex specific. Mutation Research/Fundamental and Molecular Mechanisms of Mutagenesis. 2008;642:28–36.

75 Gresham C. An investigation of various intrinsic and external factors that influence in vitro cell survival outcomes during radiation-induced bystander effect experiments. 2023. http://hdl.handle.net/11375/29000

76 Hooker AM, Bhat M, Day TK, et al. The Linear No-Threshold Model does not Hold for Low-Dose Ionizing Radiation. Radiation Research. 2004;162:447–52.

77 Cohen BL. The Linear No-Threshold Theory of Radiation Carcinogenesis Should Be Rejected. 2008;13.

78 Tubiana M, Feinendegen LE, Yang C, et al. The Linear No-Threshold Relationship Is Inconsistent with Radiation Biologic and Experimental Data. Radiology. 2009;251:13–22.

79 Lambin P, Fertil B, Malaise EP, et al. Multiphasic Survival Curves for Cells of Human Tumor Cell Lines: Induced Repair or Hypersensitive Subpopulation? Radiation Research. 1994;138:S32.

# Chapter 3 - Isolated Clones of a Human Colorectal Carcinoma Cell Line Display Variation in Radiosensitivity Following Gamma Irradiation

Desai, R.[1], Seymour, C.[1], Mothersill, C.[1]

[1]Department of Biology, McMaster University, Hamilton, ON, Canada

Accepted in Dose Response (2022).

# 3.0 Preface

The initial concept of the research presented in this chapter and methods were developed by Dr. Carmel Mothersill. Experimental work and the first draft of the paper were completed by the first author. This includes all irradiation, cell culture, experimentation, statistical analysis, and manuscript writing. All authors contributed to revision and editing of the manuscript following comments received during the peer-review process.

The following article is published by the journal of Dose-Response on September 10, 2022. The article is available online at:

https://journals.sagepub.com/doi/full/10.1177/15593258221113797

Citation: Desai R, Seymour C, Mothersill C. Isolated Clones of a Human Colorectal Carcinoma Cell Line Display Variation in Radiosensitivity Following Gamma Irradiation. Dose-Response. 2022;20(3). doi:10.1177/15593258221113797

## 3.1 Abstract

Objective: To determine whether the width of the shoulder and the size of the bystander effect are correlated using clonal lineages derived from a cultured cell line.

Methods: HCT 116 (p53 wildtype) cells were grown at cloning density and individual viable colonies were picked off and grown to establish a series of cell lines from both unirradiated and irradiated progenitors. These cell lines were then irradiated to generate full survival curves. Highly variant clones were then tested to determine the level of the bystander effect using a medium transfer protocol.

Results: The multi-target model gave the best fit in these experiments and size of the shoulder n is assessed in terms of radiosensitivity. The parent cell line has an n value of 1.1 while the most variant clones have n values of 0.88 (Clone G) and 5.5 (Clone A). Clonal lines subject to irradiation prior to isolation differed in bystander signal strength in comparison to clonal lines which were not initially irradiated (P = .055).

Conclusions: Based on these experiments we suggest there may be a link between shoulder size of a mammalian cell line and the strength of a bystander effect produced in vitro. This may have implications for radiotherapy related to out-of-field effects.

## 3.2 Introduction

The impacts of ionizing radiation (IR) on human cells are important for radiation protection, environmental risk assessment, and radiation therapy[1]. Recently, the effects of low dose IR have gained attention due both to the increasing use of IR in medical diagnostics, the use of novel protocols in radiotherapy such as FLASH and MRT, and the interest in small modular reactors as energy sources in remote environments[1,2]. High dose direct IR generally leads to significant cell death through processes such as reproductive death or apoptosis[3-5] while non-targeted and low dose radiation appears to involve other mechanisms[1,2,6,7]. Radiation-induced bystander effects (RIBE) are of particular interest since they involve cell killing, transformation and initiation of cell signaling pathways in cells that have not been directly exposed to IR but have received signals from directly exposed cells[2,8-14]. RIBE have been widely studied both in vivo and in vitro and they appear to be associated with low dose radiosensitivity[1,9,10,12,13,15-18] with some suggestion that they require wildtype p53 to be expressed[19]. This is relevant since many tumors have compromised p53 function[20-22], meaning that additional killing due to RIBE would predominantly affect normal cells around the tumor rather than the tumor itself. However, the research in this area is quite controversial with contradictory reports about RIBE even in laboratories using the same protocols and cells[23]. A possible explanation for this is “drift” within cultured cell lines leading to clonal heterogeneity in populations of genetically identical cells. To test whether this might be a factor, we

decided to revisit clonal heterogeneity with respect to clonal sensitivity. Through investigation of clonal populations we aim to approach in a more systematic way the often heterogenous nature of malignancies[24,25]. The literature often refers to clonal heterogeneity within a tumor as a "fuel for resistance" and studying this key challenge in optimizing individual therapies is necessary to advance cancer treatment[24,25]. Since radiotherapy can lead to second malignancies[26-28], some cell lines were derived from cultures of cells exposed to 1 Gy to determine whether there was greater variability in terms of radiosensitivity in these lines. With a better understanding of the heterogeneity of response in clonal sub-populations we may gain a new perspective which could improve radiation treatment[14].

# 3.3 Methods

## 3.3.1 Human Cell Cultures

The immortalized human epithelial HCT116 (p53 wildtype) cell line derived from a large intestine/colon carcinoma was used in this study. Clonal cell lines were isolated from this parent cell line. These cells were routinely cultured in Roswell Park Memorial Institute (RPMI) 1640 growth medium supplemented with 10% fetal bovine serum (FBS), 100 U/mL penicillin, 100 ug/mL streptomycin, and 2.05 mM L-Glutamine. This growth medium was also used in the bystander effect assays. Cells were grown in 75 cm2 Falcon tissue culture flasks at 37°C and 5% CO2. Subcultures

were conducted using 0.25% phenol red-free trypsin solution with 0.192 mM EDTA every 6-7 days. Trypsinized cells were neutralized using a greater volume of growth media. Cell cultures were 70–80% confluent upon culture. Cell concentrations were determined using Bio-Rad TC20 automated cell counter (Bio-Rad Life Science Research Divison, Canada). All reagents were purchased from Gibco, ThermoFisher Scientific.

### 3.3.2 Clonal Isolation

Petri dishes were seeded with 200–300 cells. These were allowed to form viable colonies of at least 50 cells. After 7 days, individual clones of various sizes were chosen for clonal expansion. These colonies were scraped off the dish and resuspended in small multiwall plates (Falcon, 6-Well Flat Bottom Tissue Culture Plate, VWR Canada). The clones were passaged into T25 flasks when confluent and grown to produce a sufficient supply of cells for the experiments. Some clones were isolated from plates where cells had been exposed to 1 Gy radiation after cells had adhered to the culture plate in order to examine the effect of this dose on subsequent clonal heterogeneity (Figure 3.1).

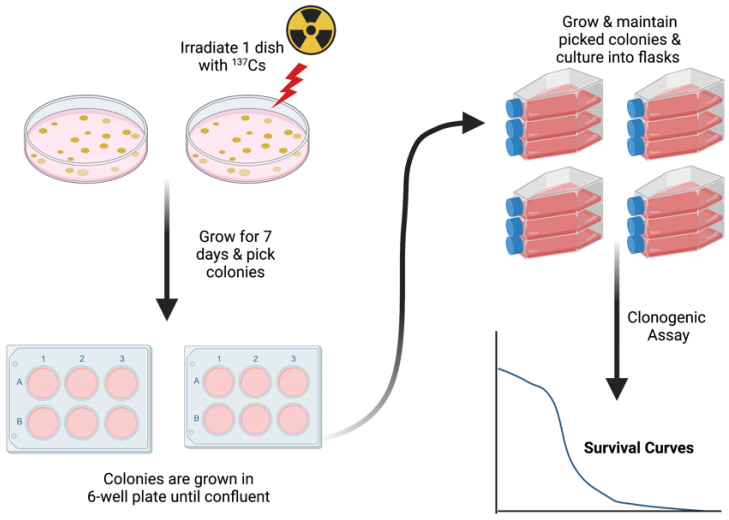


**Figure 3.1:** Diagram of clonal isolation methods.

### 3.3.3 Irradiation

All irradiations were performed using a Cesium-137 gamma-emitting source with a dose rate of 198.4 mGy/min and flasks were placed 30 cm away from the source (Taylor Radiobiology Source, McMaster University). Direct irradiations for survival curve data generation were conducted 15–20 hours post seeding. Irradiations to generate medium for bystander effect assays were also completed in this manner.

### 3.3.4 Clonogenic Survival Assay and Survival Curves

Flasks containing approximately 70% confluent cultures were used for clonogenic survival assays. Cells were removed from the flask using a Trypsin-EDTA working solution described above. Detached cells were neutralized with growth medium and mixed to form a single cell suspension. These cells were counted and plated to perform a clonogenic assay using the method described by Puck and Marcus[29]. Cell seeding densities were determined using the plating efficiencies (PE) determined for each clonal cell line. Clonogenic assays were conducted to develop full survival curves upon irradiation of cells at the following dose points: 0, 0.5, 1.0, 3.0, 5.0, 7.0, 10.0, and 15.0 Gy. This wide range in dose points provided an overall assessment at cell survival across doses. Flasks were irradiated at the appropriate dose and returned to the incubator immediately following irradiation and grown for nine days at 37°C in an atmosphere of 5% CO2 in air. On day nine, all flasks were stained with 15% Carbol Fuchsin solution (Ziehl Neelson, Millipore Sigma). Colonies were counted manually to determine the surviving fraction for each dose. The data were entered into GraphPad Prism 8 software (GraphPad Software Inc., LaJolla, CA), to generate survival curve graphs.

### 3.3.5 Bystander Effect Assay

Falcon tissue culture flasks (25 cm2 ) were seeded with cells in 5 mL growth media for the following treatments and incubated for 6 hours at 37°C and 5% CO2: plating efficiency, direct irradiation (2.0 Gy), bystander effect donor and recipient, and sham donor and recipient (Figure 3.2). Sham donor flasks were not irradiated but a medium transfer was completed from sham donor flasks to sham recipient flasks to ensure there was not an effect of medium change. All donor flasks were seeded with 100 000 cells while all other flasks were seeded with 200 cells. After 6 hours, the direct irradiation and bystander effect donor flasks were irradiated with the Cesium-137 source at 2 Gy. Following irradiation, flasks were immediately returned to the incubator for 1 hour. After 1 hour of incubation, medium transfer of donor flasks was completed. The medium from donor flasks was filtered using a 0.22-μm filter and 30 mL plastic syringe (Millipore Sigma) to ensure no cells were present in the irradiated cell culture medium (ICCM). Approximately ~15 mL media was collected from triplicate donor flasks. Growth medium from the recipient flasks was then poured off as waste and the previously filtered ICCM was added to the recipient flasks. This method of medium transfer was used for both the bystander effect and sham treatment flasks. All flasks were grown for 9 days and then stained with 15% Carbol Fuschin and counted manually.

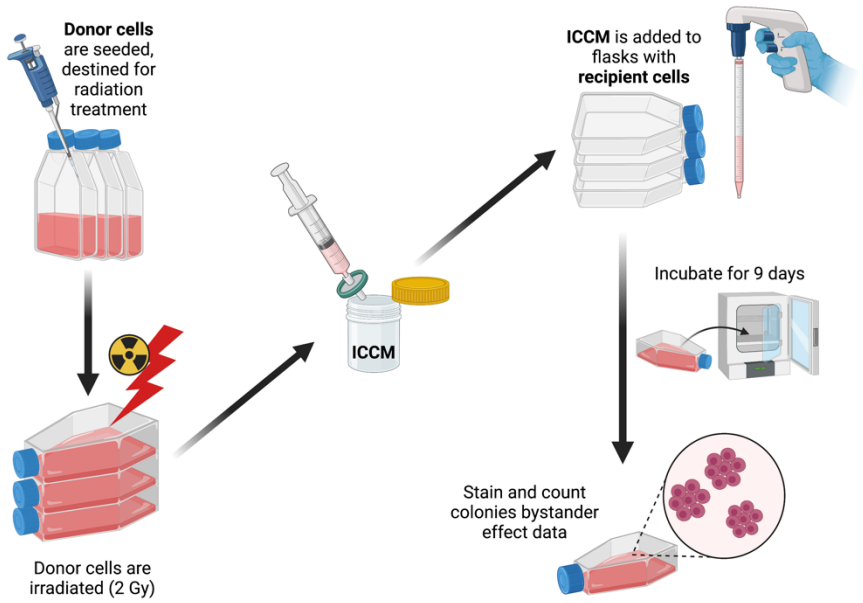


**Figure 3.2:** Bystander effect assay methods.

### 3.3.6 Statistical Analysis

For all survival curves, data are presented as a mean of three replicates in three independent trials (n=9). Least square error linear regression analyses were performed on data to produce the multi-target and linear-quadratic models using GraphPad Prism 8. Data for bystander effect assays were also collected as mean of three replicates in three independent trials. Standard error of the mean error bars are used in all figures. To determine variance between groups in bystander effect experiments, t-tests were conducted between the sham and bystander groups and the sham and direct irradiation groups for each cell line. These post hoc analyses

were performed using Welch's t-test. Significance was determined at the 95% confidence level.

## 3.4 Results

### 3.4.1 Survival Curves

Figure 3.3 displays the parent HCT116 p53+/+ line alongside all clonal cell lines derived from either an irradiated or nonirradiated population prior to clone isolation. Data were not fitted to any established model for this figure. Clonogenic survival over a dose range of 0–15 Gy after direct exposure to a cesium-137 gamma source shows variation between each clonal line. Plating efficiency variations were also observed between clonal lines and are presented in Table 1. The linear-quadratic and multi-target models were both fitted to all survival curve data. Using the linear-quadratic model, parameters alpha and beta were noted to demonstrate variation in radiosensitivity (Table 3.1). Here, we see unexpected negative values for alpha of clone A and beta for clone G (Table 3.1A). Alpha and beta values indicate cell killing proportional to the dose and cell killing proportional to the square of the dose, respectively. Negative values for such parameters have no physical meaning and suggest the fitted equation is inadequate to describe the present data. Using the multi-target model, parameters $n$ and $D_0$ are observed where n is a common indicator for

low dose radiosensitivity or the size of the cell survival curve shoulder. In comparison to the parent cell line, Clone A had the largest n value of 5.5 while Clone G had the smallest n value of 0.88 (Table 3.1A). A prominent shoulder for Clone A can be seen in Figure 4A and C. Both clone A and clone G were derived from unirradiated progenitor cells. It is apparent that curve fitting parameters obtained through either model show variation in radiosensitivity indicating the presence of heterogeneity in the initial cell HCT116 p53+/+ cell population. These curve fitting models highlight differences in cell survival response to consistent radiation doses; however, the multi-target model provided an overall better fit to data presented in this study.

**Table 3.1:** Summary of survival curve parameters obtained through survival curve fitting with the linear-quadratic and multi-target models for radiation induced cell killing. Values *n* and $D_0$ determined using the multi-target model. Alpha and beta values determined using the linear-quadratic model.

**Table 3.1A:** Cell lines derived from a control HCT 116 $p53^{+/+}$ population.

| Parameter | Parent Line | CI (95%) | Clone A | CI (95%) | Clone F | CI (95%) | Clone G | CI (95%) |
|---|---|---|---|---|---|---|---|---|
| **Multi-Target** | | | | | | | | |
| *n* | 1.119 | 0.92 – 1.4 | 5.525 | 3.1 - 30 | 1.462 | 1.3 – 1.7 | 0.8770 | 0.82 – 0.93 |
| $D_0$ | 1.834 | 1.5 - 2.2 | 1.092 | 0.68 - 1.4 | 1.754 | 1.6 – 2.0 | 1.836 | 1.7 – 2.0 |
| $r^2$ | 0.96 | | 0.95 | | 0.98 | | 1.00 | |
| **Linear-Quadratic** | | | | | | | | |
| $\alpha$ | 0.4436 | 0.36 – 0.53 | -0.05818 | -0.16 – 0.042 | 0.2843 | 0.23 – 0.34 | 0.6424 | 0.61 – 0.67 |
| $\beta$ | 0.02148 | -0.0056 - 0.057 | 0.1467 | 0.10 – 0.20 | 0.05235 | 0.033 – 0.074 | -0.01319 | -0.021 – 0.0030 |
| $r^2$ | 0.97 | | 0.95 | | 0.98 | | 1.00 | |
| **Plating Efficiency (%)** | 33.87 | | 32.16 | | 28.94 | | 25.78 | |

**Table 3.1B:** Cell lines derived from a previously 1Gy irradiated HCT 116 $p53^{+/+}$ population.

| Parameter | Clone B | CI (95%) | Clone C | CI (95%) | Clone D | CI (95%) | Clone E | CI (95%) |
|---|---|---|---|---|---|---|---|---|
| **Multi-Target** | | | | | | | | |
| *n* | 1.338 | 1.1 – 1.6 | 1.375 | 1.0 – 1.8 | 1.411 | 1.2 – 1.7 | 1.082 | 0.96 – 1.2 |
| $D_0$ | 1.670 | 1.4 – 2.0 | 1.837 | 1.5 – 2.3 | 1.350 | 1.2 – 1.6 | 2.341 | 2.1 – 2.6 |
| $r^2$ | 0.97 | | 0.94 | | 0.98 | | 0.98 | |
| **Linear-Quadratic** | | | | | | | | |
| $\alpha$ | 0.3756 | 0.29 – 0.45 | 0.2847 | 0.19 – 0.38 | 0.4006 | 0.33 – 0.47 | 0.3441 | 0.30 – 0.39 |
| $\beta$ | 0.04009 | 0.010 – 0.078 | 0.05284 | 0.018 – 0.096 | 0.08510 | 0.047 – 0.13 | 0.01764 | 0.0060 – 0.031 |
| $r^2$ | 0.97 | | 0.95 | | 0.98 | | 0.98 | |
| **Plating Efficiency (%)** | 33.87 | | 33.47 | | 24.44 | | 2747 | |

***Note:***

| | |
|---|---|
| $D_0$ | multiple event cell killing |
| *n* | size of curve shoulder |
| $\alpha$ | cell killing proportional to dose |
| $\beta$ | cell killing proportional to square of the dose |
| CI (95%) | confidence interval |

### 3.4.2 Bystander Effects

Bystander effect assays were conducted to investigate differences in bystander signal strength in the clonal cell lines. Figure 3.5 displays a response in each clonal line following a bystander medium transfer treatment. In each bystander assay donor and reporter cells are of the same clonal line so that irradiated cell culture medium (ICCM) is filtered from donor cells of a clonal line and added to reporter cells of the same clonal line. Direct groups in Figure 3.5 for all parent and clonal lines were exposed to 2 Gy direct gamma irradiation and subsequently, an expected significant decrease in cell survival compared to the sham group is observed. Of all clonal lines presented, clones A, F and D did not display a significant decrease in cell survival following addition of ICCM indicating there was no or a weak bystander signal. Figure 3.5 A and B display the cell surviving fraction of the parent and clone A, however, clone A exposed to direct ionizing radiation shows less cell death (71% surviving faction) compared to that of the parent population (57% surviving fraction). Most clonal lines derived from a non-irradiated parent line showed significantly stronger bystander signals ($P < .0001$). Clonal lines subject to irradiation prior to isolation significantly differed in bystander signal strength in comparison to clonal lines which were not initially irradiated ($P = .055$). A correlation between n value and bystander signal strength was also observed irrespective of whether the clone was derived from irradiated or non-irradiated parent populations (Figure 3.6). Figure 3.6 displays the

relationship between *n* value and surviving fraction following bystander treatment where clone A is omitted due to the unusually high shoulder size.

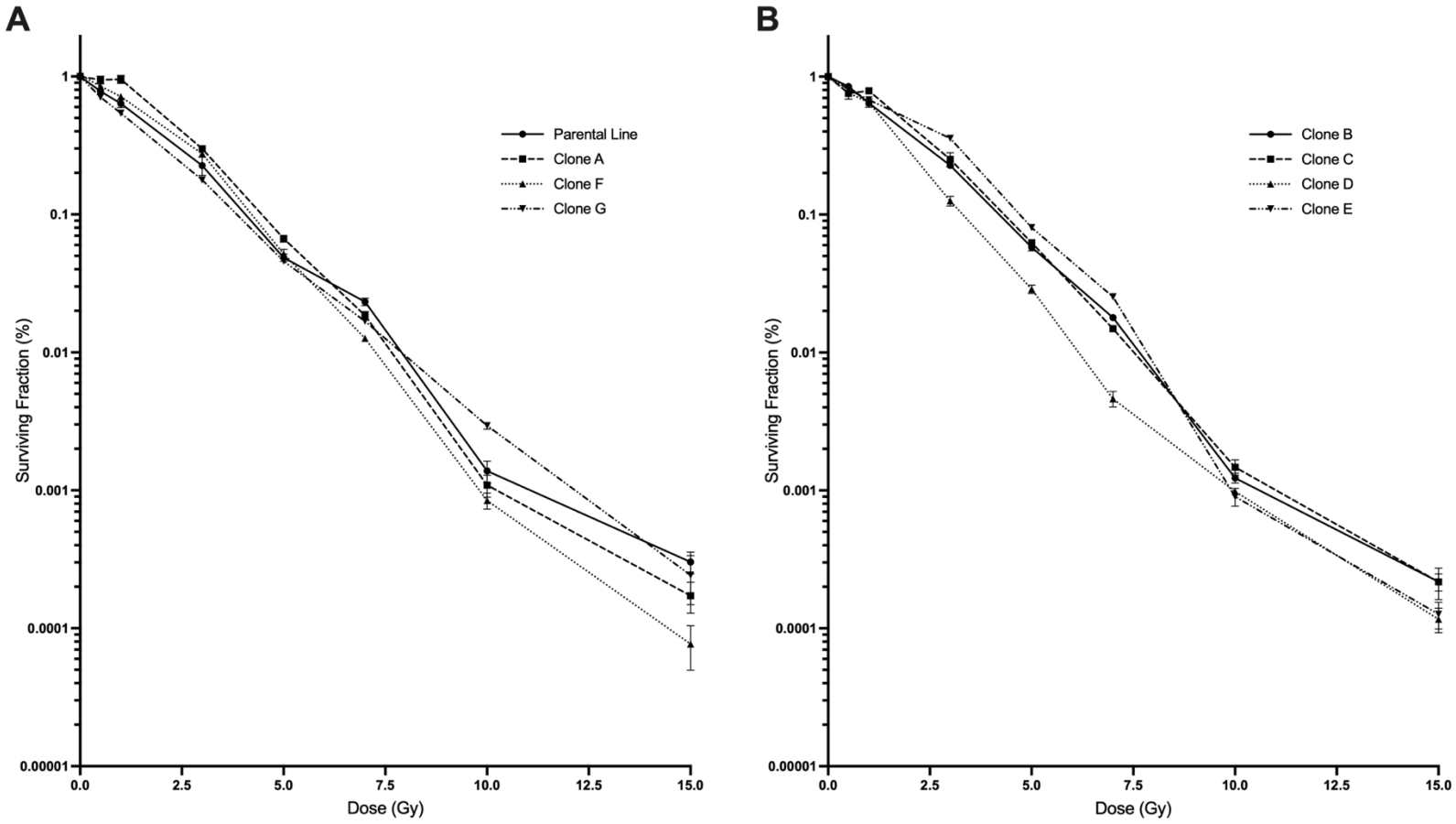


**Figure 3.3:** Survival curves of parental line, non-irradiated and irradiated progeny cell lines. (A) Parental and non- irradiated cell lines (parental, clone A, clone F, and clone G). (B) Irradiated clones (clones B, C, D, and E). Error bars are SEM for n = 9.

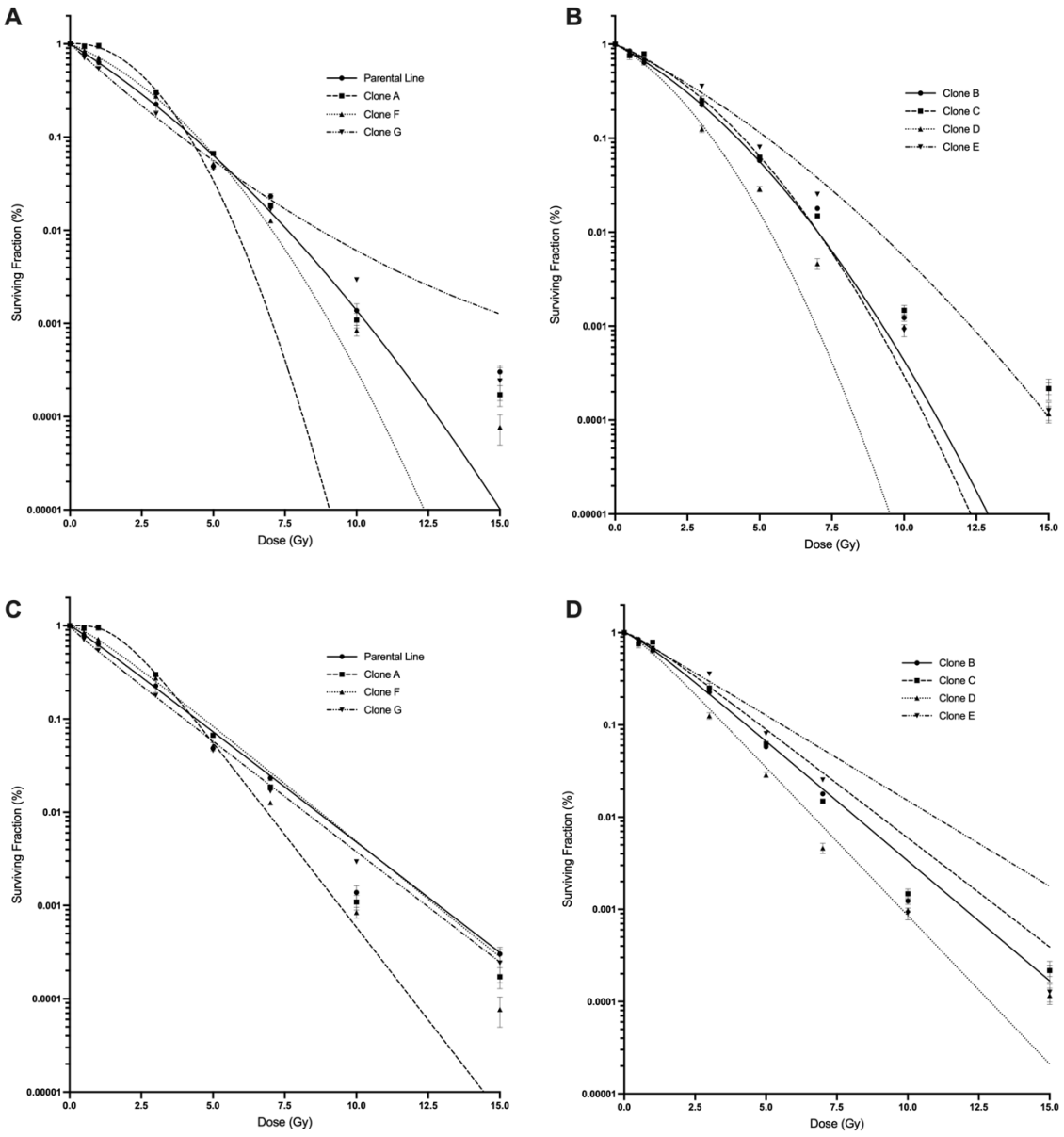


**Figure 3.4:** Survival curves of parental line, non-irradiated and irradiated progeny cell lines fit with either the multi- target or linear-quadratic model. The parental line and clones A, F, and G are derived from an initial population not exposed to radiation. Clones B, C, D, and E were initially treated with 1.0 Gy prior to clone isolation. (A) Parental line and clones A, F, and G fitted with the linear-quadratic model. (B) Clones B, C, D, and E fitted with the linear-quadratic model. (C) Parental line and clones A, F, and G fitted with the multitarget model. (D) Clones B, C, D, and E fitted with the multi-target model.

## 3.5 Discussion

Initial findings regarding sublethal damage and defective colonies sparked interest in the idea that cells exposed to x-ray radiation have the potential to form colonies of various sizes[29,30]. The data presented in this study demonstrate variability that arises in a given population of cells and how radiosensitivities differ across clonal populations. The results show that clonal populations of the same initial culture exhibit variation in radiosensitivity when subject to the same dose. When modeled with the multi-target model, a prominent shoulder region can be observed in clone A suggesting a heightened radioresistant nature compared to the parent population from which it was derived. This prominent shoulder was characteristic of a large *n* value not observed in other clonal populations derived from the same non-irradiated parent population. Most other clonal populations have a relatively smaller *n* value and overall suggest a more radiosensitive nature compared to the previously mentioned clone A. Both the multi-target and linear-quadratic models were fitted to the data because they are mathematical expressions, which have shown to be good fits to most in vitro data. However, as can be seen here, using parameters from the fittings to compare the shoulder size, especially between the two models, is misleading as the fits are very poor. Therefore, they cannot be used to derive biological mechanistic explanations. However, it is useful to present the results of these fits if only to discount them. Besides, there are several interpretations of the LQ-model apart from Chadwick and Leenhouts derivation with double strand breaks,[31,32] for example, the

ATM-shuttling hypothesis developed by Foray and his group[33,34] which proposes that delay in ATM-shuttling following radiation exposure causes radiosensitivity.

When all clonal populations were tested for the presence of bystander signals following the bystander medium transfer assay, it was demonstrated that most clonal populations regardless of their origin from a non-irradiated or irradiated population, displayed a significant reduction in cell survival following receipt of ICCM (Figure 3.4). However, clone A with the largest, and highly unusual, *n* value did not produce bystander signals suggesting a decreasing bystander signal strength with large shoulder size (Figure 3.4B). Unfortunately, the rest of the clones had n values quite close together, but a correlation plot (Figure 3.5) does suggest a trend for bystander induced survival reduction to correlate with the n value ($r^2 = 0.44$). There is a trend for n value to correlate with bystander induced reduction in survival however other additional factors could be involved. Also, while to our knowledge no previous experiments were set up to examine this relationship, there is anecdotal evidence in the literature that shoulder size and bystander signal strength are related inversely. The paper by Mothersill *et al.* (2002) examined parent cell lines and radiosensitive lines with various DNA repair defects derived from these parents.[35] Irrespective of the nature of the repair defect, all radiosensitive lines were more radiosensitive than their parent line. Also many radioresistant cell lines such as PC3 do not show bystander associated cell death while radiosensitive lines such as SW48 do show strong bystander effects.[35]

In certain clonal populations, bystander signals were not produced even though they were radiosensitive. Consistent with previous findings this could suggest the presence of a low dose hyperradiosensitivity with increased radioresistance as the dose increased (HRS/IRR) mechanism. In instances of hyperradiosensitivity a generally greater than expected response to radiation is observed. However, various studies have shown that certain cell lines only respond to bystander signals in the lower dose region where HRS is seen.[16,15]

Apart from the findings in relation to RIBE, the data in this paper suggest that the mathematical expressions based on classical target theory predictions do not provide good fits to these results. This is important to note because many of the classical experiments were done using a few cell lines such as CHO or V79 cells. These have high plating efficiencies of the order of 80-90% but limited expression of tissue of origin characteristics. Most modern radiobiology is done using lines which express important parameters related to epithelial cell or tumor function, but which have plating efficiencies below 50%. High plating efficiencies are necessary to derive meaningful target theory based conclusions. This is because of the statistical probability that radiation is the cause of a cell not forming a colony if the PE is high. With a low plating efficiency, the cause of not forming a colony need not be the radiation effect. Nowadays the focus is on molecular effects so that plating efficiency is not such an issue.

In conclusion, the data presented show marked clonal heterogeneity in cell lines derived from both irradiated and unirradiated progenitors. This manifests as differences in doubling time, plating efficiency and radiosensitivity. The data also reveal a weak correlation between shoulder size (a surrogate for low dose radioresistance) and the ability of ICCM to reduce the plating efficiency of unirradiated cells. The data also suggest that the commonly used mathematical expressions traditionally used to fit survival curve data provide poor fits to the data in this paper, possibly due to the low plating efficiency of the cell lines. In conclusion, the results may have implications for tumor radiotherapy where clonal heterogeneity is an important limitation for treatment.

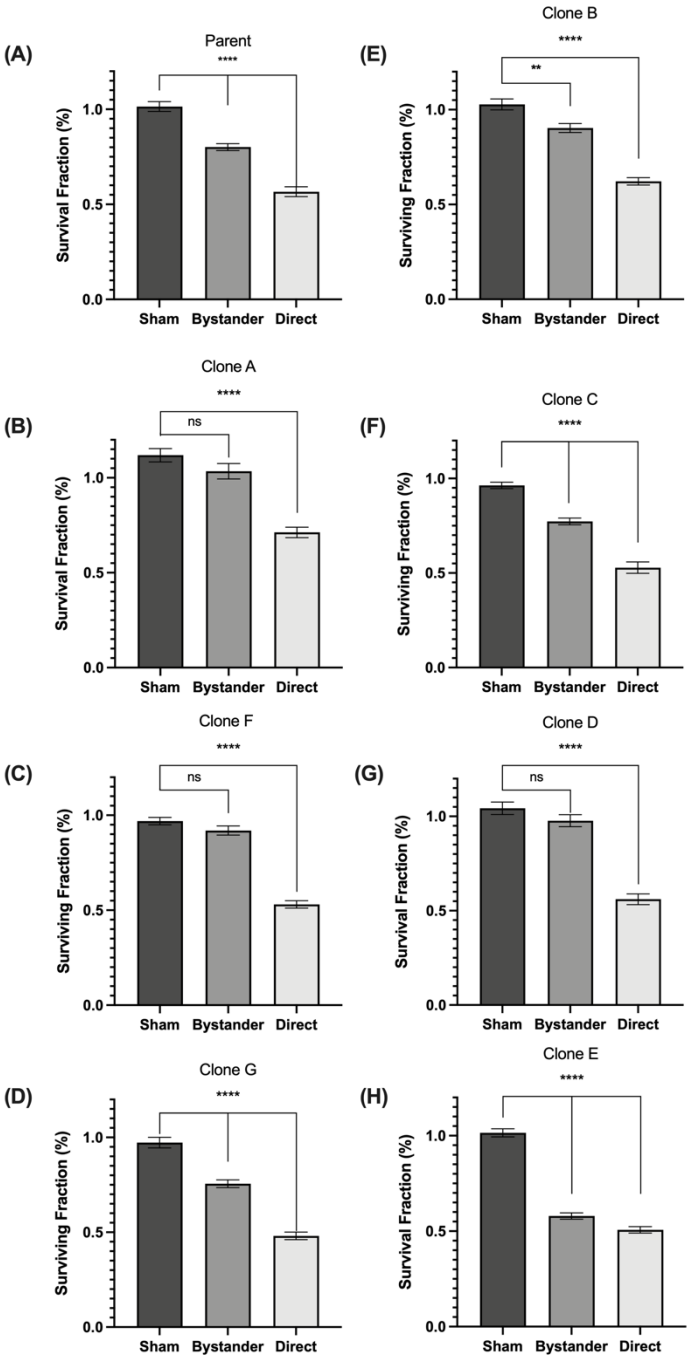


**Figure 3.5:** Recipient cells exposed to culture medium from irradiated cells. Sham represents cells exposed to cell culture control medium. Bystander represents cells exposed to irradiated cell culture medium collected from donor cells irradiated with 2.0 Gy. Direct represents cells irradiated directly with 2.0 Gy. (A-D) Bystander effect assay conducted on parent cell line and isolated clones not subject to irradiation prior to isolation. (E–H) Bystander effect assay conduced on isolated clones subject to irradiation prior to isolation. In all bystander effect assays, both recipient and donor cells are of the same parent or clonal line. All data is presented as the mean ± SEM (n = 9). (****P < .0001), (**P < .005) indicates a significant difference between treatment groups and sham.

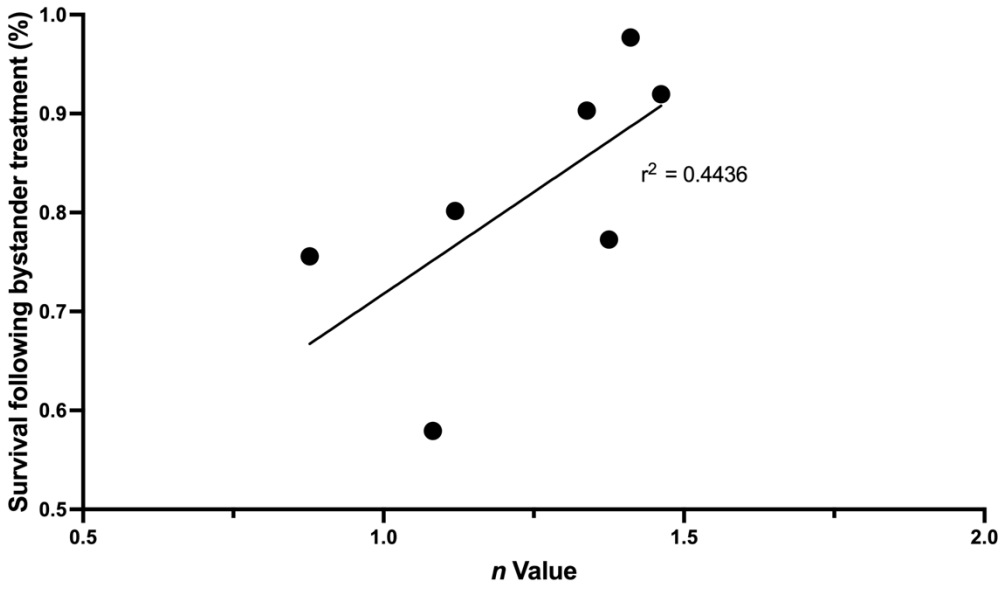


**Figure 3.6:** Correlation plot between n value or size of survival curve shoulder and percent cell survival following radiation-induced bystander treatment. Irradiation of 2 Gy is applied to donor cells before irradiated cell culture medium is collected and transferred to recipient cells. Data presented here include n values and bystander surviving fraction for the parent HCT116 p53+/+ line and clones B through G. Correlation gives an r2 value of 0.44.

## 3.6 Acknowledgements

Figures 1 and 2 created with biorender.com.

## 3.7 Declaration of Conflicting Interests

The author(s) declared no potential conflicts of interest with respect to the research, authorship, and/or publication of this article.

## 3.8 Funding

The author(s) disclosed receipt of the following financial support for the research, authorship, and/or publication of this article: This work was supported by the Canada Research Chairs 950-221284.

## 3.9 References


1. Mothersill C, Rusin A, Seymour C. Low doses and non-targeted effects in environmental radiation protection; where are we now and where should we go? Environ Res. 2017;159:484-490. doi: 10.1016/j.envres.2017.08.029.
2. Seymour CB, Mothersill C. Radiation-induced bystander effects — implications for cancer. Nat Rev Cancer. 2004;4(2):158-164. doi:10.1038/nrc1277.
3. Evans HH, DeMarini DM. Ionizing radiation-induced mutagenesis: radiation studies in Neurospora predictive for results in mammalian cells. Mutation Research/Reviews in Mutation Research. 1999;437(2):135-150. doi:10.1016/S1383-5742(99) 00080-0.
4. Moller A, Mousseau T. Biological consequences of Chernobyl: 20 years on. Trends Ecol Evol. 2006;21(4):200-207. doi:10.1016/j.tree.2006.01.008.
5. Hall EJ, Giaccia AJ. Radiobiology for the Radiologist. 7th ed.. Philadelphia, PA: Lippincott Williams & Wilkins; 2012.
6. Belyakov O V, Folkard M, Mothersill C, Prise MK, Michael B D. Bystander-induced apoptosis and premature differentiation in primary urothelial explants after charged particle microbeam irradiation. Radiat Protect Dosim. 2002;99(1):249-251. doi:10. 1093/oxfordjournals.rpd.a006775.
7. Hei TK, Zhou H, Ivanov VN, et al. Mechanism of radiationinduced bystander effects: A unifying model. J Pharm Pharmacol. 2010;60(8):943-950. doi:10.1211/jpp.60.8.0001.

8. Nagasawa H, Little JB, Tsang NM, et al. Effect of dose rate on the survival of irradiated human skin fibroblasts. Radiat Res. 1992;132(3):375. doi:10.2307/3578247.
9. Mothersill C, Seymour CB. Cell-cell contact during gamma irradiation is not required to induce a bystander effect in normal human keratinocytes: Evidence for release during irradiation of a signal controlling survival into the medium. Radiat Res. 1998; 149(3):256. doi:10.2307/3579958.
10. Prise KM. Studies of bystander effects in human fibroblasts using a charged particle microbeam. Int J Radiat Biol. 1998; 74(6):793-798. doi:10.1080/095530098141087.
11. Zhou H, Randers-Pehrson G, Waldren CA, et al. Induction of a bystander mutagenic effect of alpha particles in mammalian cells. Proc Natl Acad Sci USA. 2000;97(5):2099-2104. doi:10. 1073/pnas.030420797.
12. Prise KM, Folkard M, Michael BD. Bystander responses induced by low LET radiation. Oncogene. 2003;22(45): 7043-7049. doi:10.1038/sj.onc.1206991.
13. Azzam EI, Little JB. The radiation-induced bystander effect: Evidence and significance. Hum Exp Toxicol. 2004;23(2):61-65. doi:10.1191/0960327104ht418oa.
14. Heeran AB, Berrigan HP, O'Sullivan J. The RadiationInduced Bystander Effect (RIBE) and its Connections with the Hallmarks of Cancer. Radiat Res. 2019;192(6):668. doi:10.1667/RR15489.1.

15. Dai X, Tao D, Wu H, Cheng J. Low dose hyper-radiosensitivity in human lung cancer cell line A549 and its possible mechanisms. J Huazhong Univ Sci Technol - Med Sci. 2009;29(1): 101-106. doi:10.1007/s11596-009-0122-4.
16. Fernandez-Palomo C, Seymour C, Mothersill C. InterRelationship between Low-Dose Hyper-Radiosensitivity and Radiation-Induced Bystander Effects in the Human T98G Glioma and the Epithelial HaCaT Cell Line. Radiat Res. 2016; 185(2):124-133. doi:10.1667/RR14208.1.
17. Le M, Fernandez-Palomo C, McNeill FE, Seymour CB, Rainbow AJ, Mothersill CE. Exosomes are released by bystander cells exposed to radiation-induced biophoton signals: Reconciling the mechanisms mediating the bystander effect. In: Woloschak GE, ed., PLoS One. 2017;12(3):e0173685. doi:10. 1371/journal.pone.0173685.
18. Le M, McNeill FE, Seymour CB, et al. Modulation of oxidative phosphorylation (OXPHOS) by radiation- induced biophotons. Environ Res. 2018;163:80-87. doi:10.1016/j.envres.2018.01.027.
19. Mothersill C, Bristow RG, Harding SM, et al. A role for p53 in the response of bystander cells to receipt of medium borne signals from irradiated cells. Int J Radiat Biol. 2011;87(11): 1120-1125. doi:10.3109/09553002.2011.610866.
20. Shao J, Lu J, Zhu W, et al. Derepression of LOXL4 inhibits liver cancer growth by reactivating compromised p53. Cell Death Differ. 2019;26(11):2237-2252. doi:10.1038/s41418- 019-0293-x.

21. Bourdon JC. p53 and its isoforms in cancer. Br J Cancer. 2007; 97(3):277-282. doi:10.1038/sj.bjc.6603886.
22. Warburton HE, Brady M, Vlatkovic N, et al. p53 Regulation and ´ Function in Renal Cell Carcinoma. Cancer Res. 2005;65(15): 6498-6503. doi:10.1158/0008-5472.CAN-05-0017.
23. Groesser T, Cooper B, Rydberg B. Lack of Bystander Effects from High-LET Radiation for Early Cytogenetic End Points. Radiat Res. 2008;170(6):794-802. doi:10.1667/RR1458.1.
24. McGranahan N, Swanton C. Clonal Heterogeneity and Tumor Evolution: Past, Present, and the Future. Cell. 2017;168(4): 613-628. doi:10.1016/j.cell.2017.01.018.
25. Dagogo-Jack I, Shaw AT. Tumour heterogeneity and resistance to cancer therapies. Nat Rev Clin Oncol. 2018;15(2):81-94. doi: 10.1038/nrclinonc.2017.166.
26. Brenner DJ, Curtis RE, Hall EJ, Ron E, Second malignancies in prostate carcinoma patients after radiotherapy compared with surgery. Cancer. 2000;88(2):3982-4406. doi:10.1002/(SICI) 1097-0142.
27. Burt LM, Ying J, Poppe MM, Suneja G, Gaffney DK. Risk of secondary malignancies after radiation therapy for breast cancer: Comprehensive results. The Breast. 2017;35: 122-129. doi:10.1016/j.breast.2017.07.004.
28. Schneider U. Modeling the Risk of Secondary Malignancies after Radiotherapy. Genes. 2011;2(4):1033-1049. doi:10.3390/ genes2041033.

29. Puck TT, Marcus PI. Action of X-Rays on Mammalian Cells. J Exp Med. 1956;103(5):653-666.
30. Elkind MM, Sutton H, Moses WB. Postirradiation survival kinetics of mammalian cells grown in culture. J Cell Comp Physiol. 1961;58(S1):113-134. doi:10.1002/jcp.1030580412.
31. Leenhouts HP, Chadwick KH. Radiation induced DNA double strand breaks and chromosome aberrations. Theoret Appl Genetics. 1974;44(4):167-172. doi:10.1007/BF00277015.
32. Chadwick KH, Leenhouts HP. The Rejoining of DNA double-strand breaks and a model for the formation of chromosomal rearrangements. Int J Radiat Biol Relat Stud Phys Chem Med. 1978;33(6):517-529. doi:10.1080/09553007814550431.
33. Bodgi L, Foray N. The nucleo-shuttling of the ATM protein as a basis for a novel theory of radiation response: resolution of the linear-quadratic model. Int J Radiat Biol. 2016;92(3): 117-131. doi:10.3109/09553002.2016.1135260.
34. Devic C, Ferlazzo ML, Foray N. Influence of individual radiosensitivity on the adaptive response phenomenon: Toward a mechanistic explanation based on the nucleo-shuttling of ATM Protein. Dose-Response. 2018;16(3):155932581878983. doi: 10.1177/1559325818789836.
35. Mothersill C, Seymour CB, Joiner MC, Relationship between Radiation-Induced Low-Dose Hypersensitivity and the Bystander Effect. Radiat Res. 2002;157(5):5262-5532. doi:10. 1667/0033-7587(2002)157[0526.

# Chapter 4 - Heterogeneity of radiation response in clonal variants of a human cell line.

*Rhea Desai[1,*], Colin Seymour[1] & Carmel Mothersill[1]

[1]Department of Biology, McMaster University, Hamilton, ON, Canada,

The initial concept of the research presented in this chapter and methods were developed by Dr. Carmel Mothersill. All irradiation, cell culture, experimentation, statistical analysis and manuscript writing were completed by the first author. All authors contributed to editing of the manuscript.

# 4.0 Preface

The body of work presented in this chapter was initially conceived by Dr. Carmel Mothersill and Dr. Colin Seymour. All cell cultures, irradiation, curve fitting, and statistical analysis was completed by the first author. All authors assisted in the development of ideas throughout experimentation. The first draft of this manuscript made for publication was written by the first author and subsequently edited by all authors.

The following is a manuscript submitted to the Radiation Research journal in November 2023.

## 4.1 Abstract

The goal of this study is to investigate dose response relationships after low radiation dose exposure using clonal cell lines previously determined to vary in radiosensitivity. Clonal cell lines of a parent HCT 116 (p53 wildtype) cell line were previously isolated and grown. This series of progeny cell lines contains both unirradiated and irradiated progenitors. The latter were included to increase the potential for variation. All progeny cell lines were irradiated at doses ranging from 0.01 to 0.5 Gy and subsequently investigated for instances of low dose effects such as hyper-radiosensitivity (HRS) and increased radioresistance (IRR). The induced-repair model fitted to the data assisted in identifying the dose. At which the transition from hyperradiosensitivty (HRS) to increased radioresistance (IRR) occurred in clonal cell lines. Clonal cell lines previously shown to exhibit radiation induced bystander effects (RIBE) also exhibit a pronounced HRS/IRR transition after low dose exposure. This contradicts some previous conclusions from our group. We suggest low dose effects like RIBE and HRS/IRR may be related to p53 status of the cell line and have the ability to manifest in concert rather than mutually exclusively depending on p53 status. This research may have direct implications for improvement of low-dose radiation risk assessment and radiation protection.

## 4.2 Introduction

Low dose effects of ionizing radiation have been studied extensively over the years with regard to both acute and chronic effects as well as effects often dominating in low doses such as Non-targeted effects (NTE), hyper-radiosensitivity (HRS) and increased radioresistance (IRR) [*1–5*]. Generally, where instances of HRS/IRR are noted, a cellular sensitivity to low doses of ionizing radiation (below 0.5 Gy) are observed followed by IRR after higher doses. When observing the HRS component, a larger than expected radiosensitivity is occurring while IRR is seen as a shift to a more radioresistant cell response. This IRR has predominantly been observed to occur after doses exceeding 0.5Gy while HRS typically occurs after doses less than 0.5 Gy [*2,6,7*]. Many groups have reported HRS/IRR responses following stress from ionizing radiation in mammalian cell culture[*2,6,8–14*] and in human skin[*15*]. Research into HRS/IRR has indicated that it could be important in fractionated radiation therapy[*16,17*]. Researchers have suggested a possibility for increased effectiveness of fractionated therapy through exploitation of the HRS/IRR transition where fractionated therapy is prescribed in very small doses per fraction. For this reason, the total dose required to produce damage would decrease when the dose per fraction is less than 1 Gy. This effect was found true for mouse skin, kidney and lungs[*7,18–20*].

Due to the transition from HRS to IRR in the low dose region, modelling of these data proved difficult when using widely accepted models such as the linear-quadratic model for cell survival [*6,21–23*]. The linear-quadratic model has been demonstrated to largely underestimate the effects of low dose radiation exposures, where HRS occurs [*6,24,25*]. An overall shift to utilizing models that consider low dose sensitivities is of great importance to better portray data after low doses [*26,27*]. For example, the induced-repair model developed by Joiner and colleagues who first defined HRS/IRR has been a good option as this model contains sensitivity parameters such as $\alpha r$ and $\alpha s$ to better demonstrate effects in low doses [*10,11,24*]. To provide better standards for radiation protection and improved radiotherapy, the HRS/IRR response need further investigation [*3,7,15,28*].

Along with the HRS/IRR transition, other low dose phenomena such as the radiation-induced bystander effect (RIBE) are of interest. RIBE refers to cellular effects in a cell, tissue or organism which was not directly exposed to ionizing radiation but behaves as though it received a direct deposition of ionizing radiation as a result of signals emitted from irradiated counterparts[*29–31*]. While much research has focused on low dose effects, less focus has been on how the effects may present together. Our group has aimed to investigate the relationship between these low dose effects to better understand the mechanisms in vitro. An early paper [*4*] using lines known to display (or not) HRS/IRR suggested that RIBE and HRS were mutually exclusive however in 2016, Fernandez-Palomo et al. conducted studies on the T98G and HaCaT cell lines where combinations of

these cells were tested to observe bystander signals. For example, media collected from irradiated T98G cells was applied to recipient HaCaT cells and vice versa, to observe if a bystander response would be induced. The T98G cells were previously determined to display a strong HRS/IRR transition while HaCaT cells did not display low-dose hypersensitivity. Using the RIBE medium transfer assay [*30*], medium from irradiated T98G cells was found to decrease cell survival in both T98G and HaCaT recipient cells. However, medium from HaCaT cells increased cell survival in recipient T98G cells and decreased cell survival in HaCaT cells. It was also noted that T98G cells only displayed RIBE when exposed to doses less than 1 Gy. Ultimately it was suggested that the relationship between HRS/IRR and RIBE is more complex than previously understood and the effect often varies depending on the cells and dose in question. This clarified the previous understanding that HRS/IRR and RIBE are mutually exclusive mechanisms.

A study in 2022 by Desai et al. aimed to further investigate cell survival following ionizing radiation using popular curve fitting models [*27*]. Here the goal was to investigate potential heterogeneity in a cell population and the effects this may have on radiosensitivity. Clonal cell lines were isolated from an HCT 116 $p53^{+/+}$ parent population and survival curves were developed and fit with the multi-target and linear-quadratic models. Medium transfer bystander assays were also conducted on the parent and all clonal lines and a link between radiosensitivity and RIBE was determined. Overall, cell lines determined to be more radiosensitive produced strong bystander signals while the more

radioresistant lines did not [*27*]. However, there was still a gap in our understanding of whether the HRS/IRR transition was also present. Due to the high doses involved in the study, it was not possible to make any assumptions about low dose-response relationships. Therefore, it was decided to experiment using low doses. The present study utilizes the same parent and clonal cells lines from Desai et al. 2022 to investigate radiosensitivity in low doses.

## 4.3 Methods

### 4.3.1 Cell Culture

The HCT116 (p53 wildtype) cell line was originally derived from a large intestine/colon carcinoma. Clonal cell lines were previously isolated by our group [*27*] to give rise to 7 clonal HCT116 cell lines. These cell lines are designated clone A to clone G. The parent HCT116 cell line was also maintained for comparison. All cells were regularly cultured in Roswell Park Memorial Institute (RPMI) 1640. RPMI 1640 was supplement with 10% fetal bovine serum (FBS), 100 U/mL penicillin, 100 ug/mL streptomycin, and 2.05 mM L-Glutamine. Cell cultures were grown in 75 $cm^2$ Falcon tissue culture flasks at 37 °C and 5% $CO_2$. Cells were detached for experimentation and subcultures using 25% phenol red-free trypsin solution with 0.192 mM EDTA every 5-7 days and subsequently

neutralized using a greater volume of growth media. Cells were cultured when 70 to 80% confluent. All mentioned reagents were purchased from Gibco, ThermoFisher Scientific.

### 4.3.2 Cell Irradiations

Irradiations were conducted using a Cesium-137 source with a dose rate of 198.4 mGy/min. To achieve desired doses with time of exposure, flasks were consistently placed 30cm away from the source (Taylor Radiobiology Source, McMaster University). Direct irradiations for survival curve data were conducted 15-20 hours post cell seeding.

### 4.3.3 Clonogenic Survival Assay

Confluent cell culture flasks were used for clonogenic survival assays. Cells were detached from tissue culture flasks using the Trypsin-EDTA working solution described previously and neutralized with supplemented RPMI 1640 growth medium. Cell seeding concentrations were determined using the Bio-Rad TC20 automated cell counter (Bio-Rad Life Science Research Division, Canada). Cells were seeded in T25 Falcon tissue culture flasks to perform a clonogenic assay using the method described by Puck and Marcus [*32*]. Clonogenic assays were conducted to develop low-dose survival curves. Cells were seeded and irradiated at the following dose points: 0, 0.01, 0.03, 0.05, 0.1, 0.3, and 0.5 Gy. This

range in dose points allowed for assessment of cell survival in the low dose range. Parameter results from Desai et al. 2022 were also re-analyzed and stated in Table 1 for complete full range data. Following irradiation, flasks were immediately returned to the incubator and grown for nine days at 7°C in an atmosphere of 5% CO2 in air. Flasks were stained with 15% Carbol Fuchsin solution (Ziehl Neelson, Milipore Sigma) on day nine of growth. Colonies were then counted manually and surviving fraction for each dose was determined. GraphPad Prism 10 software (GraphPad Software Inc., LaJolla, CA) was used to generate survival curve graphs and to fit curves.

### 4.3.4 Statistical Analysis

All data presented is a mean of three independent trials using three replicates (n=9). Least square error linear regression analyses were performed on data to produce the linear-quadratic and induced-repair models using GraphPad Prism 10.

## 4.4Results

Figures 1-8 display the HCT116 $p53^{+/+}$ parent cell line along with all previously isolated clones. All clones were derived from an irradiated (Figures 4.3, 4.4, 4.5 and 4.6) or non-irradiated (Figures 4.1, 4.2, 4.7, and 4.8) parent population prior to clone isolation.

All Figures 4.1 to 4.8 demonstrate changes in cell survival following a low dose radiation exposure to a Cesium-137 gamma emitting source. All cell survival curves are fitted with the induced-repair model and linear-quadratic model. To build on previous findings from Desai *et al.* 2022, linear-quadratic curve fittings (in Table 4.1 of that paper) are included while induced-repair model fittings show an improvement in low dose curve fits. Clonal variation in radiosensitivity following direct exposure of doses ranging from 0 to 15 Gy is evident in all survival curves. Large scale curves with dose points from 0 to 15 Gy show overall downward trends in cell survival following radiation but graphs zoomed into the low dose range display further cell killing in low doses, not visible in the full range survival curve (small panel in Figures 4.1- 4.8). Curve fitting parameters are summarized in Table 4.1. When low dose data are fitted with the linear-quadratic model, our physical understanding of radiation effects is not represented accurately by the mathematical model. Particularly where negative beta values are report

**Table 4.1:** A comparison of survival curve fitting parameters using the (A) linear-quadratic and (B) induced-repair model.

**(A) Linear Quadratic Model**

| Cell Line | Progeny of Irradiated Progenitors | Desai et al. (2022) | | | | | Combined Data (0.0, 0.01, 0.03, 0.05, 0.1, 0.3, 0.5, 1.0, 3.0, 5.0, 7.0, 10, 15) | | | | |
|---|---|---|---|---|---|---|---|---|---|---|---|
| | | $\alpha$ | CI (95%) | β | CI (95%) | $r^2$ | $\alpha$ | CI (95%) | β | CI (95%) | $r^2$ |
| Parent Line | | 0.44 | 0.36-0.53 | 0.021 | -0.0056-0.057 | 0.97 | 0.44 | 0.35-0.52 | 0.023 | -0.0063-0.061 | 0.96 |
| Clone A | | -0.058 | -0.16-0.042 | 0.15 | 0.10-0.20 | 0.95 | 0.059 | -0.029-0.15 | 0.10 | 0.069-0.14 | 0.95 |
| Clone B | Yes | 0.38 | 0.29-0.45 | 0.040 | 0.010-0.078 | 0.97 | 0.47 | 0.40-0.54 | 0.012 | -0.010-0.041 | 0.97 |
| Clone C | Yes | 0.28 | 0.19-0.38 | 0.053 | 0.018-0.096 | 0.95 | 0.43 | 0.34-0.52 | 0.012 | -0.013-0.046 | 0.95 |
| Clone D | Yes | 0.40 | 0.33-0.47 | 0.085 | 0.047-0.13 | 0.98 | 0.52 | 0.39-0.65 | 0.036 | -0.016-0.11 | 0.93 |
| Clone E | Yes | 0.34 | 0.30-0.39 | 0.018 | 0.0060-0.031 | 0.98 | 0.50 | 0.40-0.60 | -0.013 | -0.025-0.011 | 0.90 |
| Clone F | | 0.28 | 0.23-0.34 | 0.052 | 0.033-0.074 | 0.98 | 0.39 | 0.29-0.49 | 0.021 | -0.0068-0.059 | 0.93 |
| Clone G | | 0.64 | 0.61-0.67 | -0.013 | -0.021-0.0030 | 1.0 | 0.66 | 0.59-0.73 | -0.019 | -0.032-0.0086 | 0.97 |

**(B) Induced-Repair Model**

| Cell Line | Progeny of Irradiated Progenitors | $ar$ | CI (95%) | $as$ | CI (95%) | β | CI (95%) | $as/ar$ | $d_c$ | CI (95%) | $r^2$ |
|---|---|---|---|---|---|---|---|---|---|---|---|
| **Parent Line** | | 0.38 | 0.29-0.48 | 3.4 | 1.9-11 | 0.039 | 0.0054-0.083 | 9.0 | 0.087 | 0.027-0.16 | 0.97 |
| **Clone A** | | 0.018 | -0.049-0.086 | 9.5 | 3.3-15 | 0.12 | 0.090-0.15 | 5.2e2 | 0.045 | 0.031-0.14 | 0.97 |
| **Clone B** | Yes | 0.39 | 0.33-0.44 | 4.3 | 3.4-5.4 | 0.036 | 0.015-0.061 | 11 | 0.098 | 0.076-0.12 | 0.99 |
| **Clone C** | Yes | 0.083 | -0.22-0.23 | 2.6 | 1.9-3.5 | 0.12 | 0.066-0.23 | 32 | 0.27 | 0.19-0.44 | 0.97 |
| **Clone D** | Yes | 0.44 | 0.36-0.53 | 18 | 12-27 | 0.068 | 0.026-0.12 | 40 | 0.034 | 0.025-0.048 | 0.97 |
| **Clone E** | Yes | 0.33 | 0.26-0.39 | 6.2 | 5.2-7.4 | 0.022 | 0.0059-0.041 | 19 | 0.15 | 0.12-0.17 | 0.98 |
| **Clone F** | | 0.33 | 0.28-0.40 | 13 | 9.4-19 | 0.037 | 0.017-0.061 | 40 | 0.044 | 0.033-0.061 | 0.98 |
| **Clone G** | | 0.59 | 0.52-0.63 | 4.6 | 3.7-5.8 | 0.0032 | -0.016-0.028 | 8.0 | 0.096 | 0.073-0.12 | 0.99 |

**Table 4.2:** Summary of induced-repair model parameters with consideration of HRS and RIBE.

| Line | $\alpha r$ | $\alpha s$ | $d_c$ | HRS | RIBE |
|---|---|---|---|---|---|
| Parent | 0.38 | 3.4 | 0.087 | X | X |
| A | 0.018 | 9.5 | 0.045 | X | |
| B | 0.39 | 4.3 | 0.098 | X | X |
| C | 0.083 | 2.6 | 0.27 | X | X |
| D | 0.44 | 18 | 0.034 | X | |
| E | 0.33 | 6.2 | 0.15 | X | X |
| F | 0.33 | 13 | 0.044 | X | |
| G | 0.59 | 4.6 | 0.096 | X | X |

To better model low dose data, curves are fitted with the induced-repair model (Equation 4.1). This model described by Lambin *et al.* comprises parameters characteristic of the induced-repair process which give insight into the radiosensitive or radioresistant nature of the cell line (Table 4.1). Specifically, parameters $\alpha r$ and $\alpha s$ provide this information (Table 4.1.B). Parameter $\alpha r$ represents the slope of the linear component's resistant portion, while $\alpha s$ describes the slope of the linear component's sensitive portion. Table 4.1.B states $\alpha s/\alpha r$ ratio values representing the magnitude of induced radioprotection as dose increases [*9]*. When the $\alpha s$ term is equal to the $\alpha r$ term, induced-repair is no longer sufficient and radiation exposure is mainly lethal. It is important to note, these parameters are originally derived from the linear-quadratic model to better represent low dose effects. Values for $d_c$ can also be found in Table 4.1.B. where maximum HRS is observed and a transition to IRR begins.

$$S = \exp\left(-\alpha r\left(1 + \left(\frac{\alpha s}{\alpha r} - 1\right)e^{\frac{-d}{d_c}}\right)d - \beta d^2\right) \tag{4.1}$$

Using the induced-repair model, instances of HRS/IRR are observed (Figures 1-8). The parent line and all clonal lines display the HRS/IRR transition (Figure 8). Out of all the cell lines presented, clone G displays a greater than expected level of cell killing at low doses but continues to trend downwards starting from even the smallest doses. Regardless of whether clonal lines were isolated from a pre-irradiated progenitor population, there is an overall variance in radiosensitivity between clonal lines as evident by the curve fitting parameters and cell survival curves. The parent line (Figure 1) and all clonal lines A to G (Figures 2-8) display a greater than expected level of cell killing at doses generally below 0.1 Gy but beyond this point there is a transition towards increased radioresistance to low doses.

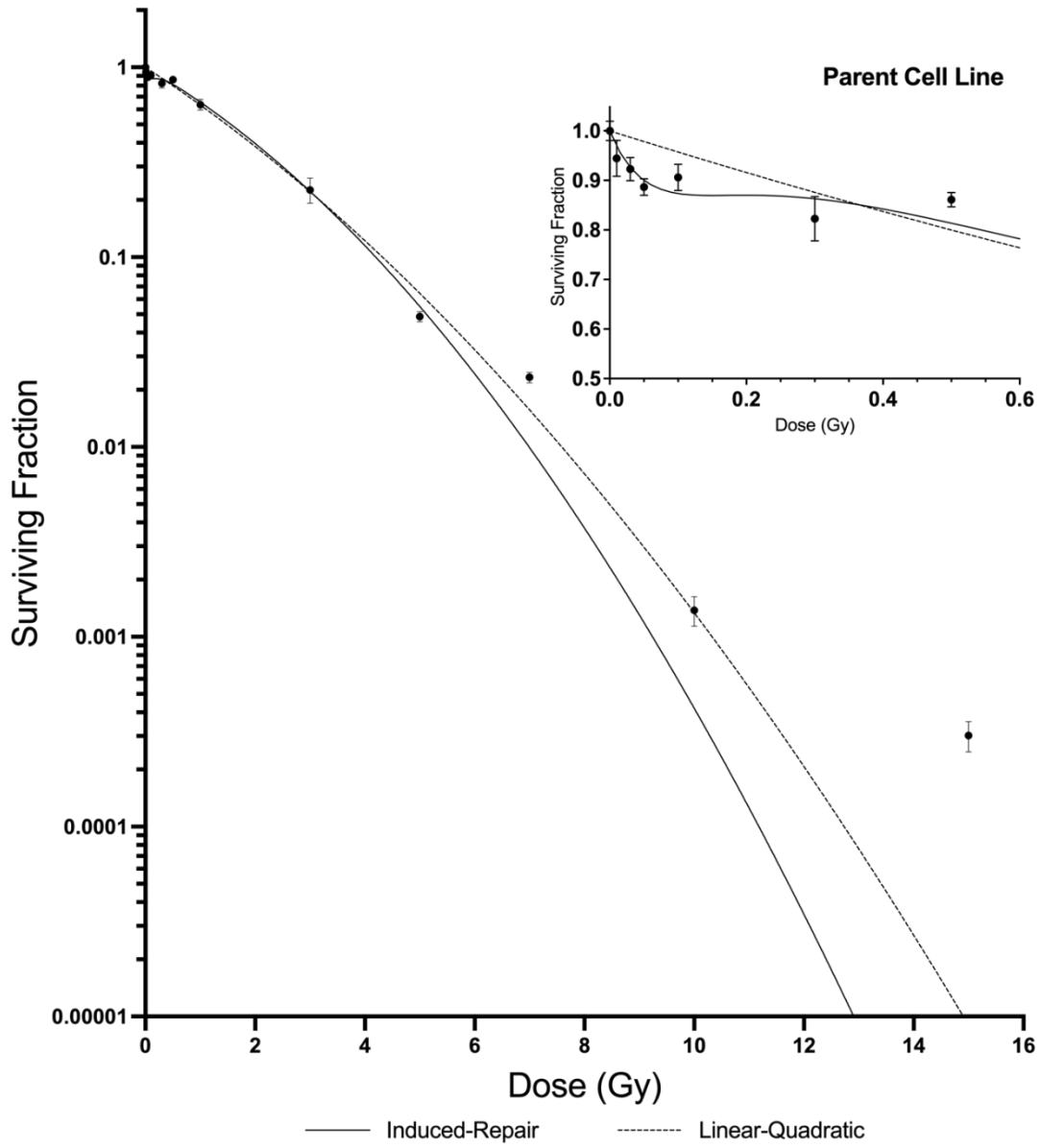


**Figure 4.1:** Cell survival curve of parent HCT 116 $p53^{+/+}$ cell line. Data points are fitted using the Induced-Repair and Linear-Quadratic models for cell survival following ionizing radiation. Dose points are 0, 0.01, 0.03, 0.05, 0.1, 0.3, 0.5, 1.0, 3.0, 5.0, 7.0, 10.0, 15.0. Error bars are standard error of the mean for n=9.

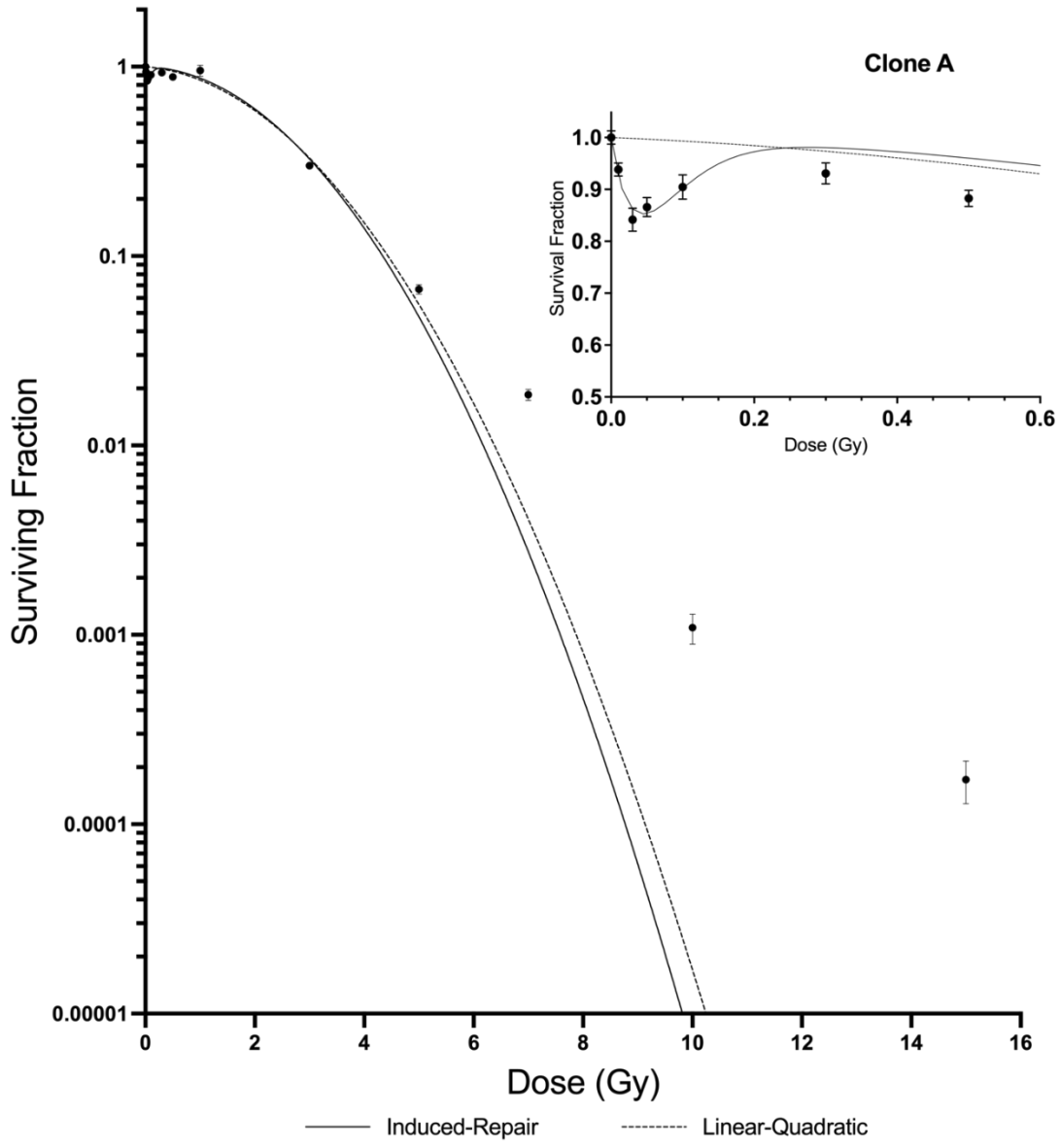


**Figure 4.2:** Cell survival curve of clone A derived from parent HCT 116 $p53^{+/+}$ cell line. Data points are fitted using the Induced-Repair and Linear-Quadratic models for cell survival following ionizing radiation. Dose points are 0, 0.01, 0.03, 0.05, 0.1, 0.3, 0.5, 1.0, 3.0, 5.0, 7.0, 10.0, 15.0. Error bars are standard error of the mean for n=9.

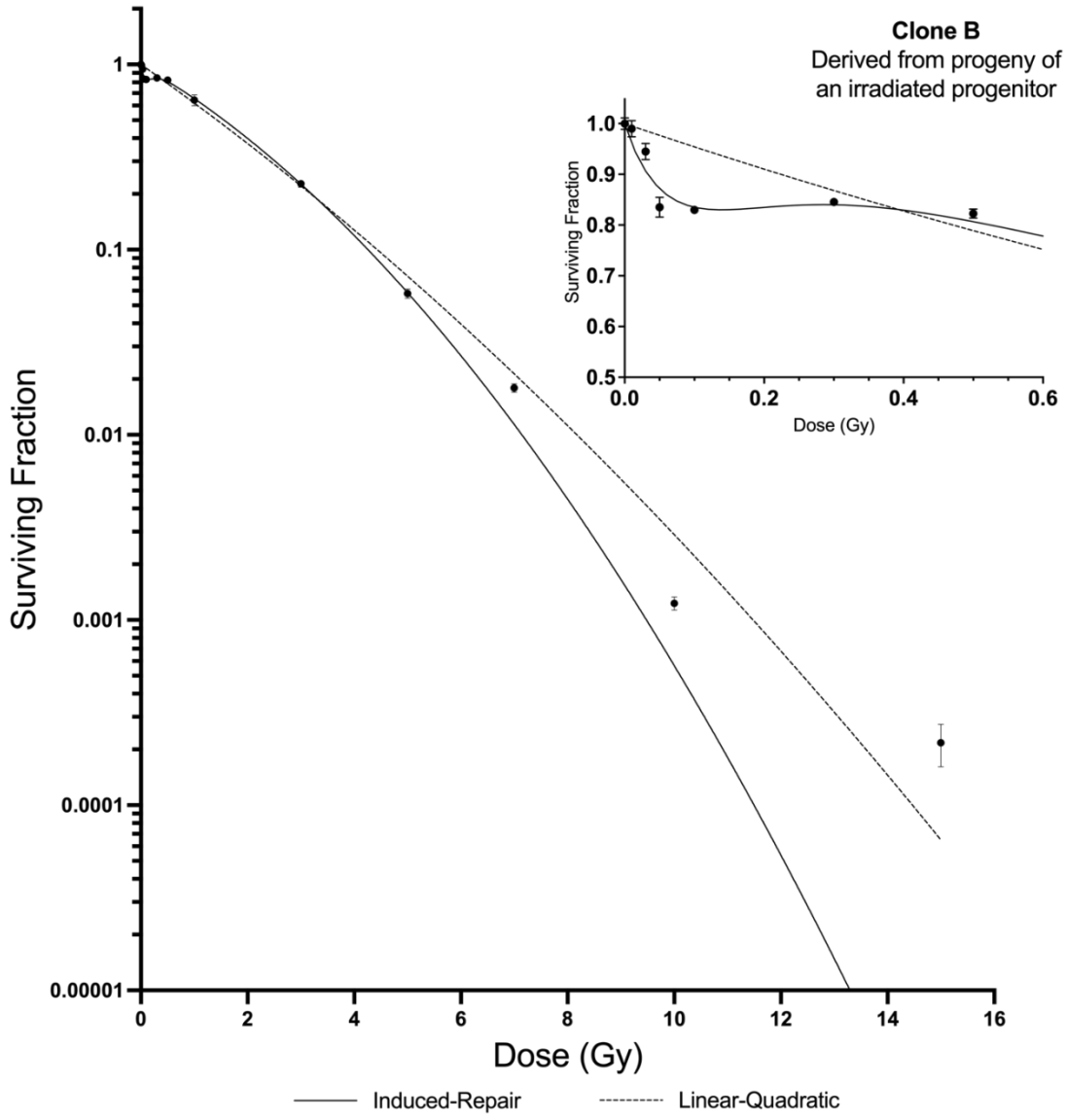


**Figure 4.3:** Cell survival curve of clone B derived from an irradiated parent HCT 116 $p53^{+/+}$ progenitor population. Data points are fitted using the Induced-Repair and Linear-Quadratic models for cell survival following ionizing radiation. Dose points are 0, 0.01, 0.03, 0.05, 0.1, 0.3, 0.5, 1.0, 3.0, 5.0, 7.0, 10.0, 15.0. Error bars are standard error of the mean for n=9.

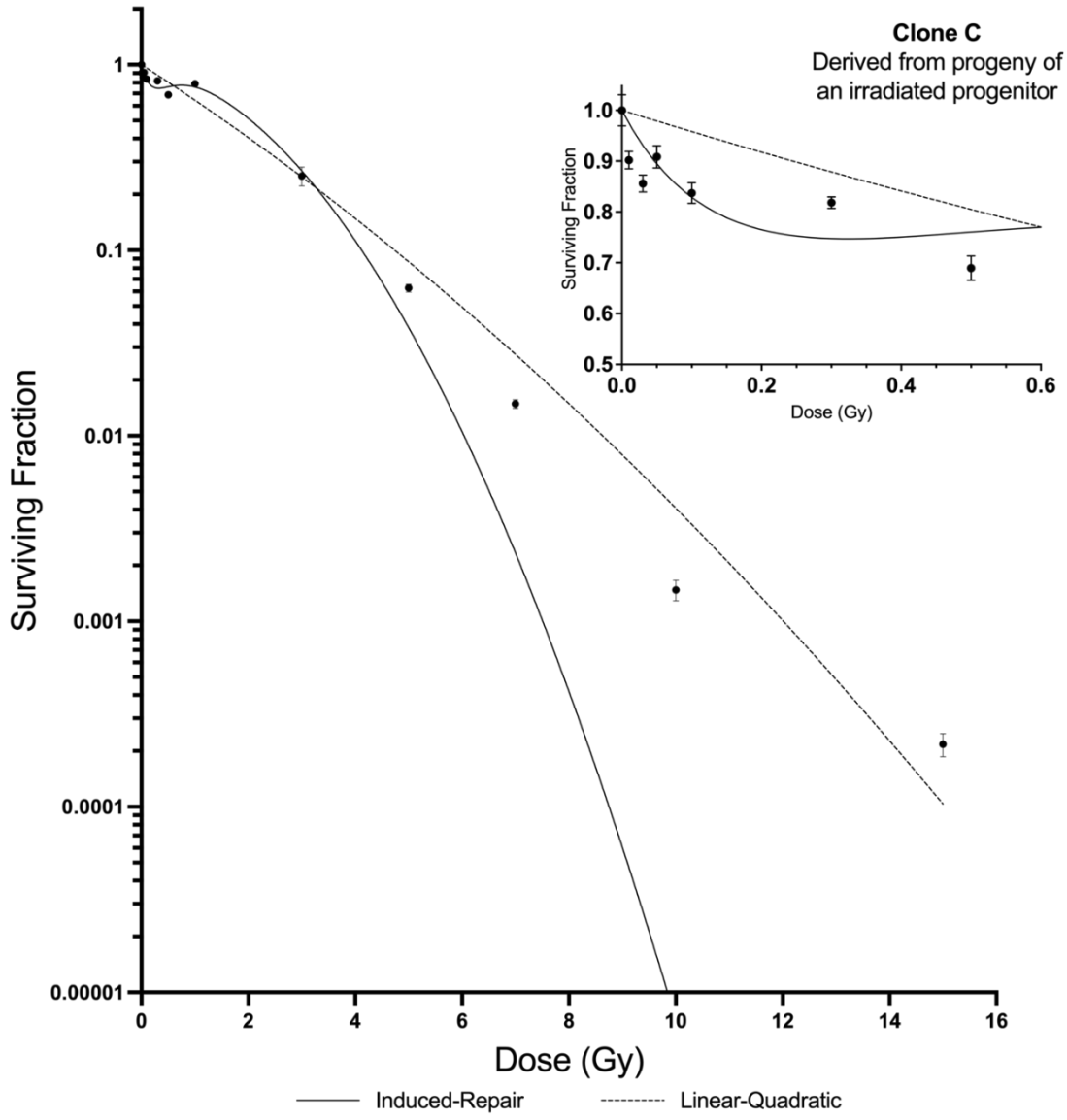


**Figure 4.4:** Cell survival curve of clone C derived from an irradiated parent HCT 116 $p53^{+/+}$ progenitor population. Data points are fitted using the Induced-Repair and Linear-Quadratic models for cell survival following ionizing radiation. Dose points are 0, 0.01, 0.03, 0.05, 0.1, 0.3, 0.5, 1.0, 3.0, 5.0, 7.0, 10.0, 15.0. Error bars are standard error of the mean for n=9.

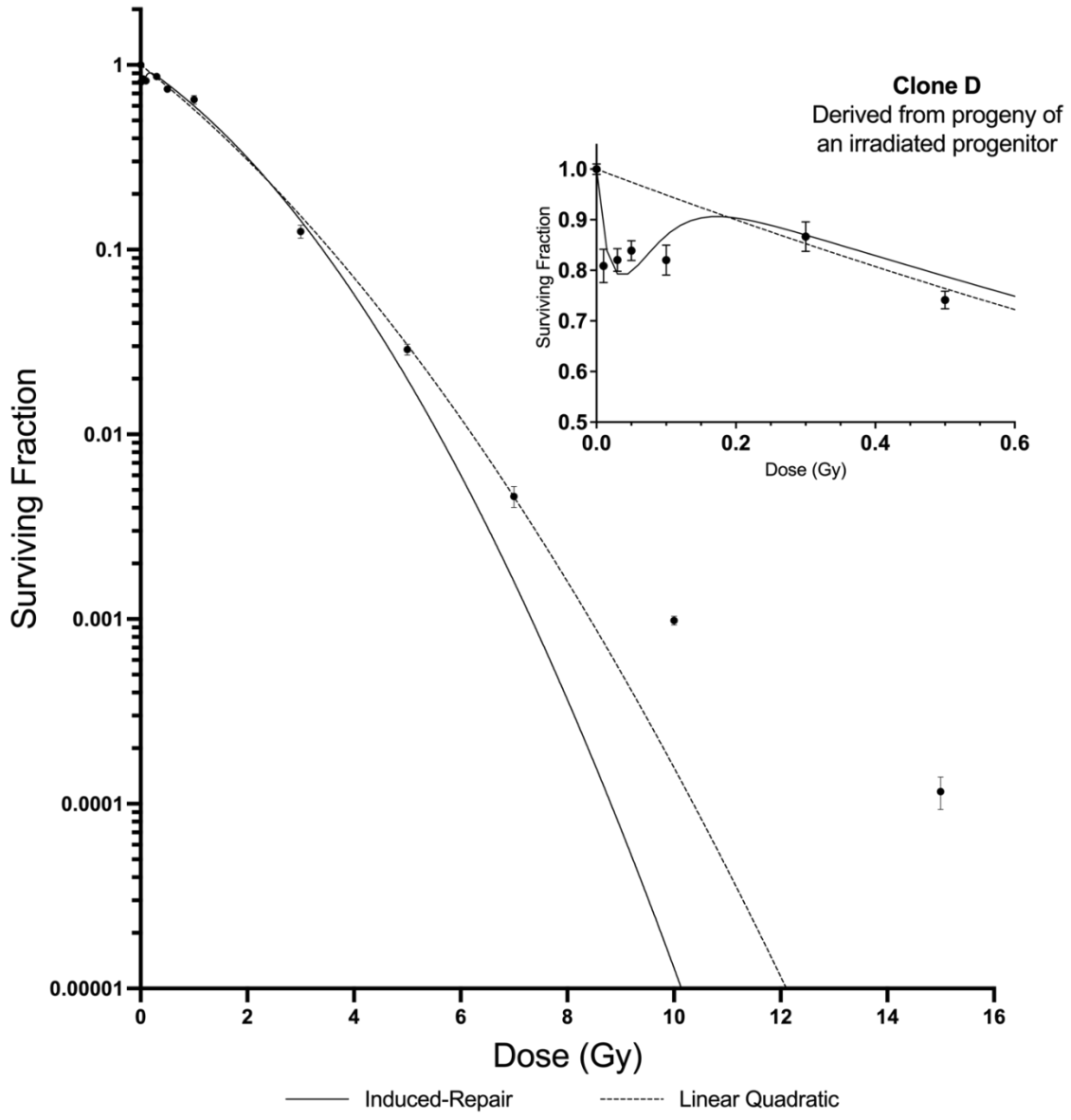


**Figure 4.5:** Cell survival curve of clone D derived from an irradiated parent HCT 116 $p53^{+/+}$ progenitor population. Data points are fitted using the Induced-Repair and Linear-Quadratic models for cell survival following ionizing radiation. Dose points are 0, 0.01, 0.03, 0.05, 0.1, 0.3, 0.5, 1.0, 3.0, 5.0, 7.0, 10.0, 15.0. Error bars are standard error of the mean for n=9.

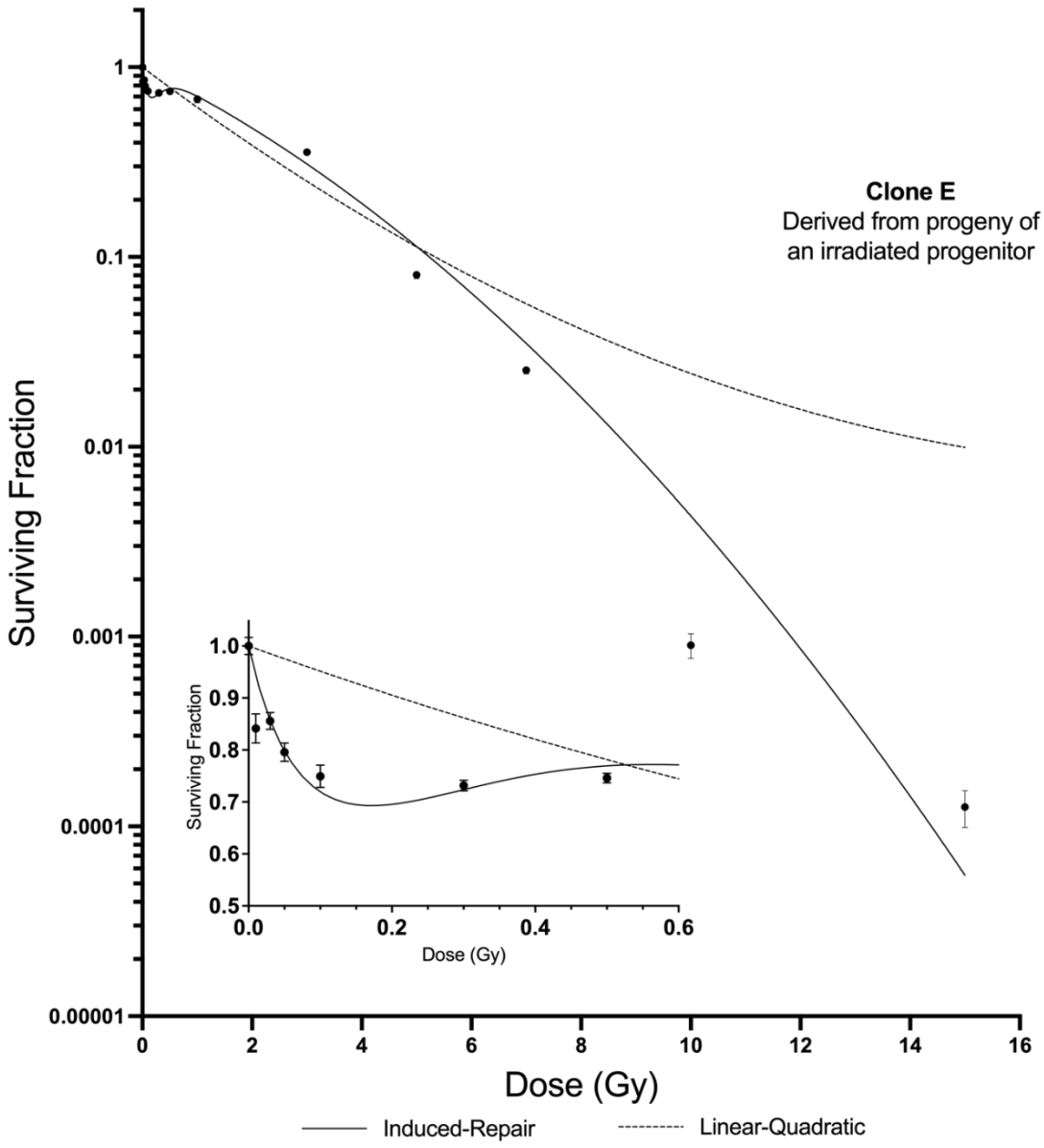


**Figure 4.6:** Cell survival curve of clone E derived from an irradiated parent HCT 116 $p53^{+/+}$ progenitor population. Data points are fitted using the Induced-Repair and Linear-Quadratic models for cell survival following ionizing radiation. Dose points are 0, 0.01, 0.03, 0.05, 0.1, 0.3, 0.5, 1.0, 3.0, 5.0, 7.0, 10.0, 15.0. Error bars are standard error of the mean for n=9.

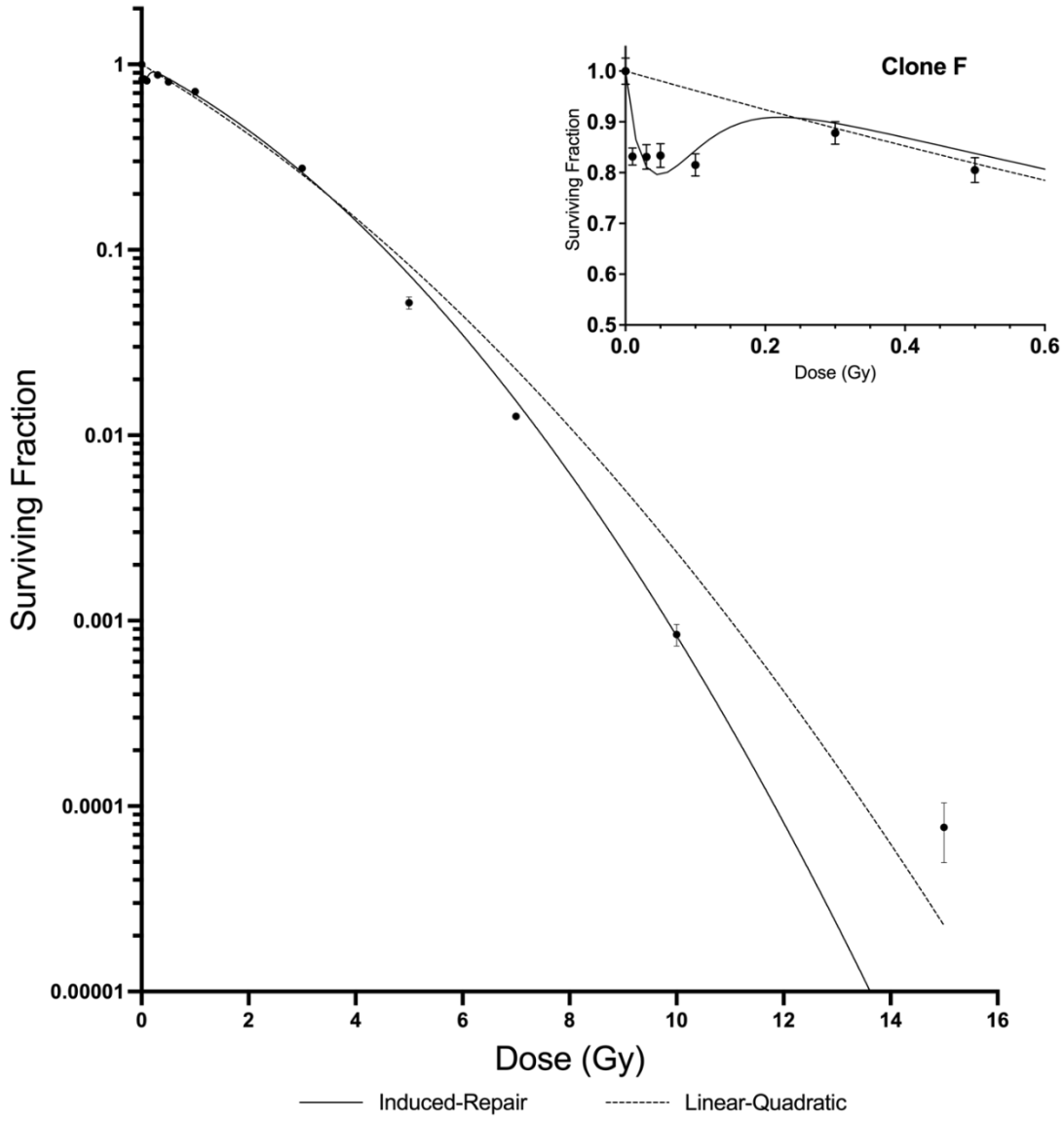


**Figure 4.7:** Cell survival curve of clone F derived from parent HCT 116 $p53^{+/+}$ cell line. Data points are fitted using the Induced-Repair and Linear-Quadratic models for cell survival following ionizing radiation. Error bars are standard error of the mean for n=9.

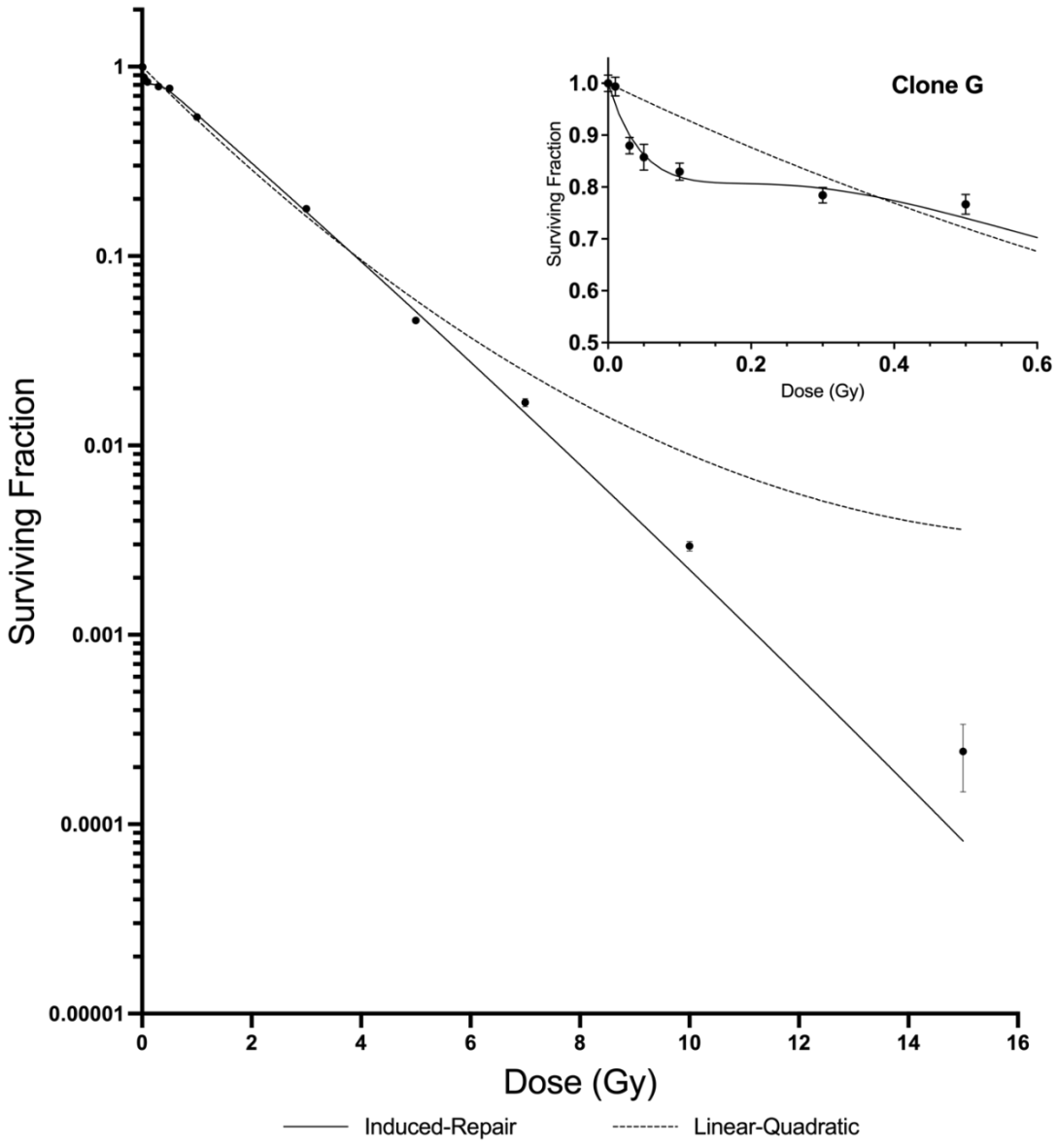


**Figure 4.8:** Cell survival curve of clone G derived from parent HCT 116 $p53^{+/+}$ cell line. Data points are fitted using the Induced-Repair and Linear-Quadratic models for cell survival following ionizing radiation. Dose points are 0, 0.01, 0.03, 0.05, 0.1, 0.3, 0.5, 1.0, 3.0, 5.0, 7.0, 10.0, 15.0. Error bars are standard error of the mean for n=9.

## 4.5 Discussion

Low dose radiation phenomena such as HRS/IRR and RIBE continue to be an area of interest due to new research on how these effects are present in conjunction with one another. Widely used models like the linear-quadratic model have been shown not to describe accurately, low dose cell killing because they tend to underestimate the effects of low dose radiation [*6,7,21,24*]. To address these low dose related issues, certain groups have worked to describe cellular and molecular pathways involved with the HRS/IRR transition, but others have taken a more mechanistic approach of investigation. In the past our group has investigated the HRS/IRR transition in the context of the bystander effect [*2*,6] to better understand when these effects are likely to occur in low doses and how we can better our efforts towards radiation protection. The data presented in this study build on previous work by our group which demonstrated a link between radiosensitive clonal populations and their ability to produce bystander signals. We found that the more radiosensitive clonal cell lines (small survival curve shoulder) displayed the bystander effect while the most radioresistant did not. We also found that the overall parent cell line from which all clonal lines were isolated was generally radiosensitive with a small survival curve shoulder size and thus was able to produce bystander signals. However, it was also noted that certain clonal populations with similar shoulder size and sensitivity were not able to produce the bystander effect. Thus, we postulated that there may be other low dose effects acting alongside RIBE.

There are various instances of HRS/IRR in laboratory and clinical settings that offer likely causes for the phenomena to occur, such as defective DNA repair or cell cycle regulation while other groups have suggested the phenomena useful in improving cancer treatments by sensitizing tumours [*1,3,7,11,22,28*]. The data presented here focus primarily on a mechanistic understanding of the link between bystander effects and low-dose HRS/IRR.

To test this idea, low dose survival curves ranging from 0 to 0.5 Gy were developed and instances of HRS were identified. Interestingly in 2022 Desai *et al*., found clones A, D and F were not able to produce bystander signals but all other clones including the parent population exhibited RIBE. Clone A, determined to be the most resistant did not display the bystander effect but did indeed show the HRS/IRR transition below 0.1 Gy. On the other hand, the previously determined most radiosensitive line, clone G, did not show a strong HRS/IRR transition. There was no apparent influence of whether clones were derived from irradiated progeny or not. In this study we demonstrate a link between HRS and RIBE. Previous work from our group initially reported HRS/IRR and RIBE as mutually exclusive [*2*]. Later work however[*6*] found that in the T98G line, which shows HRS/IRR, bystander signals were only seen in the HRS dose range and not in the IRR dose range (0.01Gy). This suggested that IRR mechanisms inactivated RIBE. In the present work we show various instances where both mechanisms may occur concurrently. For example, clone G which did not display the strongest HRS/IRR was still able to produce RIBE at a

dose of 2 Gy. Alternatively Clone A determined in this study to be an HRS clonal line, did not produce RIBE at 2 Gy. Values for $d_c$ listed in Table 4.1.B are all doses below 0.27 Gy which emphasizes the importance of this research in low doses showing that low dose radiation does have a relatively significant effect on cell survival which is often overlooked when commenting on the effects of ionizing radiation. The results also emphasize the importance of looking over a wide dose range and in many cell lines before making sweeping statements! In regard to what might underlie this variation in the relationship between HRS and RIBE, we have shown previously that both p53 null or deficient and p53 wild type cells have ability to produce bystander signals however cells responding to the signal or cells designated as reporter cells in the RIBE medium transfer assay must have normal p53 status to show RIBE over a range of doses. This might help explain previous results by our group which have shown RIBE only in HRS zone doses [*6,33*]. T98G is a p53 null cell line while HCT $116^{+/+}$ has wild type p53. It is possible that when p53 wild type is present, cells are able to respond to RIBE signals across the whole dose range but if p53 is null or mutant, they either have no RIBE or lose the capacity to respond as the IRR mechanisms kicks in. Further work with a greater variety of cell lines might address this question. Lines with mutant p53 may show the bystander effect in the very low dose region while wild type lines maintain the bystander effect response over a larger dose range [*6,33*]. Clearly more work needs to be done to clarify the low dose response relationship and the influence of HRS/IRR, RIBE and p53 status.

In conclusion, we have demonstrated that clonal populations isolated from a heterogeneous HCT116 $p53^{+/+}$ parent cell line exposed to ionizing radiation display various instances of the HRS/IRR transition. It was found that models like the induced-repair model are useful in demonstrating low dose effects while the linear-quadratic model provides little to no information in low doses. The linear-quadratic model is evidently not appropriate for low range survival curve fitting as they were developed with the aim of modeling high doses rather than low dose effects. We also demonstrate that whether bystander signals are produced or not, effects of HRS can lead to the overall increased sensitivity of a cell line in low doses. This is of particular interest when calculating risk to low dose exposures which currently may be too liberal in approach. Understanding the mechanisms of these low dose effects and the doses at which they may be produced will ultimately lead to better radiation therapies and protection efforts [*3,7,15,28*].

## 4.6 Acknowledgements

We acknowledge the grant support for this work from the Natural Sciences Resource Council (NSRC) and Canada Research Chairs 950-221284.

## 4.7 Declaration of Conflicting Interests

The author(s) declared no potential conflicts of interest with respect to the research, authorship, and/or publication of this article.

## 4.8 References


*1.* Leonard BE. Thresholds and transitions for activation of cellular radioprotective mechanisms – correlations between HRS/IRR and the 'inverse' dose-rate effect. *International Journal of Radiation Biology*. 2007;83:479–89.

*2.* Ryan LA, Seymour CB, Joiner MC, *et al.* Radiation-induced adaptive response is not seen in cell lines showing a bystander effect but is seen in lines showing HRS/IRR response. *International Journal of Radiation Biology*. 2009;85:87–95.

*3.* Thomas C, Martin J, Devic C, *et al.* Impact of dose-rate on the low-dose hyper-radiosensitivity and induced radioresistance (HRS/IRR) response. *International Journal of Radiation Biology*. 2013;89:813–22.

*4.* Mothersill C, Seymour CB, Joiner MC. Relationship between Radiation-Induced Low-Dose Hypersensitivity and the Bystander Effect. *Radiation Research*. 2002;157:526–32.

*5.* Cherubini R, De Nadal V, Gerardi S, *et al.* Lack of hyper-radiosensitivity and induced radioresistance and of bystander effect in V79 cells after proton irradiation of different energies. *Radiation Protection Dosimetry*. 2011;143:315–9.

*6.* Fernandez-Palomo C, Seymour C, Mothersill C. Inter-Relationship between Low-Dose Hyper-Radiosensitivity and Radiation-Induced Bystander Effects in the Human T98G Glioma and the Epithelial HaCaT Cell Line. *Radiation Research*. 2016;185:124–33.

*7.* Joiner MC, Marples B, Lambin P, *et al.* Low-dose hypersensitivity: current status and possible mechanisms. *International Journal of Radiation Oncology*Biology*Physics*. 2001;49:379–89.

*8.* Lambin P. Might intrinsic radioresistance of human tumour cells be induced by radiation? *International Journal of Radiation Biology*. 1996;69:279–90.

*9.* Lambin P, Fertil B, Malaise EP, *et al.* Multiphasic Survival Curves for Cells of Human Tumor Cell Lines: Induced Repair or Hypersensitive Subpopulation? *Radiation Research*. 1994;138:S32.

*10.* Lambin P, Mailaise E, Joiner MC. The effect of very low radiation doses on the human bladder carcinoma cell line RTl12. *Radiotherapy and Oncology*. 1994;32:63–72.

*11.* Lambin P, Marples B, Fertil B, *et al.* Hypersensitivity of a Human Tumour Cell Line to Very Low Radiation Doses. *International Journal of Radiation Biology*. 1993;63:639–50.

*12.* Short, C. Mayes, M. Woodcock, H. Jo S. Low dose hypersensitivity in the T98G human glioblastoma cell line. *International Journal of Radiation Biology*. 1999;75:847–55.

*13.* C. Short, S. A. Mitchell, P. Boulto S. The response of human glioma cell lines to low-dose radiation exposure. *International Journal of Radiation Biology*. 1999;75:1341–8.

*14*. Wouters BG, Sy AM, Skarsgard LD. Low-Dose Hypersensitivity and Increased Radioresistance in a Panel of Human Tumor Cell Lines with Different Radiosensitivity. *Radiation Research*. 1996;146:399.

*15*. Harney J, Shah N, Short S, *et al.* The evaluation of low dose hyper-radiosensitivity in normal human skin. *Radiotherapy and Oncology*. 2004;70:319–29.

*16*. Schoenherr D, Krueger SA, Martin L, *et al.* Determining if low dose hyper-radiosensitivity (HRS) can be exploited to provide a therapeutic advantage: A cell line study in four glioblastoma multiforme (GBM) cell lines. *International Journal of Radiation Biology*. 2013;89:1009–16.

*17.* Prasanna A, Ahmed MM, Mohiuddin M, *et al.* Exploiting sensitization windows of opportunity in hyper and hypo- fractionated radiation therapy. *Journal of Thoracic Disease*. 2014;6.

*18*. Joiner MC, Denekamp J, Maughan RL. The Use of 'Top-up' Experiments to Investigate the Effect of Very Small Doses Per Fraction in Mouse Skin. *International Journal of Radiation Biology and Related Studies in Physics, Chemistry and Medicine*. 1985;49:565–80.

*19.* Joiner MC, Johns H. Renal Damage in the Mouse: The Response to Very Small Doses per Fraction. *Radiation Research*. 1988;114:385.

*20.* Parkins CS. The linear quadratic fit for lung function after irradiation with X-rays at smaller doses per fraction than 2 Gy. *British Journal of Cancer*. 1986;320–3.

*21.* Shun Wong C, Minkin S, Hill RP. Linear-quadratic model underestimates sparing effect of small doses per fraction in rat spinal cord. *Radiotherapy and Oncology*.

*22.* Harney J, Short SC, Shah N, *et al.* Low dose hyper-radiosensitivity in metastatic tumors. *International Journal of Radiation Oncology*Biology*Physics*. 2004;59:1190–5.

*23.* Thames HD, Ang KK, Stewart FA, *et al.* Does Incomplete Repair Explain the Apparent Failure of the Basic LQ Model to Predict Spinal Cord and Kidney Responses to Low Doses Per Fraction? *International Journal of Radiation Biology*. 1988;54:13–9.

*24.* Garcia LM, Leblanc J, Wilkins D, *et al.* Fitting the linear–quadratic model to detailed data sets for different dose ranges. *Phys Med Biol*. 2006;51:2813–23.

*25.* Bodgi L, Foray N. The nucleo-shuttling of the ATM protein as a basis for a novel theory of radiation response: resolution of the linear-quadratic model*. *International Journal of Radiation Biology*. 2016;92:117–31.

*26.* Hanu C, Wong R, Sur RK, *et al.* Low-dose non-targeted radiation effects in human esophageal adenocarcinoma cell lines. *International Journal of Radiation Biology*. 2017;93:165–73.

*27.* Desai R, Seymour C, Mothersill C. Isolated Clones of a Human Colorectal Carcinoma Cell Line Display Variation in Radiosensitivity Following Gamma Irradiation. *Dose-Response*. 2022;20:155932582211137.

*28*. Mothersill CE, Moriarty MJ, Seymour CB. Radiotherapy and the potential exploitation of bystander effects. *International Journal of Radiation Oncology*Biology*Physics*. 2004;58:575–9.

*29*. Azzam EI, Little JB. The radiation-induced bystander effect: evidence and significance. *Hum Exp Toxicol*. 2004;23:61–5.

*30*. Mothersill C, Seymour CB. Cell-Cell Contact during Gamma Irradiation Is Not Required to Induce a Bystander Effect in Normal Human Keratinocytes: Evidence for Release during Irradiation of a Signal Controlling Survival into the Medium. *Radiation Research*. 1998;149:256.

*31*. Seymour CB, Mothersill C. Radiation-induced bystander effects — implications for cancer. *Nat Rev Cancer*. 2004;4:158–64.

*32*. Puck TT, Marcus PI. Action of X-Rays on Mammalian Cells. 1956;103:653–66.

*33*. Mothersill C, Bristow RG, Harding SM, *et al.* A role for p53 in the response of bystander cells to receipt of medium borne signals from irradiated cells. *International Journal of Radiation Biology*. 2011;87:1120–5.

# Chapter 5 - Influence of sex of the cell line on the bystander effect and low dose irradiation.

Rhea Desai[1,*], Colin Seymour[1] & Carmel Mothersill[1]

[1]Department of Biology, McMaster University, Hamilton, ON, Canada

The initial concept of the research presented in this chapter and methods were developed by Dr. Carmel Mothersill. All irradiation, cell culture, experimentation, statistical analysis and manuscript writing were completed by the first author. All authors contributed to editing of the manuscript.

# 5.0 Preface

The body of work presented in this chapter was initially conceived by Dr. Carmel Mothersill and Dr. Colin Seymour. All cell cultures, irradiation, curve fitting, and statistical analysis was completed by the first author. Troubleshooting of experiments was completed by the first author with advisory from all authors of this manuscript. The first draft of this manuscript made for publication was written by the first author and subsequently edited by all authors.

The following is a manuscript submitted to the Radiation Research journal in November 2023.

# 5.1 Abstract

This study aims to investigate whether bystander effects following radiation exposure can be modulated by the sex of the donor from which the cell line was originally derived. Previous research suggested using donor explants, a greater sensitivity in females compared to males. Survival curves were developed with doses ranging from 0.01 to 3.0 Gy for four fibroblast cell lines. Two cell lines from males and two from females. Of these cell lines one male and one female line were null for Artemis. The protein Artemis has been found to be involved in the repair of radiation induced DNA double strand breaks and thus Artemis-null cell lines have compromised ability to repair DNA breaks which render the lines more radiosensitive. For this reason, Artemis-null lines were included as controls for radiosensitivity. Low dose hypersensitivity (HRS) and radiation induced bystander effect (RIBE) is noted in both male and female derived cell lines. A significant difference in cell survival is reported following both direct and bystander exposure to radiation between the male (1BR.3) and female (48BR) cell lines. The 48BR (female) cell line was found to show a more sensitive response to both direct and bystander irradiation compared to 1BR.3 (male). Our findings of greater female radiosensitivity support previous data and suggest there is an influence of donor sex on the non-targeted effects of ionizing radiation. An unexpected finding that RIBE did not depend on Artemis status may suggest that DNA damage repair status is not relevant to RIBE induction.

## 5.2 Introduction

Ionizing radiation is known to have the ability to cause damage in living systems due to energy deposition in DNA. There are various factors that can influence the way a system may react to the stress of radiation. These can include age, genetics, lifestyle factors, comorbidities, and sex [*1*]. All of these complex factors can impact the radiosensitivities of different populations and the way in which systems may respond or be damaged by radiation. The literature [*1–3*] has noted that of these factors, sex is often overlooked but research on this particular factor has considerable relevance for radiation protection [*1*]. This paper aims to build on findings of notable differences between the male and female response to ionizing radiation by focusing on low dose responses which are both clinically and environmentally relevant. In order to address this question of radiosensitivity, Artemis-null female and male cell lines are included as a control for radiosensitivity. Due to the compromised status of Artemis, a greater sensitivity to radiation in these lines is expected. This helps establish a good comparison against male and female lines with normal Artemis status.

There is a large body of evidence that supports the idea that males and females respond to ionizing radiation differently. Research groups have investigated the disparity in radiosensitivity between males and females in animals and have found alterations in cellular pathways such as apoptosis and DNA methylation [*3–5*]. For example, male and

female mice show differences through epigenome analysis which revealed sex-specific disparities in DNA and histone methylation, DNA methyltransferases and methyl-binding proteins when tissues are exposed to ionizing radiation. The liver and spleens of female mice revealed increased hypomethylation. Brain tissues and overall behavior were also altered more in females. Such investigations have found a greater long term radiosensitivity in females over males.

The Life Span Study based on data collected from Japanese survivors of Hiroshima and Nagasaki has been a major source for information on health effects because the cohort consists of survivors of varying sex and age [*6,7*]. It is evident that cancer risk is increased in these high dose exposed populations and that individuals exposed at a younger age have a higher associated risk of cancer (pediatric females being most sensitive [*7*]). Whether acute doses below 0.5 Gy significantly increased risk of radiation induced disease is less understood. So, while research suggests some role of sex-linked effects in response to radiation exposure, focused efforts are still needed in low doses.

Studies have also reported differences in acute and chronic exposure to ionizing radiation and such effects have been observed in various environmental and clinical settings. For example, a study by Pogribny et al., reports that radiation-induced DNA methylation changes were both sex and tissue dependent following acute and chronic radiation exposures [*5*]. Following a 5 Gy X-ray acute exposure, significant genome hypomethylation was observed in female mice livers. Alternatively, no significant change

was observed in male mice livers. When studying chronic exposures, no significant DNA methylation was noted. Other studies have also investigated different tissues with varying times post irradiation with the general understanding being epigenetic processes affected by ionizing radiation vary in tissues, organs, and sex of the organism.

In a 2008 study by Koturbash et al. the radiation induced bystander effect (RIBE) was investigated with respect to the level of radiation induced DNA damage [*3*]. The radiation-induced bystander effect refers to cells, tissues or organisms that were not exposed to direct ionizing radiation but behave as though they were. It was found that there is a difference in RIBE between males and females and that male spleen tissue showed a greater level of DNA damage. Interestingly the group emphasizes the need for further investigation of bystander spleens of male and female mice due to *in vitro* data that suggests a temporal difference in cellular response [*3*]. Overall they reported a greater loss of DNA methylation and accumulation of DNA damage in spleen of whole body and head-exposed male mice than females but note the mechanisms of sex differences should be further investigated [*1,3*]. Furthermore, a 2001 study by Mothersill et al. investigated the role of gender, smoking status and the existence of a bladder malignancy on production of bystander signals using tissues from more than 100 patients [*8*]. An overall significant difference between males and females was observed using HPV-G cells as reporter cells for the bystander medium transfer assay. It was concluded that females displayed more toxicity to bystander effects than males [*8*]. Previous work by a student in our group

analyzed published bystander data available in literature to determine whether there was any commonality in studies from different laboratories with regard to a number of factors influencing RIBE. One of these factors was the sex of the cell line. [*2*]. The conclusion based on these studies involving 64% male cell lines and 32% female cell lines was that female cell lines, on average produced a larger reduction in cell survival compared to male cell lines.

This evolving understanding of the various factors involved in an ionizing radiation induced response peaks further curiosity about non-targeted effects. While groups work to elucidate underlying processes and mechanisms, these confounding factors such as sex in the context of non-targeted effects should also be given attention. To further understand the influence of sex on RIBE, the present study investigates four cell lines for changes in radiosensitivity following a low dose range of ionizing radiation exposure.

## 5.3 Methods

### 5.3.1 Cell culture

Four cell lines (1BR.3, 48BR, CJ176 and F02/385) were used in both survival curve and radiation induced bystander effect assays. Cell lines 1BR.3 (Artemis wild type) and CJ176 (Artemis null) are of male origin and 48BR (Artemis wild type) and F02/385 (Artemis null) are of female origin. Artemis null cell lines are included in experiments to ensure radiosensitivity in these cell lines. A cell lines were provided by the Genome Damage and Stability Center in the United Kingdom. All cells were cultured regularly using Dulbecco's Modified Eagle Medium (DMEM) supplemented with 15% FBS, 100 U/ml penicillin, 100 ug/mL streptomycin, and 20.5 mM L-Glutamine. Growth media was changed weekly, and cells were cultured when 70-80% confluent. Cell cultures were frown in 75 $cm^2$ Falcon tissue culture flasks (VWR Canada) and incubated at 37°C and 5% $CO_2$. Cells were trypsinized for cell culture and experiments using 25% phenol red-free trypsin solution combined with 0.192 mM EDTA when growth was confluent. All reagents were purchased from Gibco, ThermoFisher Scientific.

### 5.3.2 Irradiations

The McMaster Taylor Radiobiology Cesium-137 source was used for all irradiations. The source had a dose rate of 198.4 mGy/min during the experiments at a source to flask distance of 30 cms.

### 5.3.3 Survival Curve Assays

Cell cultures grown to confluence were used to set up for clonogenic survival assays. Cells were detached using the trypsin working solutions described in 2.1. Trypsinized cultures were neutralized with a greater volume of DMEM growth media. Cell seeding concentrations were determined using a Bio-Rad TC20 automated cell counter (Bio-Rad Life Science Research Division, Canada). For all experiments cells were seeding in T25 Falcon tissue culture flasks (VWR Canada). T25 flasks were seeded using the clonogenic assay method described previously by Puck and Marcus[9]. In this assay, low densities (300 cells) of cells destined for irradiation are plated in T25 flasks. Plating efficiencies of approximately 30% were achieved. Clonogenic assays were used to develop survival curves with doses of 0, 0.01, 0.03, 0.05, 0.1, 0.3, 0.5, 1.0, 2.0 and 3.0 Gy. Low dose, dose points were chosen to observe ionizing radiation effects in the low dose range. After irradiation all experimental flasks were immediately returned to the incubator and grown for 11 days at 37°C in an atmospheric environment of 5% $CO_2$ in air. Media was then

discarded, and flasks were stained with 15% Carbol Fuchsin solution (Ziehl Neelson, Milipore Sigma) on day 11 of growth. Cell colonies were then counted and surviving fraction was determined. GraphPad Prism 10 software (GraphPad Software Inc., LaJolla CA) was used to create survival curve graphs.

### 5.3.4 Radiation-Induced Bystander Effect Assay

T25 Flacon flasks were used for all bystander effect assay. Cells were seeded in the T25 flasks with 5mL DMEM growth media (described in 5.3.1) and incubated for 6 hours at 37°C and 5% $CO_2$. Plating efficiency, direct irradiation (2.0 Gy), bystander effect donor and recipient, and sham donor and recipient flasks were seeded for each trial. Sham donor flasks were not irradiated but serve as a medium transfer control to confirm no effect of the assay's medium change. All donor flasks were seeded with 150 000 cells while all other flasks were seeded with 300 cells. Post 6-hour incubation, direct irradiation and bystander effect donor flasks were irradiated as described in 5.3.2 to 2.0 Gy. Upon completion of irradiation, flasks were returned to the incubator for an hour and then medium transfer of donor medium to recipient flasks was completed. Medium from recipient flasks was discarded and donor media was transferred using a 0.22-μm filter and 30 mL plastic syringe (Millipore Sigma). A filter was used on the syringe to ensure no cells were transferred to the recipient flasks. This medium transfer bystander assay technique was used for both

bystander effect and sham treatment flasks. All flasks were then incubated as previously described for 10 days and stained with 15% Carbol Fuschin on the final day. Colonies could then be counted, and data was used to make bar graphs for treatment comparison using GraphPad Prism 8.

### 5.3.5 Statistical Analysis

Survival curve and bystander data in this study is a result of a mean of three independent trials using three replicates (n=9). Least square error linear regression analyses were used to produce induced-repair model fits using GraphPad Prism 10 (GraphPad Software Inc., LaJolla CA). Standard error of the mean (SEM) error bars is used in all figures. Variance between groups in the bystander effect assays was determined using t-tests between the sham and bystander and sham and direct irradiation groups. Post hoc analyses completed using Welch's t-test. Significance was determined at the 95% confidence interval.

# 5.4 Results

## 5.4.1 Low Dose Cell Survival Curves

Cell survival curves are found in Figures 5.1 to 5.4 fitted with the induced-repair model. Here variances in radiosensitivity are observed between male cell lines and female cell lines and findings are summarized in Table 5.1. Both Artemis-null cell lines; male (CJ176) and female (F02/385), display a rapid decrease in cell survival. The $\alpha s/\alpha r$ ratio indicates the magnitude of induced radioprotection as dose increases[10] and $d_c$ represents the dose where there is maximum HRS and a transition to IRR. Values for $\alpha s$ can also be found in Table 5.1, directly indicating radiosensitivity. As expected in the Artemis-null cell lines CJ176 and F02/385, their radiosensitivity in low doses is much greater than their normal counterparts 1BR.3 and 48BR respectively. This shows hyperradiosensitivity in the very low doses. When comparing normal male 1BR.3 to normal female 48BR, it is evident that 48BR is more radiosensitive in low doses. This is again shown by the larger $\alpha s$ value for 48BR cells compared to 1BR.3 cells.

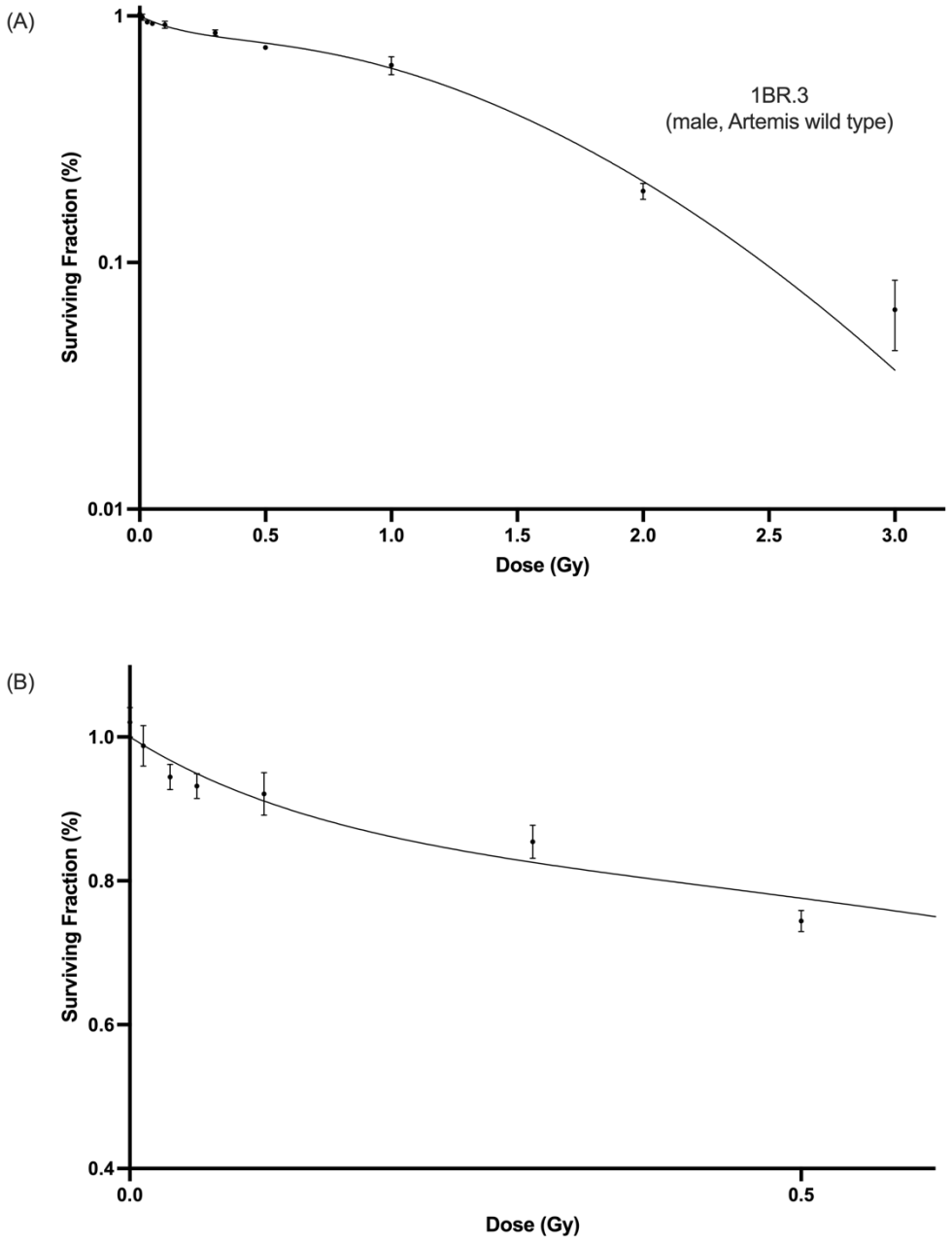


**Figure 5.1:** Cell survival curve for 1BR.3 (male, Artemis wild type) cells exposed to Cesium-137 gamma radiation for doses of 0 to 3.0 Gy. Data are fitted with the Induced-Repair model. (A) Full survival curve for 1BR.3 cells. (B) Enlarged survival curve portion with dose points between 0 and 0.5 Gy. Error bars are SEM for n=9.

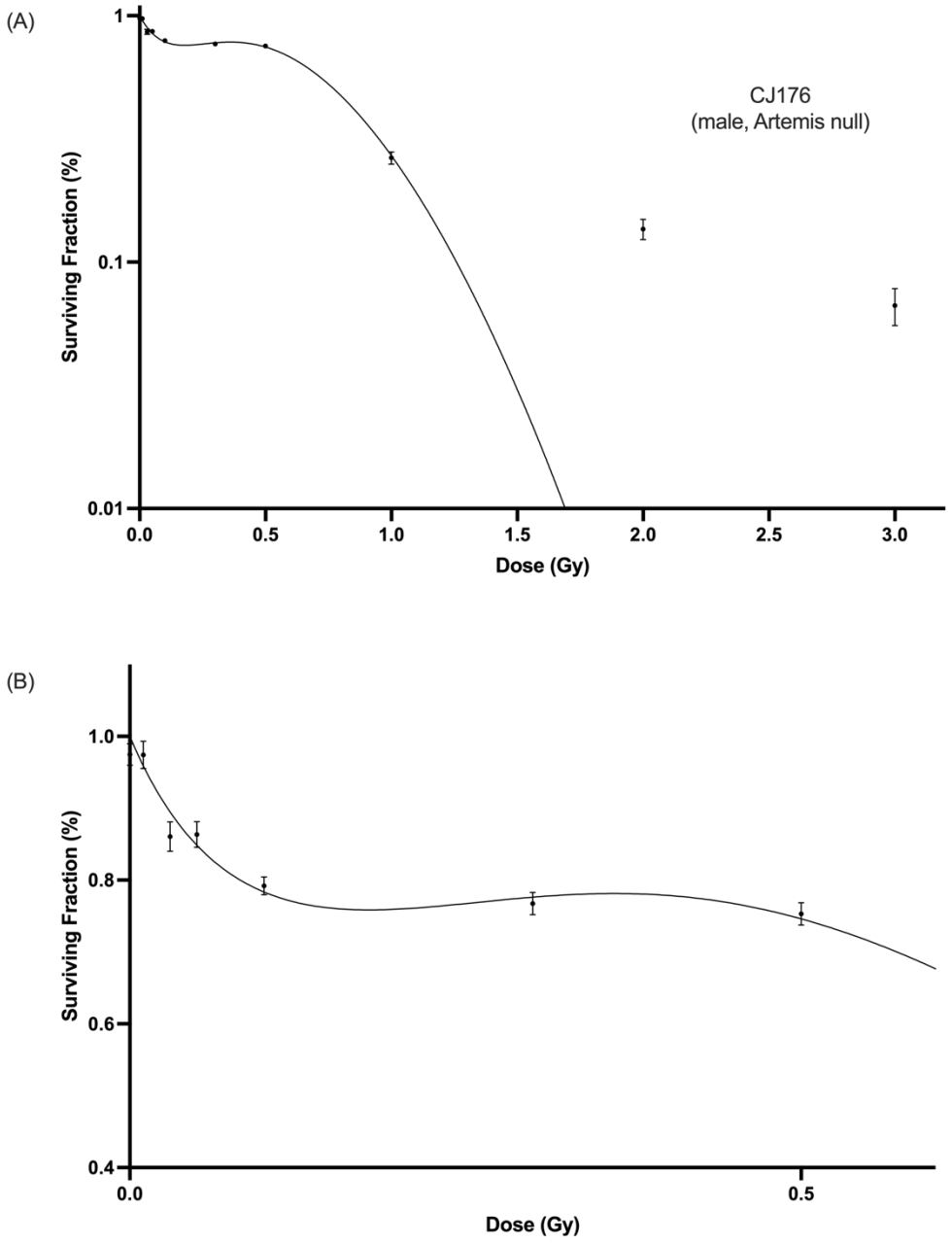


**Figure 5.2:** Cell survival curve for CJ176 (male, Artemis null) cells exposed to Cesium-137 gamma radiation for doses of 0 to 3.0 Gy. Data are fitted with the Induced-Repair model. (A) Full survival curve for CJ176 cells. (B) Enlarged survival curve portion with dose points between 0 and 0.5 Gy. Error bars are SEM for n=9.

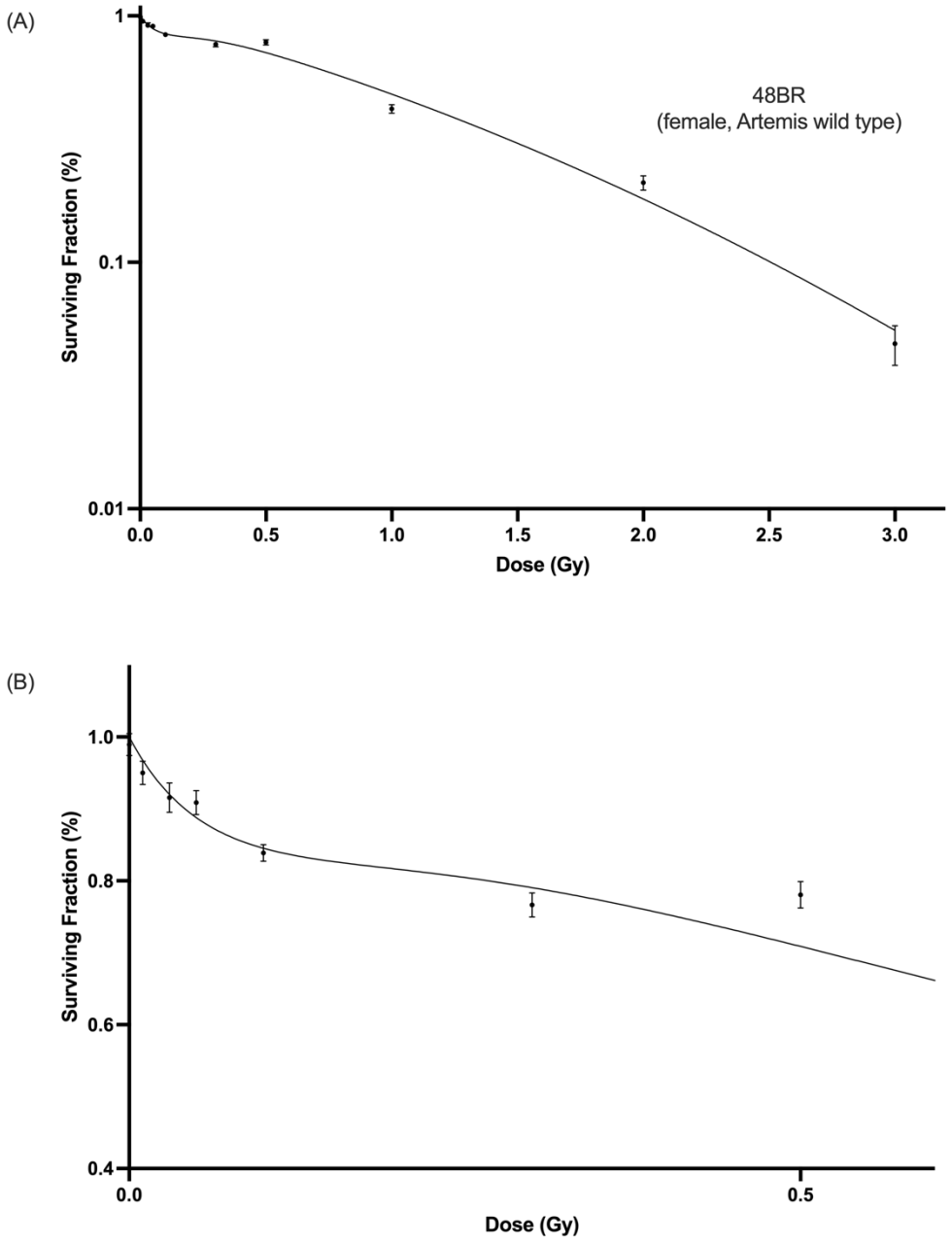


**Figure 5.3:** Cell survival curve for 48BR (female, Artemis wild type) cells exposed to Cesium-137 gamma radiation for doses of 0 to 3.0 Gy. Data are fitted with the Induced-Repair model. (A) Full survival curve for 48BR cells. (B) Enlarged survival curve portion with dose points between 0 and 0.5 Gy. Error bars are SEM for n=9.

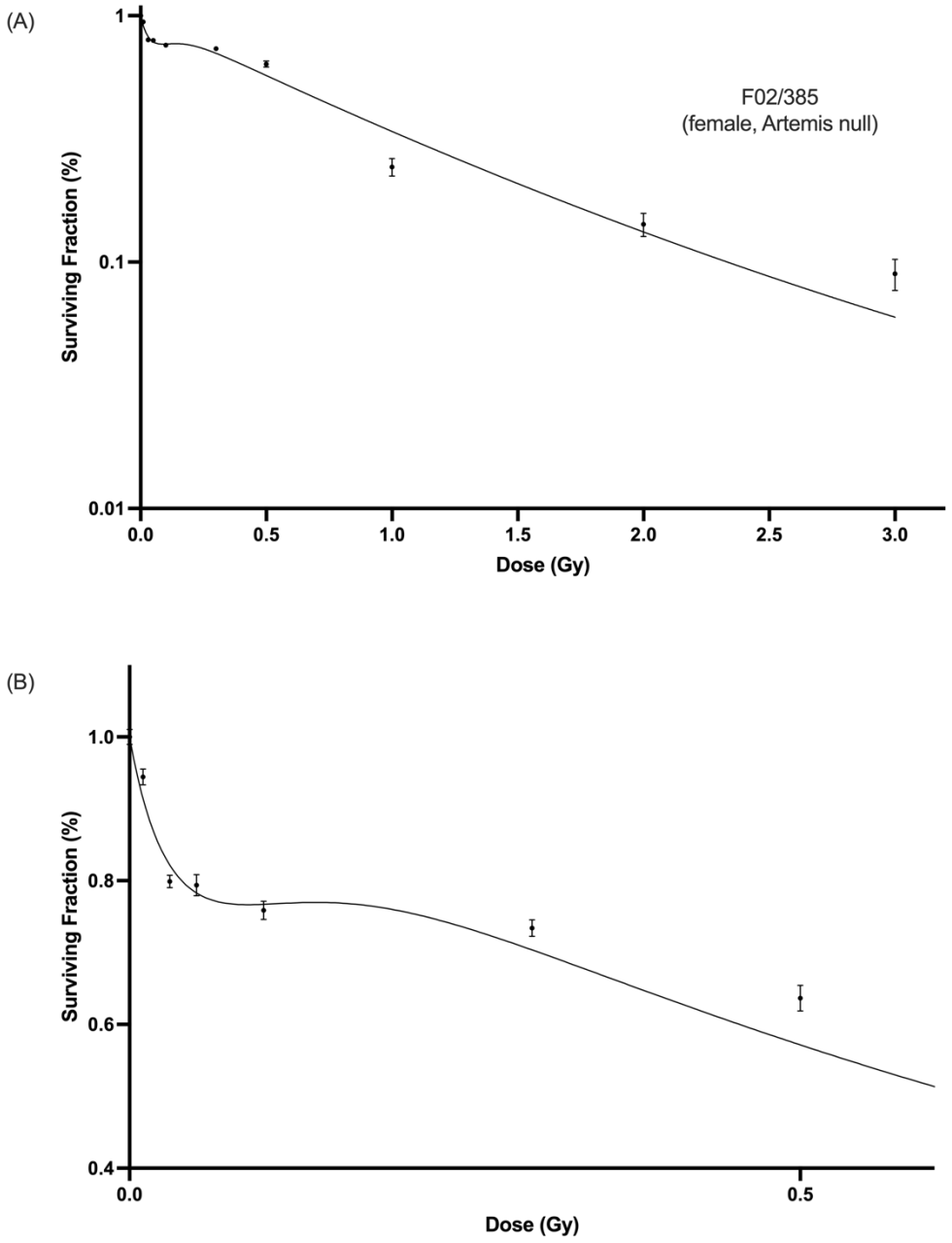


**Figure 5.4:** Cell survival curve for F02/385 (female, Artemis null) cells exposed to Cesium-137 gamma radiation for doses of 0 to 3.0 Gy. Data are fitted with the Induced-Repair model. (A) Full survival curve for F02/385 cells. (B) Enlarged survival curve portion with dose points between 0 and 0.5 Gy. Error bars are SEM for n=9.

**Table 5.1:** A summary of survival curve fitting parameters using the Induced-Repair model.

| Parameter | F02/385 | CI (95%) | 48BR | CI (95%) | CJ176 | CI (95%) | 1BR.3 | CI (95%) |
|---|---|---|---|---|---|---|---|---|
| $\alpha r$ | 1.2 | 1.0-1.3 | 0.61 | 0.49-0.72 | -0.80 | -4.8-0.15 | 0.10 | *-0.40 |
| $\alpha s$ | 10 | 8.1-14 | 3.5 | 2.5-5.1 | 4.4 | 3.3-5.9 | 1.2 | 0.65-2.4 |
| β | -0.071 | -0.15-0.052 | 0.12 | 0.051-0.21 | 2.1 | 1.0-5.3 | 0.33 | -0.081-* |
| $d_c$ | 0.055 | 0.043-0.071 | 0.098 | 0.060-0.14 | 0.18 | 0.10-0.44 | 0.33 | 0.16-* |
| $\alpha s/\alpha r$ | 8.3 | | 5.8 | | -5.6 | | 7.2 | |
| $r^2$ | 0.97 | | 0.97 | | 0.96 | | 0.95 | |

* - unbound confidence interval value

### 5.4.2 Radiation Induced Bystander Effect

RIBE assays were conducted to investigate differences in bystander signals between male and female cell lines. Figure 5 demonstrates the differences in cell survival following either receipt of irradiated cell culture medium or through a direct 2.0 Gy dose of ionizing radiation. Both donor and recipient cells in each scenario are of the same origin. For comparison, a sham group is also included to indicate there is no effect of the medium transfer RIBE assay on the bystander and direct treatment groups. All cell lines displayed sensitivity to direct irradiation and bystander medium transfer. RIBE was also observed in all cell lines regardless of sex or Artemis status. Female cell line 48BR displayed a stronger bystander effect response and increased cell killing following exposure to irradiated cell culture medium compared to male cell line 1BR.3. Both 48BR and 1BR.3 cell lines are normal for Artemis status. When comparing cell lines null for Artemis status to each other, they did not exhibit a significant difference in response to direct or bystander radiation. Comparison between the two male cell lines revealed a significant difference in survival following both direct and bystander irradiation however the same comparison between the female cell lines did not result in a significant difference. These findings are summarized in Table 5.2.

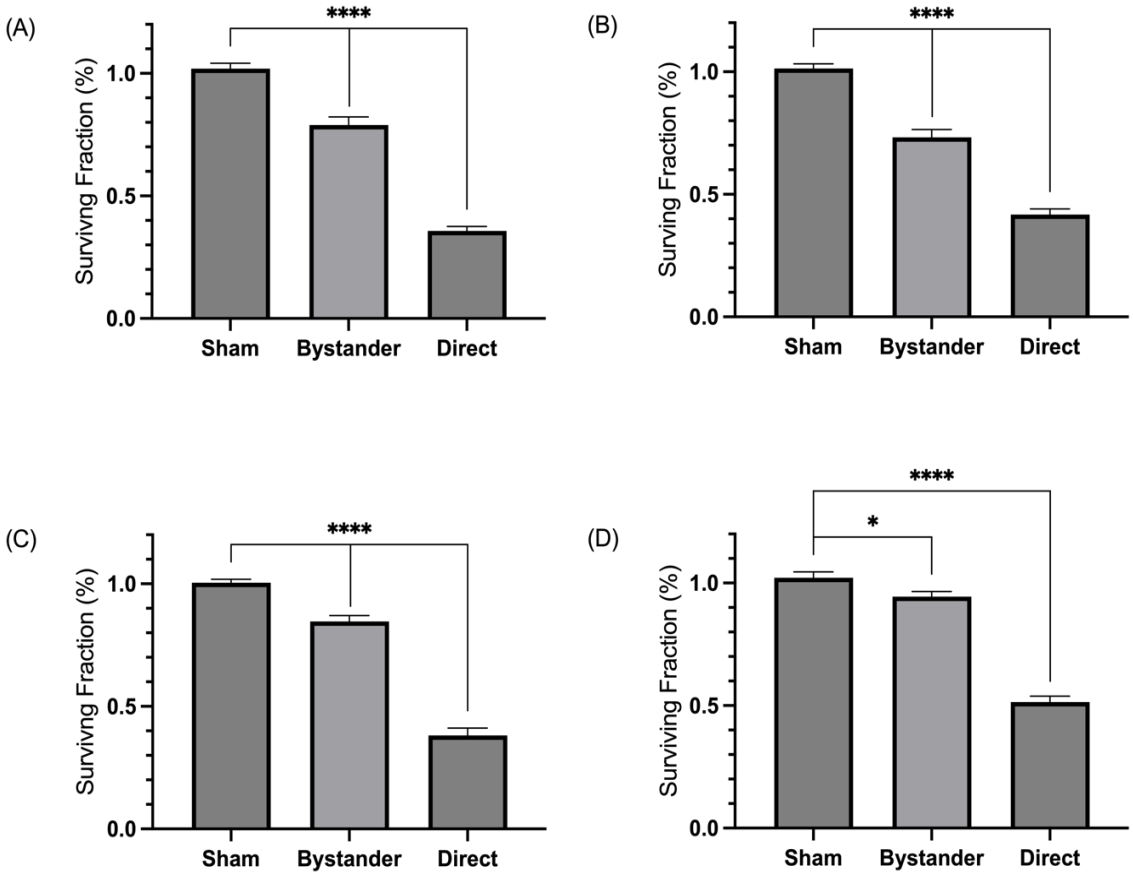


**Figure 5.5:** Radiation induced bystander effect (RIBE) assays using for (A) F02/385 (female, Artemis null), (B) 48BR (female, wild type), (C) CJ176 (male, Artemis null) and (D) 1BR.3 (male, wild type) cell lines. For all cell lines donor and recipient cells are of the same kind. Sham represents a RIBE protocol control exposed to only transferred cell culture medium from non-irradiated donor cells. Bystander represents cells exposed to irradiated cell culture medium collected from donor cells irradiated with 2.0 Gy. Direct represents cells irradiated directly with 2.0 Gy. All data is presented as the mean ± SEM (n = 9). (****$p < .0001$), (*$p < 0.05$) indicates a significant difference between treatment groups and sham.

**Table 5.2:** Statistical differences between response to direct ionizing radiation and bystander radiation of cell lines with varying Artemis status. 1BR.3 and CJ176 are of male origin and 48BR and F02/385 are of female origin.

| Cell Lines | Artemis Status | Sex of Cell Line | Direct Ionizing Radiation | Bystander Radiation |
|---|---|---|---|---|
| 1BR.3 vs. 48BR | both wild type | 1BR.3 male<br>48BR female | $p<0.05$ | $p<0.0001$ |
| CJ176 vs. F02/385 | both null | CJ176 male<br>F02/385 female | ns | ns |
| 1BR.3 vs. CJ176 | 1BR.3 wild type<br>CJ176 null | 1BR.3 male<br>CJ176 male | $p<0.05$ | $p<0.05$ |
| 48BR vs. F02/385 | 48BR wild type<br>F02/385 null | 48BR female<br>F02/385 female | ns | ns |

# 5.5 Discussion

Overall, a greater sensitivity to the bystander signals is observed in females compared to males (Figure 5.7) which opposes the *in vivo* RIBE data published by Koturbash et al. in 2008. This finding in cell culture is an interesting result as much data on sex effects of ionizing radiation heavily supports the idea that female species are more sensitive to radiation damage due to the presence of reproductive tissues and organs which is not the case in the present study. This finding suggests a greater than expected role of hormones or x-linked factors. While differences are noted between our cell culture work and *in vivo* work by other groups, it is important to note that different species may vary in response to stress such as radiation. Data published by Mothersill et al. in 2001 using HPV-

G reporter cells provides supporting evidence for findings of this present study [*8*]. A greater decrease in clonogenic cell survival when cells are treated with irradiated cell culture medium from female donors compared to male donors was concluded [*8*].

This study also highlights differences in the bystander effect in cell lines of male or female origin. Ionizing radiation can be utilized clinically and diagnostically to help with the treatment of diseases, however the effects it may have on neighboring cell populations can be of concern. Additionally, as radiation science research aims to improve standards for safety, it is important to consider the non-targeted effects of radiation and how the role of sex can affect outcomes. In this study we test four cell lines; two male and two female, to better understand RIBE. Of the four cell lines, two are null for the protein Artemis. Artemis is known to function in ionizing radiation induced double strand break repair [11]. Artemis null cell lines CJ176 (male) and F02/385 (female) are used as controls for radiosensitivity to ionizing radiation. Cell lines 1BR.3 (male) and 48BR (female) have normal Artemis status.

Comparison of all cell lines reveals a novel finding that there is no significant difference in cell survival following direct or bystander irradiation between female 48BR and F02/385 cell lines (Table 5.2) meaning the presence or absence of the *ARTEMIS* gene does not affect female radiation response in these experiments. However, a significant

difference was observed in the direct and bystander irradiated groups for male cell lines 1BR.3 and CJ176. Here cells null for Artemis that have impaired ability to repair double strand DNA breaks do show a more radiosensitive response both to direct irradiation and to bystander signals. The *ARTEMIS* gene has been reported to be responsible for diseases such as radiosensitive-severe combined immunodeficiency (RS-SCID) and various studies both *in vitro* and *in vivo* have noted the protein Artemis is required for the non-homologous end joining (NHEJ) pathway in DSB repair [*11–18*]. Cells deficient in Artemis experience increased sensitivity to ionizing radiation compared to their normal counterparts [*11,12,18*]. Since a significant difference is not observed between the two female cell lines used, we put forward evidence that DNA is not the only primary target of low dose ionizing radiation [*20,21*]. In classical radiation biology, target theory describes that cells contain at least one critical target that if hit by a track of ionizing radiation would kill the cell or produce some type of damaging effect [*21–23*]. This target has been widely accepted as DNA however, researchers have postulated other possible targets [*20,24*]. To further elucidate the mechanisms in play here, further research questioning the targets of low dose ionizing radiation is required. Particularly due to the interconnectedness of DNA to a majority of biological processes, evidence for other targets of ionizing radiation damage can be difficult to obtain.

Today, much research relies on the use of the linear-quadratic (LQ) model to model cell killing following ionizing radiation exposure, but when modeling dose response

relationships particularly in low doses, the LQ model often underestimates possible effects [*10,25–28*]. Previous findings by Desai et al. highlighted the poor fit of the linear-quadratic model and suggested difficulties in low dose modeling. For this reason, data in this present study are fit using the induced-repair (IR) model found to provide a better fit particularly in low doses [*25*]. As evident in Figures 5.1 to 5.4, low dose HRS is observed where a greater than expected reduction in cell survival is evident at low doses following a bout of increased radioresistance at doses generally greater than 0.1 Gy. This low dose effect is modeled more accurately using the IR model.

In summary, this paper supports other in vitro work suggesting human female cells and tissue explants are more sensitive to RIBE signals than males, but it disagrees with in vivo studies in mice suggesting that males have a more sensitive response. An unexpected finding was that in the female cell lines the presence or absence of the *ARTEMIS* gene did not affect either the direct response to low dose radiation or the bystander response. However, in males Artemis null cells were more radiosensitive and had greater sensitivity to bystander signals. This study highlights the importance of continued investigation of low dose effects of ionizing radiation with particular attention to sex for improving recommendations on radiation safety.

## 5.6 Acknowledgements

We acknowledge the grant support for this work from the Natural Sciences Resource Council (NSRC) and Canada Research Chairs 950-221284.

## 5.7 Declaration of Conflicting Interests

The author(s) declared no potential conflicts of interest with respect to the research, authorship, and/or publication of this article.

## 5.8 References


1 Narendran N, Luzhna L, Kovalchuk O. Sex Difference of Radiation Response in Occupational and Accidental Exposure. *Front Genet*. 2019;10:260.

2 Gresham C. *An investigation of various intrinsic and external factors that influence in vitro cell survival outcomes during radiation-induced bystander effect experiments.* 2023. http://hdl.handle.net/11375/29000

3 Koturbash I, Kutanzi K, Hendrickson K, *et al.* Radiation-induced bystander effects in vivo are sex specific. *Mutation Research/Fundamental and Molecular Mechanisms of Mutagenesis*. 2008;642:28–36.

4 Kovalchuk O, Burke P, Besplug J, *et al.* Methylation changes in muscle and liver tissues of male and female mice exposed to acute and chronic low-dose X-ray-irradiation. *Mutation Research/Fundamental and Molecular Mechanisms of Mutagenesis*. 2004;548:75–84.

5 Pogribny I, Raiche J, Slovack M, *et al.* Dose-dependence, sex- and tissue-specificity, and persistence of radiation-induced genomic DNA methylation changes. *Biochemical and Biophysical Research Communications*. 2004;320:1253–61.

6 Kamiya K, Ozasa K, Akiba S, *et al.* Long-term effects of radiation exposure on health. *The Lancet*. 2015;386:469–78.

7 Hasegawa A, Tanigawa K, Ohtsuru A, *et al.* Health effects of radiation and other health problems in the aftermath of nuclear accidents, with an emphasis on Fukushima. *The Lancet*. 2015;386:479–88.

8 Mothersill C, Rea D, Wright EG, *et al.* Individual variation in the production of a 'bystander signal following irradiation of primary cultures of normal human urothelium. *Carcinogenesis*. 2001;22:1465–71.

9 Puck TT, Marcus PI. Action of X-Rays on Mammalian Cells. 1956;103:653–66.

10 Lambin P, Fertil B, Malaise EP, *et al.* Multiphasic Survival Curves for Cells of Human Tumor Cell Lines: Induced Repair or Hypersensitive Subpopulation? *Radiation Research*. 1994;138:S32.

11 Riballo E, Doherty A, Smith GCM, *et al.* A Pathway of Double-Strand Break Rejoining Dependent upon ATM, Artemis, and Proteins Locating to ⁄-H2AX Foci. *Molecular Cell*.

12 Woodbine L, Grigoriadou S, Goodarzi AA, *et al.* An Artemis polymorphic variant reduces Artemis activity and confers cellular radiosensitivity. *DNA Repair*. 2010;9:1003–10.

13 Kurosawa A, Adachi N. Functions and Regulation of Artemis: A Goddess in the Maintenance of Genome Integrity. *JRR*. 2010;51:503–9.

14 Li L, Salido E, Zhou Y, *et al.* Targeted Disruption of the Artemis Murine Counterpart Results in SCID and Defective V(D)J Recombination That Is Partially Corrected with Bone Marrow Transplantation. *The Journal of Immunology*. 2005;174:2420–8.

15 Ma Y, Pannicke U, Schwarz K, *et al.* Hairpin Opening and Overhang Processing by an Artemis/DNA-Dependent Protein Kinase Complex in Nonhomologous End Joining and V(D)J Recombination. *Cell*. 2002;108:781–94.

16 Ulus-Senguloglu G, Arlett CF, Plowman PN, *et al.* Elevated expression of artemis in human fibroblast cells is associated with cellular radiosensitivity and increased apoptosis. *Br J Cancer*. 2012;107:1506–13.

17 Darroudi F, Wiegant W, Meijers M, *et al.* Role of Artemis in DSB repair and guarding chromosomal stability following exposure to ionizing radiation at different stages of cell cycle. *Mutation Research/Fundamental and Molecular Mechanisms of Mutagenesis*. 2007;615:111–24.

18 Jeggo P. The Greek Goddess, Artemis, reveals the secrets of her cleavage. *DNA Repair*. 2002;1:771–7.

19 Sridharan DM, Whalen MK, Almendrala D, *et al.* Increased Artemis levels confer radioresistance to both high and low LET radiation exposures. *Radiat Oncol*. 2012;7:96.

20 Mothersill C, Seymour CB. Radiation-induced bystander effects and the DNA paradigm: An "out of field" perspective. *Mutation Research/Fundamental and Molecular Mechanisms of Mutagenesis*. 2006;597:5–10.

21 Nomiya T. Discussions on target theory: past and present. *Journal of Radiation Research*. 2013;54:1161–3.

22 Powers EL. Considerations of Survival Curves and Target Theory. *Phys Med Biol*. 1962;7:3–28.

23 Kadhim M, Salomaa S, Wright E, *et al.* Non-targeted effects of ionising radiation—Implications for low dose risk. *Mutation Research/Reviews in Mutation Research*. 2013;752:84–98.

24 Mothersill C, Seymour C. Targets, pools, shoulders, and communication – a reflection on the evolution of low-dose radiobiology. *International Journal of Radiation Biology*. 2019;95:851–60.

25 Fernandez-Palomo C, Seymour C, Mothersill C. Inter-Relationship between Low-Dose Hyper-Radiosensitivity and Radiation-Induced Bystander Effects in the Human T98G Glioma and the Epithelial HaCaT Cell Line. *Radiation Research*. 2016;185:124–33.

26 Ryan LA, Seymour CB, Joiner MC, *et al.* Radiation-induced adaptive response is not seen in cell lines showing a bystander effect but is seen in lines showing HRS/IRR response. *International Journal of Radiation Biology*. 2009;85:87–95.

27 Thomas C, Martin J, Devic C, *et al.* Impact of dose-rate on the low-dose hyper-radiosensitivity and induced radioresistance (HRS/IRR) response. *International Journal of Radiation Biology*. 2013;89:813–22.

28 Desai R, Seymour C, Mothersill C. Isolated Clones of a Human Colorectal Carcinoma Cell Line Display Variation in Radiosensitivity Following Gamma Irradiation. *Dose-Response*. 2022;20:155932582211137.

# Chapter 6 - Conclusion

The research conducted in this thesis sought to explore low dose responses in a variety of situations. Through exploring heterogeneity of a cell line as well as the influence of factors such as sex on radiosensitivity, a better understanding of low dose effects is achieved. Dose-response relationships derived from high dose exposures do not extrapolate to the low dose region due to evidence of low dose effects [1,2]. However certain dose-response relationships such as data modelled with the induced-repair model represent the low dose region with improvement [3]. This is emphasized throughout this thesis and is summarized below. This final chapter summarizes main findings of this thesis and recommendations for future work.

## 6.1 Main Findings

### 6.1.1 Isolated clones of a human colorectal carcinoma cell line display variation in radiosensitivity following gamma irradiation

The work presented in Chapter 3 aimed to identify variation in radiosensitivity in clonal populations of an HCT 116 p53 wild type cell line. Seven clonal lines were isolated from the parent population and grown for use in developing cell survival curves. The parent and all clonal lines were irradiated with doses ranging from 0.5 to 15 Gy and fitted with two commonly used models to describe the dose-response relationship. The linear-quadratic model and multi-target model were used, and it was determined that the multi-target model provided the overall best fits. Medium transfer bystander effect assays were also conducted for the parent and all clonal lines. Upon analysis of curve fitting parameters and bystander effect assay results, a relationship was determined between the extrapolation number, *n*, from the multi-target model and the extent to which bystander cell killing occurred. Clone A had the largest *n* value while Clone G had the smallest. It was found that Clone A did not respond to non-targeted exposure to radiation through the bystander medium transfer assay, but Clone G did show a significant reduction in cell survival following receipt of the bystander medium transfer. Variation of clonal populations in their

response to bystander treatment also lends evidence to the heterogeneity of the initial cell population, ultimately contributing to the overall sensitivity of the cell line.

### 6.1.2 Heterogeneity of radiation response in clonal variants of a human cell line.

Chapter 4 took a closer look at low dose radiation responses and built on the work presented in Chapter 3. Using the previously derived clonal cell lines, the low dose portion of all cell line survival curves was expanded giving insight to the presence of low dose phenomena such as the transition of HRS to increased IRR. All clonal lines were irradiated to include six doses in the range of 0.01 to 0.5 Gy. Survival curves were then fitted with the linear-quadratic and induced-repair models. It is evident that even with an extensive data set, the linear-quadratic model has difficulty accurately representing low dose data. The induced-repair model provided a better fit to the data due to parameters designed to represent low dose effects. Low dose hyperradiosensitivity was found in the parent and all clonal lines below 0.27 Gy. This shows that low dose exposures have the potential to significantly influence overall dose-response relationships. It was also found that the radiation induced bystander effect and low dose hyperradiosensitivity can occur concurrently in a cell line suggesting the mechanisms may be linked. These findings build on previous work by our group that once suggested RIBE and HRS/IRR to be mutually exclusive

mechanisms [4] and the range in which these responses can occur together may only be in a select dose range [5] suggesting that p53 has a role in the range of doses in which these two phenomena can occur.

### 6.1.3 Influence of sex of the cell line on the bystander effect and low dose irradiation.

The work reported in Chapter 5 aimed to investigate whether there is a role or influence of sex of a cell line on RIBE. The interest of this study was focused on low dose effects and RIBE. Here four cell lines (two male and two female) were used and of these four cell lines, two are null for the protein Artemis (one male and one female). The null cell lines were included as a control for radiosensitivity since Artemis is involved in DNA double strand break repair and thus Artemis-null cell lines render more radiosensitive. Survival curves were developed with doses in the range of 0.01 to 3.0 Gy and curves were fitted with the induced-repair model previously determined to describe low dose effects more accurately. It was found that the two Artemis-null cell lines were most radiosensitive, but the normal female cell line (48BR) was more sensitive than the normal male cell line (1BR.3). This was evident through the alpha curve fitting parameters $\alpha s$ designed to demonstrate low dose responses. Low dose hyperradiosensitivity was observed in all cell lines. RIBE medium transfer assays were also conducted on all four cell lines and a significant

reduction in cell survival was evident in all cell lines. Most notably, the female normal cell line 48BR displayed a significantly higher reduction in cell survival following bystander medium transfer compared to the normal male 1BR.3 cell line.

## 6.2 Concluding Statements & Future Work

The work presented in this thesis investigated low dose responses to radiation and analyzed various curve fitting models. Through demonstration of instances in which HRS and RIBE are observed, a better understanding of low dose effects is gained. Exploring the commonly used HCT 116 p53 wild type cell line revealed heterogeneity adding to the overall radiosensitivity of the cell line and found HRS in very low doses. The influence of sex of the cell line on RIBE and low dose HRS highlights the importance of continued focus on low doses. Thus, future work should continue to investigate cell lines with interest in p53 status, sex and other factors which may contribute to the overall radiosensitivity of a cell line, tissue or organism. Factoring in all of these components will contribute to elucidating the pathways which render living systems more radiosensitive and vulnerable to chronic and acute exposure.

## 6.3 References


1 Desai R, Seymour C, Mothersill C. Isolated Clones of a Human Colorectal Carcinoma Cell Line Display Variation in Radiosensitivity Following Gamma Irradiation. *Dose-Response*. 2022;20:155932582211137.

2 Mothersill C, Rusin A, Seymour C. Low doses and non-targeted effects in environmental radiation protection; where are we now and where should we go? *Environmental Research*. 2017;159:484–90.

3 Lambin P, Fertil B, Malaise EP, *et al.* Multiphasic Survival Curves for Cells of Human Tumor Cell Lines: Induced Repair or Hypersensitive Subpopulation? *Radiation Research*. 1994;138:S32.

4 Mothersill C, Seymour CB, Joiner MC. Relationship between Radiation-Induced Low-Dose Hypersensitivity and the Bystander Effect. *Radiation Research*. 2002;157:526–32.

5 Fernandez-Palomo C, Seymour C, Mothersill C. Inter-Relationship between Low-Dose Hyper-Radiosensitivity and Radiation-Induced Bystander Effects in the Human T98G Glioma and the Epithelial HaCaT Cell Line. *Radiation Research*. 2016;185:124–33.